Air source heat pump modelling for dynamic building simulation tools based on standard test data

Eric Baster B.Sc. M.Sc.

A thesis submitted for the
degree of Doctor of Philosophy

Energy Systems Research Unit
Department of Mechanical and Aerospace Engineering
University of Strathclyde, Glasgow

March 14, 2017

Declaration of authenticity

This thesis is the result of the author's original research. It has been composed by the author and has not been previously submitted for examination which has led to the award of a degree.

Signed: _____

Date: _____

Abstract

Air source heat pumps (ASHP) are increasingly of interest in the UK and Europe, due to national commitments around emissions reductions and the greater use of renewables. This raises issues around the optimisation of installation design approaches, and the potential for ASHP to contribute to demand flexibility. Dynamic modelling is a useful tool for addressing such issues. It is also beginning to play a role in performance estimation under National Calculation Methodologies.

There is currently no broadly accepted method for the creation of models of air-to-water heat pump performance for dynamic building simulation tools based on standard testing processes. Such a method is proposed. An analysis of ASHP theory and behaviour is undertaken, and used to inform a review of modelling methods in the literature. The "grey box" approach is selected, and adapted to work with data of the type output by European Standard EN 14511 for the performance testing of heat pumps.

The wide applicability of the proposed modelling method is demonstrated through application to EN 14511 data for 45 ASHP units. Three of the models developed are implemented in building energy simulation tool ESP-r.

Simulations results are within the range found in field trials, and are comparable to the predictions of other modelling methods. The method can differentiate between higher and lower quality ASHP, and predictions follow expected trends when the parameters of the modelled heating system are changed. It is concluded that the method is valid for simulations focussing on the integrated performance of building and heating systems.

The main limitation found is that humidity can have a significant impact on performance, and EN 14511 performance data does not allow sensitivity to humidity to be assessed. Recommendations are made for extensions to standard testing processes to aid the production of dynamic models.

Acknowledgements

I am grateful to my supervisor, Dr Paul Tuohy, for his insight and encouragement; to my family, for their unwavering support; John, for always being ready to share his huge wealth of technical knowledge; Katie, Thom and John again - I'll miss office lunchtimes and late nights; and Mike, Julian and Michael - your friendship and Tuesday night pub quiz chat kept me going! And last but not least - thank you, Gordon.

Contents

List of Figures

List of Tables

Nomenclature

Symbols used throughout	
Φ	Heat transfer rate
P	Electrical Power
θ	Temperature
RH	Relative humidity
M	Mass
$\dot{m}$	Mass flow rate
c_p	Specific heat
$\bar{c}$	Mass-weighted average specific heat
U	U value
A	Surface area

Suffixes used throughout	
a	Air
w	Water
i	Inlet
o	Outlet
ss	Steady state

Symbols appearing in particular chapters	
	Chapter 2
W	Work
γ	Isentropic efficiency factor
P_1 and P_2	Evaporator and Condenser pressure respectively
$\dot{v}$	Volume flow rate
r_v	Inbuilt volume ratio (scroll compressor)
V_s	Swept volume
f	Rotations per second
ρ	Density
	Chapter 4
$\Delta\theta_w$	Difference between water inlet and outlet temperature
COP_{std}	COP determined during testing
COP_Δ	COP adjusted for water flow rate
t_{df}	Defrost duration
t_{on}, t_{off}	Time since start up, shutdown respectively
τ_{on}, τ_{off}	Time constant of transients at start up, shut down
Φ_d	Heat output including defrost adjustment
COP_d	COP including defrost adjustment
ΔCOP	COP frosting adjustment term
t_{ff}	Time between defrosts
E_{df}	Energy to defrost
	Chapter 5
ϵ	Effectiveness (heat exchanger)
NTU	Number of transfer units
$\dot{C}$	Specific heat of a fluid multiplied by $\dot{m}$
UA_c	Heat transfer parameter between fluids in condenser
θ_c	Condensing temperature of refrigerant

Chapter 1

Introduction

1.1 Background

Heat pumps operate by augmenting input energy with thermal energy absorbed from the environment. At a domestic scale, practically all are electrically driven and operate on the vapour compression cycle. The ratio of thermal energy delivered to electrical energy input - known as coefficient of performance or COP - can range from less than 2 up to more than 5 in favourable conditions [1], making them a potentially attractive method of heat supply. COP however is highly dependent on variables such as weather and output temperature.

The UK has seen an increased interest in heat pumps in recent years, due to changes to building regulations and the CO_2 emissions reduction commitments included in the UK and Scotland Climate Change Acts. The depth of these cuts would require a switch from gas as the main source of heating to electricity generated using non-emitting means, prompting government support for their installation through the Renewable Heat Incentive [2]. Air-to-water heat pumps are seen by many as having the most potential: they have lower capital cost than ground source heat pumps, more flexible installation requirements, and unlike air-to-air heat pumps they can operate in familiar UK wet central heating systems and provide hot water.

Field trials of ASHP systems conducted in the UK have shown very mixed performance. Figure 1.1 depicts “system efficiencies” (COP measured over a year, including auxiliary power loads) recorded by the Energy Saving Trust [3]. There is clearly still some work to be done to examine how best to deploy heat pumps in current energy systems. A key reason

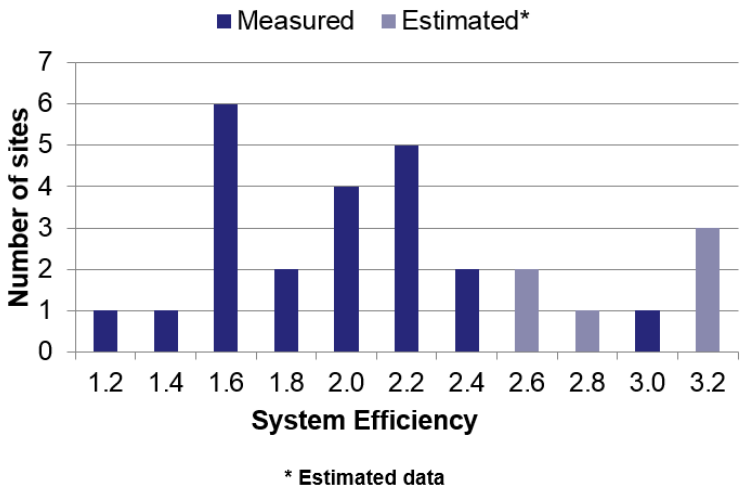

Figure 1.1: ASHP field trial results (Energy Saving Trust [3])

is that heat pumps are highly sensitive to the conditions under which they operate: the design and control of the installation are vitally important, and the heat pump cannot be considered in isolation from the building and heating system it is coupled to.

A further active topic of research relates to the role of heat pumps in future energy systems. A number of recent studies [4, 5] consider the use of thermal storage to shift electricity consumption away from peak times, to ease grid constraints, smooth out demand or to take advantage of surplus renewable generation.

In both these research areas, dynamic whole-building energy simulation tools are highly valuable. Within such tools, there is currently no broadly-accepted method for producing models of air-to-water heat pump units [6]. Although several different ASHP models for building energy simulation tools have been put forward, these have relied on specifically-measured, non-standard data. A method is desirable which makes use of standard, independent test data. Such a method - as well as contributing to the previously mentioned research areas - may be informative during the future development of building standards. The role of dynamic simulation as a compliance tool is expected to expand; in the UK, dynamic simulation is already an approved method for demonstrating compliance with Approved Document L2A of the UK building regulations for new, non-domestic buildings [7].

Within Europe, independent performance testing of air source heat pumps is often carried out to European Standard EN 14511 [8]. Whilst EN 14511 is not mandatory, it is the closest there is to a universal standard. Elements of EN 14511 are at the time of writing

requirements for support schemes such as the UK Renewable Heat Incentive (air-to-water heat pumps for heating only were added in 2014 [2]), as well as the European Heat Pump Association's Quality Label [9] (introduced in 2009). There are therefore strong incentives for manufacturers to use it. Furthermore at least one independent test centre [1] regularly publishes a subset of EN 14511 tests, and there is a relatively large pool of data on which methods can be trialled.

1.2 Aims and approach

The focus of this work is on the development of a method for producing models of on-off controlled air source heat pump (ASHP) performance for use in building energy simulation, based on performance data produced by European Standard EN 14511 on the performance testing of heat pumps[1].

The approach taken is to first critically review existing modelling approaches, and the data available from testing. Based on this, a grey box method is proposed as most appropriate. In order to test the applicability of the approach, such a model is developed within dynamic building simulation tool ESP-r [10] using EN 14511 data for exemplar air source heat pumps. The method is documented with the intent that it could be used in other dynamic simulation tools.

1.3 Contributions

The main contributions of this thesis are:

- an analysis of ASHP behaviour and performance characteristics;
- a review of standard test processes for ASHP and resulting data outputs;
- an assessment of methods currently used to model heat pumps in dynamic simulation and the associated data requirements;

[1] Modulating ASHP, generally using inverter driven compressors, are available. However when this project was initiated, these were relatively rare. Of the 41 sets of EN 14511 test data obtained in 2013 and analysed in A, only six had the ability to modulate their output - and for these, only full load test data was available.

- an updated dynamic modelling method tailored to standard test data, but with a gap around the determination of transient elements;
- the application of the method to over 40 sets of ASHP data;
- the implementation of the method in ESP-r;
- application of validation tests to the method;
- a discussion of the method's usefulness, applicability and limitation;
- the capture of the approach in a methodology that can be applied by others;
- suggestions as to how standard testing should be improved in future, to better enable dynamic modelling; and
- a discussion of the method's potential uses, and what the findings mean for the increased use of dynamic modelling as a National Calculation Methodology or to show compliance with building regulations.

1.4 Document structure

In chapter 2, the theory behind ASHP behaviour is reviewed, in order to better enable the assessment of modelling methods. A shortage of data for validation means that a thorough exploration of theory is particularly important.

European Standard EN 14511 for the performance testing of heat pumps (as it applies to air-to-water heat pumps) is then assessed in chapter 3. The aim of the thesis is to develop an ASHP modelling method for dynamic simulation environments which can be informed by EN 14511 results.

Chapter 4 reviews ASHP modelling methods in the literature, categorising them as either black box, grey box or component-based approaches. A grey-box approach is identified as most suitable.

Chapter 5 proposes a methodology for the modelling of fixed capacity ASHP based on standard test data. The generality of the method is tested by the application of key aspects to test data for 45 ASHPs. In chapter 6, validation tests are applied to the method.

The extent to which the proposed method achieves the aims of this work, and its relationship to other works in the literature, is discussed in chapter 7. Limitations and are considered, and extensions to standard testing which would enable it to better meet the needs of dynamic modelling are recommended.

Chapters 8 and 9 sets out the conclusions and areas for further work emerging from the thesis.

Chapter 2

Key air source heat pump performance characteristics

A thorough understanding of key ASHP performance characteristics is required before modelling methods are discussed in later chapters. The most important of these characteristics is that thermal output and power load vary constantly. This chapter first considers how refrigerant pressures in the condenser and evaporator influence these quantities, then examines the factors influencing the condenser and evaporator pressures themselves. Steady state operation is initially discussed, before transient behaviour around start up and shut down is looked at separately. The impact of humidity on ASHP is also discussed separately, then lastly the differences between fixed and variable capacity ASHP are noted.

A key characteristic of ASHP performance is that their thermal output and power load are highly sensitive to the external conditions in which they operate - ambient air temperature, moisture content and heating system water flow temperature are particularly important. Thermal output and power load vary independently: their ratio, COP, is also sensitive to operating conditions. Most ASHP installations will experience a wide range of conditions during normal operation.

A comprehensive understanding of the basis for ASHPs' sensitivity is important for the review and development of modelling methods, particularly in the absence of extensive data for validation. Unfortunately there is a lack of good theoretical explanations in the literature.

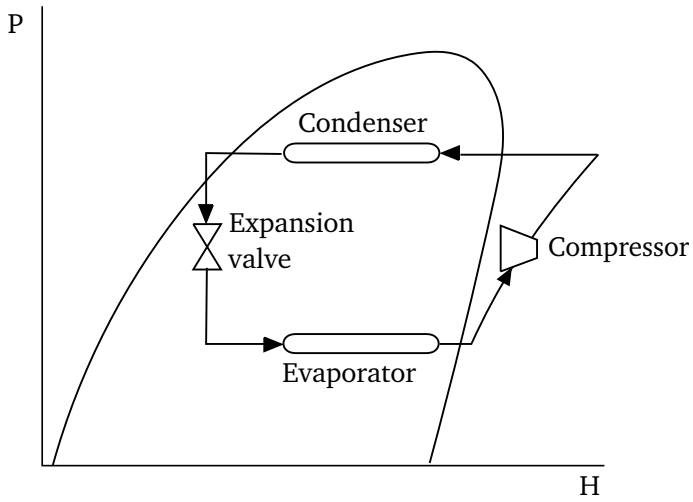

Figure 2.1: Schematic of cycle components

Many authors make reference to Carnot's theorem regarding the maximum efficiency of a heat engine operating between two heat reservoirs. One shortcoming of this approach is that Carnot's theorem relates only to COP - on its own, this is not sufficient to model the performance of a heat pump. More importantly, the idealised heat engine associated with his theorem is too simple to illustrate various aspects of real heat pump behaviour.

This section therefore comprises a review of theory taking as the starting point the interactions of the components of the heat pump cycle. The description is split into two parts: the first, section 2.1, covers the relationship between thermal output and power load and the key variables of the refrigerant cycle (namely refrigerant pressures in the evaporator and condenser). The second, spread across subsections 2.2 and 2.4, covers the links between these variables and the operating conditions.

ASHP for domestic use operate on the vapour compression cycle. The basic cycle is depicted in figures 2.1 and 2.2. Heat energy from the environment evaporates a refrigerant at low pressure and temperature. The vapour is compressed then allowed to condense at some higher pressure and temperature, releasing energy. The refrigerant then passes through an expansion device, returning to the evaporator as a liquid-vapour mix to begin the cycle again. Heat pumps are an appealing method of heating because in normal operation the rate of heat delivered is greater than the rate of work done in compression.

In most if not all ASHPs, active control of the refrigerant cycle is required. This is because the compressor may be damaged if the refrigerant at its inlet is not fully evaporated. In

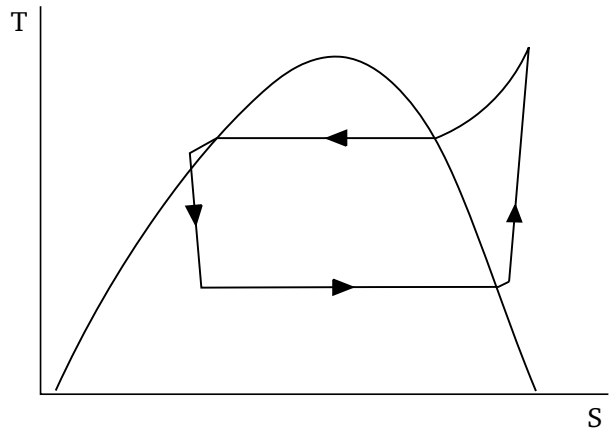

Figure 2.2: Temperature-entropy diagram of typical cycle

order to ensure no droplets are present, heat pumps are fitted with an adjustable expansion device. This is controlled either mechanically or electronically such that refrigerant leaving the evaporator is superheated by a fixed amount. The degree of superheating should be sufficient to ensure no droplets form in the compressor suction line, but not so high that compressor work is unnecessarily increased. There are occasional variations to the basic design described here, including additional components such as accumulators, receivers or subcooling loops; however most would not alter the essential characteristics of heat pump behaviour.

2.1 Drivers of variation in thermal output and power load

In this subsection the relationships between thermal output and power load and evaporator and condenser pressures are explored. Mechanisms linking variation in the thermal output to variation in evaporating and condensing pressures are explained. The links to evaporating pressure are stronger. Variations in power load are also driven by variation in evaporating and condensing pressures, though this time often condensing temperature is more important. The arguments relate to heat pumps using "conventional" refrigerants (typically R404A, R407C, and R410). Heat pumps using CO_2 as a refrigerant employ a transcritical cycle and are slightly different: the same relationships apply, but condensation occurs above the liquid-vapour dome in the temperature-entropy diagram and follows a curved path, meaning there isn't a single identifiable temperature at which condensation occurs.

Power consumption is dominated by the compressor, though it is also consumed by a

number of different components: the controls, the fan which draws air over the evaporator coils, and any water circulation pump, crank case, tray heater and freeze protection fitted. Classically, the work done W in adiabatic compression of an ideal gas is given by equation 2.1, and depends on both inlet pressure P_1 (effectively evaporating pressure) and outlet pressure P_2 (effectively condensing pressure). Here $\dot{v}$ denotes volume flow rate, and γ isentropic expansion factor. It is worth taking a moment to consider that, whilst this equation relates work to evaporating and condensing *pressures*, in *qualititative* descriptions of the link between work and evaporating and condensing pressures, "pressure" could in fact be exchanged for "temperature": at any point in the liquid-vapour dome, knowledge of either pressure or temperature is all that is required to determine the other, and (for the refrigerants encountered in this work at least) a higher temperature indicates a higher pressure and vice versa.

$$W = \frac{\gamma}{\gamma - 1} \dot{v}_1 P_1 \left[\left(\frac{P_2}{P_1} \right)^{\frac{\gamma}{\gamma - 1}} - 1 \right] \tag{2.1}$$

Modern ASHPs' compressor power consumption, however, is commonly much more sensitive to condensing pressure than evaporating pressure. Once the reader is familiar with the arguments in the following section (which show that air temperature is a key determiner of evaporator pressure, and water temperature of condensing pressure), this greater sensitivity to condensing pressure is readily apparent from studying fig. 2.3 and many of the graphs of ASHP in appendix A: There is little correlation between power load and air temperature. Cuevas et al. [11] suggest that this is a peculiar feature of scroll compressors. They developed semi-empirical model of compressor work (eq. (2.2)), which aims to take into account not just the work done to compress a pocket of gas from scroll closing to opening, but also heat flow through the material of the compressor wall and any mismatch between actual and built-in pressure ratio. It can be seen that when the relation between scroll inbuilt volume ratio[1] r_v and γ is as given in eq. (2.3), the influence of evaporating pressure would disappear. V_s denotes swept volume.

$$W = \frac{P_1 \times V_s}{\gamma - 1} \left(r_v^{\gamma - 1} - \gamma \right) + \frac{P_2 \times V_s}{r_v} \tag{2.2}$$

[1] Scroll inbuilt volume ratio is the ratio of the volume of the gas pocket at the instant the scroll inlet closes to its volume at the instant the scroll outlet opens.

$$r_v = \gamma^{\frac{1}{\gamma-1}} \tag{2.3}$$

The thermal output of an ASHP is essentially the rate of heat transfer in the condenser from refrigerant to heating system water. In normal operation the refrigerant will undergo de-superheating, condensation and subcooling before leaving the condenser. The majority of the heat transferred is latent heat of condensation.

This leads to an important point: as the refrigerant is always completely condensed before it leaves the condenser, the mass flow rate of refrigerant being delivered to it is a major influence on the rate of heat transfer. The more refrigerant being delivered and condensed, the greater the thermal output of the ASHP.

Assuming the heat pump in question is equipped with a scroll compressor[2], the mass flow rate of refrigerant is:

$$\dot{m} = V_s f \rho \tag{2.4}$$

Swept volume V_s (interpreted for a scroll compressor as the volume of the gas packet immediately after the scroll closes) is a fixed parameter of the compressor hence, for a fixed rotational speed f, mass flow rate is proportional to ρ, the density of the refrigerant at the scroll inlet. Density is dictated by the state of the refrigerant in the evaporator. A higher evaporating pressure corresponds to a higher refrigerant density, which leads to a higher mass flow rate of refrigerant being delivered to the condenser.

In summary then, the thermal output of an ASHP in steady-state operation is closely linked to the mass flow rate of refrigerant passing through the condenser, which in turn is determined by evaporating pressure. As evaporating pressure increases, density at the scroll intake, mass flow rate and thermal output all increase too. As mentioned previously,

[2]In this description, it is assumed the ASHP uses a scroll compressor with a synchronous motor. Scroll compressors certainly appear to be the most common type in domestic ASHP: a survey undertaken by the author in April 2014 of the ASHP listed in the UK governments SAP Product Characteristics Database found that, where the manufacturer's brochures listed the type of compressor used, this was always a scroll. No indication was found as to whether synchronous or asynchronous motor types are most common - a synchronous motor is assumed because it simplifies the reasoning. The thermal output of an ASHP which use a reciprocating compressor or an asynchronous motor is still influenced by evaporating pressure through the mechanism described: however it is also influenced by condensing pressure. In both cases increasing condenser pressure decreases refrigerant mass flow rate and thus thermal output. In the case of an asynchronous motor this happens through increased slip a higher pressures. With a reciprocating compressor, increased condenser pressure reduces volumetric efficiency: a greater mass of gas remains in the compressor's clearance volume at the end of a stroke.

because in the evaporator the refrigerant is undergoing a phase change, either pressure or temperature is enough to specify its state - and a higher pressure corresponds to a higher temperature. It is therefore also true to say that as evaporating *temperature* increases, thermal output of the ASHP increases.

The scale of this affect can be seen by looking at refrigerant property charts. It appears from ASHP test centre reports [1] that the large majority of current domestic-scale ASHP use R407c as the refrigerant. Density for R407c in the saturated vapour state at 220 kPa (about −20 °C) is 9.5 $\mathrm{kg\,m^{-3}}$, whereas density at 480 kPa (about 0 °C) is more than double this value at 19.8 $\mathrm{kg\,m^{-3}}$.

A smaller but still significant mechanism links condensing pressure and thermal output. The latent heat of condensation in common refrigerants isn't constant – the width of the liquid-vapour dome in a pressure-enthalpy diagram reduces as pressure and temperature increase. This means that the energy delivered to the condenser for a given refrigerant mass flow rate - and therefore ASHP thermal output - also reduces as condensing pressure increases.

Again the scale of this affect can be seen in refrigerant property charts. The latent heat of condensation for R407c at 1600 kPa (about 40 °C) is 173 $\mathrm{kJ\,kg^{-1}}$, whereas at 2600 kPa (about 60 °C) it is 20% lower at 138 $\mathrm{kJ\,kg^{-1}}$.

Up to this point, energy losses throughout the refrigerant cycle due to friction and heat exchange with the environment have been ignored. There is also a heat gain at one point, in some ASHP at least. Hermetic and semi-hermetic compressors use refrigerant leaving the evaporator to provide cooling to motor coils prior to compression. An investigation of the effects of these losses and gains is beyond the scope of this thesis - whilst of interest to a heat pump manufacturer, this level of detail proved unnecessary for the analysis and development of modelling methods presented later in this work.

In summary ASHP thermal output is not constant but is heavily dependent on evaporating pressure, and to a lesser extent on condensing pressure. ASHP power load is also variable, largely dictated by condensing pressure. To complete the picture, consideration must be given to how evaporating and condensing pressures relate to operating conditions.

2.2 Drivers of variation in evaporating and condensing pressures

This section gives a qualitative description of which variables influence evaporating and condensing pressures and hence heat pump thermal output and power consumption. A comprehensive picture is needed for the assessment of modelling methods.

If a heat pump has been off for some time, the refrigerant in the evaporator will be in thermal equilibrium with the outdoor air, and the refrigerant in the condenser will be in thermal equilibrium with the heating system water in the condenser. When the compressor switches on, it acts together with the expansion valve to increase the pressure in the condenser and decrease the pressure in the evaporator. The evaporating temperature is thus reduced below that of the air, and condensing temperature increased above that of the heating system water. This provides the driving force for heat transfers from air to refrigerant in the evaporator, and from refrigerant to heating system water in the condenser.

If the temperatures and flow rates of the ambient air and heating system return water into the ASHP remain steady, after several minutes the evaporating and condensing pressures will stabilise in a dynamic equilibrium state, such that the rate of heat transfer across the evaporator is equal to heat removed by the refrigerant flow; the heat transfer across the condenser is equal to the rate of heat delivered by the refrigerant flow; and the condenser rate of heat transfer is equal to the evaporator rate of heat transfer plus the heat added to the refrigerant during compression (minus any losses). The equilibrium state will be characterised by an evaporating temperature several degrees below that of the air; and a condensing temperature a few degrees greater than that of the inflowing heat system water.

The equilibrium state reached by the refrigerant cycle will be sensitive to changes in the boundary conditions. If, for example, the temperature of the heating system water inflow at the condenser increases or its mass flow rate decreases (perhaps if thermostatic radiator valves are used), the heat transfer rate across the condenser will decrease. A complex set of interactions within the refrigerant cycle will ensue, resulting in pressure and temperature in the condenser increasing until the system is again in equilibrium.

As the condensing pressure is now higher, there will be an associated increase in power load. Depending on the characteristics of the compressor, there may also be a drop in

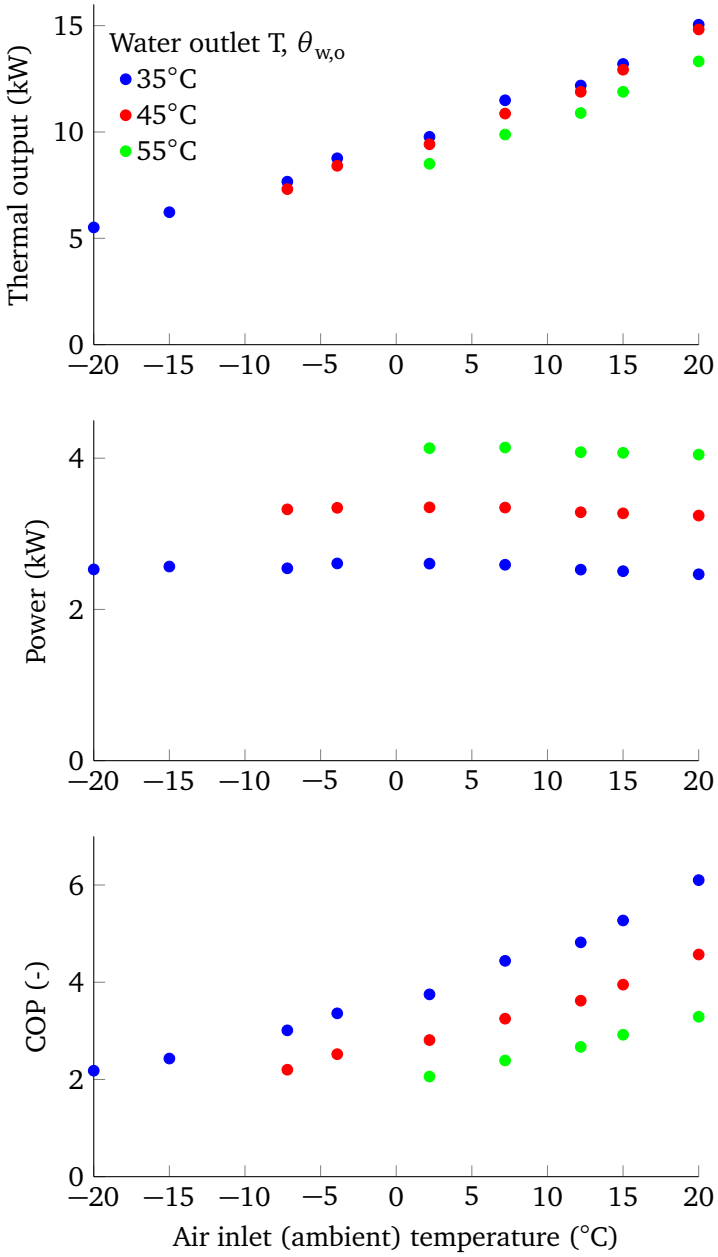

Figure 2.3: EN 14511 test data for an example ASHP [12] showing sensitivity to air inlet and water outlet temperatures

thermal output. Should the water temperature fall rather than rise, or its flow rate increase, the opposite would occur. There is likely to be some hunting behaviour, caused by the thermostatic expansion valve, whilst the new equilibrium state is sought.

Boundary conditions at the evaporator inlet are more complex. This is because the air passing through the evaporator is a mixture of dry air and water vapour, which in some circumstances can condense or freeze on the evaporator surface. A discussion of the impact of humidity on performance is left for subsection 2.4, as it is complex enough to merit separate discussion; here only variations in air temperature are considered.

Variations in air temperature or flow rate effect the equilibrium state reached by the cycle in a similar way to variations in water temperature or flow rate. A drop in air temperature or flow rate would result in a smaller rate of heat transfer across the evaporator. The amount of superheating of the refrigerant would fall, triggering the expansion valve to close up slightly. The pressure in the evaporator will reduce, increasing the rate of heat transfer until a new equilibrium state is reached. This state will be result in a smaller thermal output. Should the air temperature or flow rate rise, the opposite would occur.

Figure 2.3 illustrates the sensitivity of ASHP performance to variation in air inlet (ambient) and water outlet temperatures. Whilst the previous theory discussion has dealt with water inlet rather than outlet temperature, these are closely enough linked that the latter can serve as a proxy for the former in this discussion of general trends. The underlying data was obtained from technical specifications published by a major manufacturer [12].

The major trends in thermal output and power consumption that would be expected from the theory outlined up to this point are clearly visible. Increasing air inlet temperature causes an increase in thermal output. There is minimal impact on power consumption, consistent with the scroll compressor model put forward by Cuevas et al.. Increasing water temperature has a small negative impact on thermal output, and significantly increases power consumption. These trends in thermal output and power load as operating conditions change are one of the key points in this subsection.

In the case of thermal output, the size of variations is consistent with the theoretical causes set out in the previous section. Property tables for refrigerant R407c suggested that a 20 °C increase in evaporating temperature (taken in isolation) implies a doubling of thermal output - the change seen in fig. 2.3 when air temperature increases by the same amount is

close to this scale, though other effects clearly have an impact too. The previous section also suggested that an increase in condensing temperature of 20 °C should lead to a reduction in thermal output of around 20% - again, a similar size of reduction is apparent in fig. 2.3 when water outlet temperature increases by 20 °C.

A second key point from this discussion is that in steady state operation, a particular set of operating conditions implies particular evaporating and condensing temperatures, which in turn always relate to particular values for thermal output and power load. Thus steady state thermal output and power load can be predicted from knowledge of operating conditions only. This concept is the basis for the equation-fit models discussed later.

A related observation is that, if two different sets of operating conditions correspond to the same steady state evaporating and condensing pressures, they will have the same thermal output and power load. It was described earlier how either increasing the temperature or decreasing the flow rate of water arriving at the condenser would increase the condensing temperature, leading to an increase in power consumption and a smaller decrease in thermal output. If, however, one was to increase the temperature and *increase* the flow rate by carefully determined amounts such that the rate of heat transfer between refrigerant and water stayed the same, there would be no effect on condensing temperature and thermal output and power consumption would be unchanged. Creffig:WflowDiag1 is a depiction of temperature and flows in the condenser. The solid line depicts a case with high water inlet temperature and flow rate, and the dotted line depicts a case with lower temperature and flow. The rate of heat transfer is the same for both, and so condensing temperature is unaffected. This observation is employed in the method for adjusting performance test data to different water flow rates described in section 5.5.

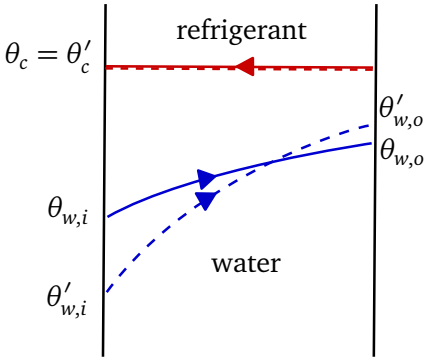

Figure 2.4: Temperatures in the condenser under different water flow rates

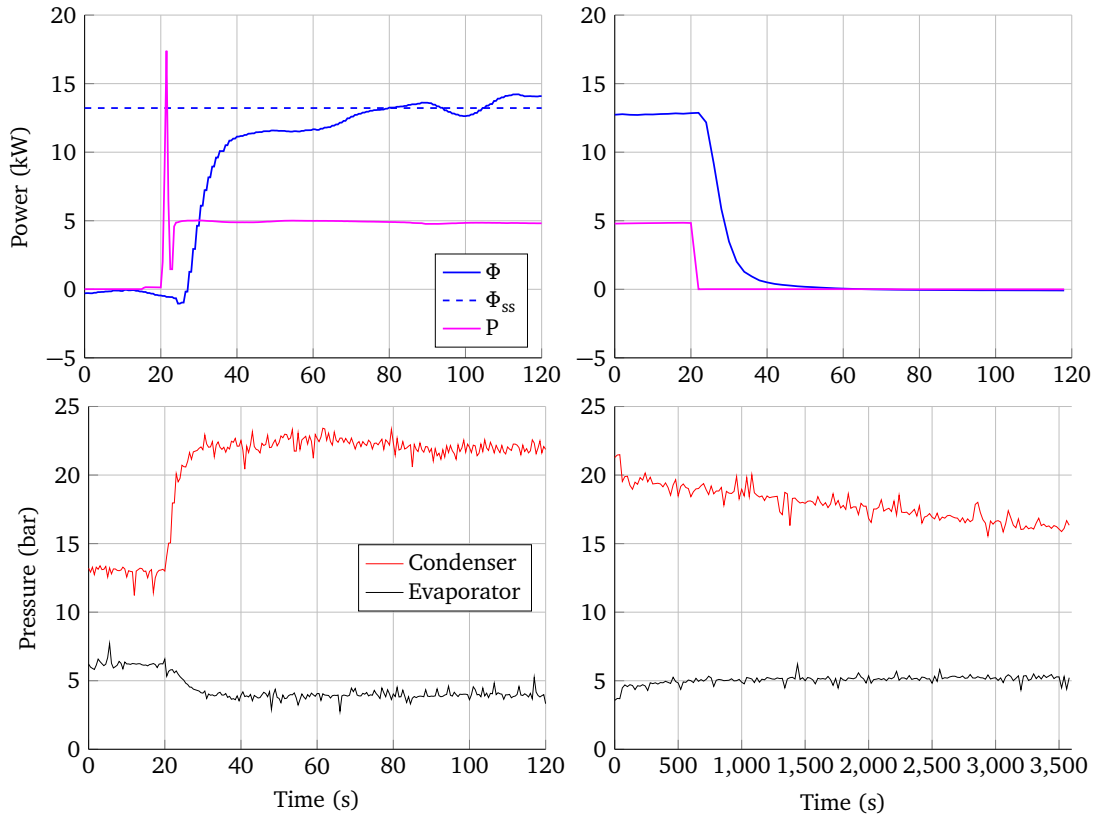

Figure 2.5: ASHP start-up (left) and shutdown (right)

2.3 Transient behaviour

In previous sections, steady-state behaviour has been the focus. However when modelling a system, its transient behaviour must also be considered as this will affect performance. This behaviour is most visible around startup and shutdown, events which represent very rapid changes in operating conditions.

Figure 2.5 shows the variation in output, power load and evaporating and condensing pressures around start up and shut down events for an air-water ASHP with nominal thermal output 16 kW. The data was collected and described by Uhlmann and Bertsch [13]. Power load initially spikes before settling at its steady state value after just 5 seconds, whereas thermal output Φ takes nearly a minute to reach its steady state value Φ_{ss} [3]. Prior to start up the heat pump had been off for more than 10 hours.

The delay in attaining full thermal output is due to two interlinked factors: the thermal inertia of the refrigerant and heat pump components, and the need to re-establish the

[3] "steady state value" in this instance was taken to be the mean value over the 30 minute time interval beginning 2 minutes after start up.

difference in refrigerant pressure between the evaporator and condenser. The pressure difference declines during off periods as the refrigerant and heat pump components approach ambient temperature. There is also some degree of refrigerant leakage from the high pressure to low pressure sides through imperfect seals in the compressor, expansion valve and four-way reversing valve (if present). The ASHP depicted in fig. 2.5 re-establishes the steady state pressure difference in less 15 seconds, so it seems that much of the delay in attaining full thermal output is due to the thermal inertia - i.e. the thermal mass of key components, the condenser in particular, which absorb energy until it their steady state operating temperatures are reached.

Some of the additional energy input at start up is reclaimed at shutdown. The water circulation pump appears to continue operating for approximately 5 seconds after the compressor stops running, and momentum prolongs the flow for even longer. Uhlmann and Bertsch remark that more energy could be reclaimed in this way if the pump was run for longer. ASHP which continue to circulate water for two minutes after compressor shutdown have been described [14].

Uhlmann and Bertsch conclude that, for this ASHP, the overall reduction in COP due to transient behaviour is no more than 2% so long as run times were maintained above 15 minutes. A separate (non-peer-reviewed) study, in which a test installation was monitored, found that run times of 8 minutes were sufficient to ensure performance close to lab test values [15]. When modelling a sensibly-sized ASHP installation, it is therefore debatable whether or not transient behaviour necessarily needs to be included. Its inclusion would however be useful for studies where an ASHP may be pushed beyond “ideal” operation, such as sizing studies or investigation of control approaches.

In summary, transient behaviour is visible following rapid changes in operating conditions —namely, start up and shut down events. Experimental data suggests that the main factor in large scale transient behaviour is the thermal inertia of the ASHP, rather than the need to re-establish the correct pressure ratio. The impact of transient behaviour on long term performance is likely to be just a few percent in well-functioning installations, though potentially more in (for example) oversized installations, and its inclusion in modelling is therefore desirable .

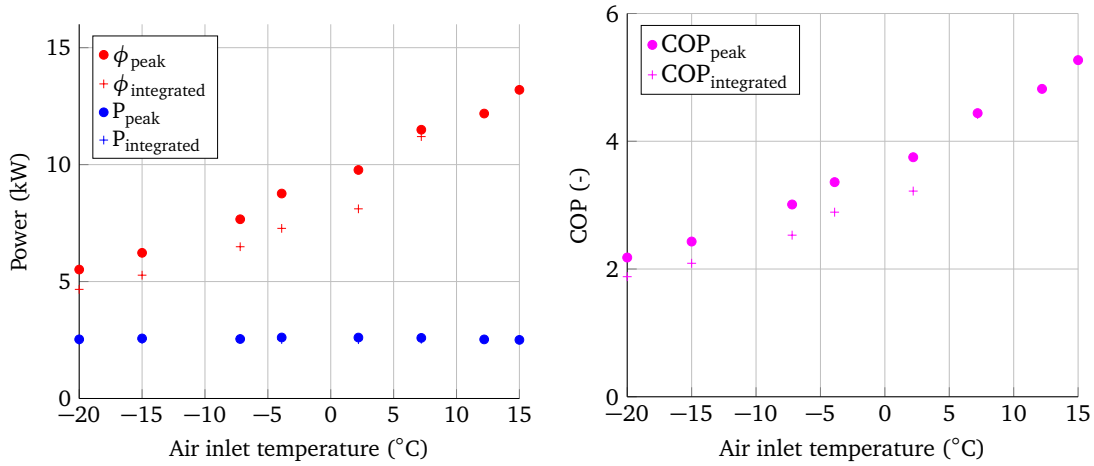

Figure 2.6: Example of ASHP manufacturer's data [17] showing difference between peak (defrosts excluded) and integrated (defrosts included) performance at a range of air inlet temperatures

2.4 Humidity and evaporator frosting

Section 2.2 described how variation in air temperature at the evaporator inlet affects thermal output and power consumption by changing the evaporating pressure. For simplicity, it was temporarily assumed that the air was dry; in reality the air flowing through a ASHP evaporator will be a mixture of dry air and water vapour. In certain climatic conditions this can have significant repercussions for ASHP performance, and this should be taken account of in models.

During normal operation the evaporator surface is several degrees cooler than the air flowing over it. Thus there is the potential for condensation or frost to form, and this can have a significant effect on ASHP performance. Though the additional heat transfer provided by the phase change is beneficial to performance, frost build up is harmful and if unchecked would eventually prevent operation. ASHPs therefore must include a defrost mechanism. The vast majority of systems employ either the reverse cycle or hot gas bypass defrost methods [16], both of which periodically stop the normal function of the refrigerant cycle so that the evaporator can be heated and the accumulated ice melted. These interruptions are themselves costly to performance, but necessary to prevent total shutdown in colder weather.

There is surprisingly little in the literature which addresses the impact of humidity

on ASHP seasonal or *integrated*[4] performance. The evidence that was found is described below, and suggests that the impact is significant enough to require addressing in any ASHP modelling method.

For example, figure 2.6 compares an ASHP's integrated performance with its peak, unfrosted performance in the same conditions [17]. At 2 °C, thermal output is reduced by 17%, and COP by 14%. Unfortunately it is not known what humidity levels were used in testing. A Swiss Government report for which 13 ASHPs (7 with reverse cycle defrost and 6 with hot gas bypass) were tested found that COP was typically reduced by 10-15% by defrosting [18]. Using a simplified first principles approach Vocale et al. found integrated COP in some conditions could be 16% lower than peak. Simulations using climate data for Bologna, Italy, suggest that over a year the reduction in COP could be 13%.

Broadly, condensation/frosting occurs in the evaporator when the moist air passing through it is cooled beyond saturation point. The variables which determine whether condensation or frosting are occurring are thus air dry bulb temperature $\theta_{a,i}$, dew point temperature θ_{dp} and the evaporator surface temperature θ_{evap} [20].

In a typical ASHP the difference between $\theta_{a,i}$ and θ_{evap} is such that condensation/frosting only occurs when the entering air is already at more than 50-60% saturation [21, 22]. At humidity levels lower than this, θ_{evap} is generally warmer than θ_{dp}, and hence air cannot be cooled beyond saturation.

Condensation tends to freeze rather than running off when θ_{evap} is −3 °C or lower [23]; for many ASHP this appears to correspond to a $\theta_{a,i}$ of between 5 °C and 7 °C [22].

Evaporator surface temperature is therefore a crucial variable for predicting frost growth. It is important to note that the difference between $\theta_{a,i}$ and θ_{evap} varies from ASHP to ASHP, due to factors such as evaporator geometry, air velocity [24], compressor characteristics and even refrigerant fill.

Furthermore, the ASHP's operating conditions also cause variations in the difference; for example if the water output temperature of the heat pump is 55 °C, its thermal output will be relatively low; the rate of heat transfer at the evaporator will be small, and the difference between $\theta_{a,i}$ and θ_{evap} reduced. If the water output temperature is 35 °C, its thermal output

[4]Integrated performance is used in this work to refer to thermal output, power load and COP averaged over one or more frosting-plus-defrost-period cycles

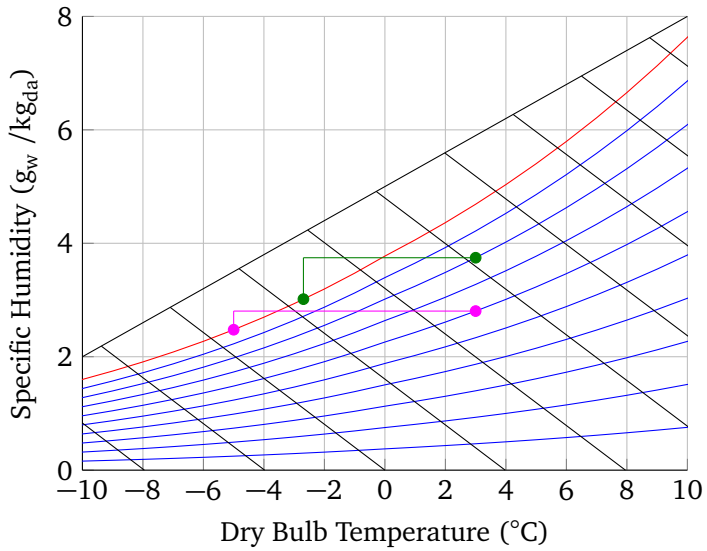

Figure 2.7: Frosting process represented on a simplified psychrometric chart

will be higher and the difference larger.

In addition, condensation and frosting themselves effect θ_{evap}. In the former case, the additional latent heat transfer means that evaporating temperature increases. In the latter case, the obstruction of air flow by the frost reduces the heat transfer, and the evaporating temperature decreases [22]. Predicting precisely when an ASHP would be affected by condensation or frosting is not straightforward.

Assuming condensation or frosting is occurring, the rate increases with increasing relative humidity. The rate also increases the warmer the temperature, due to the steepening of the saturation curve (fig. 2.7); more water is condensed for a given amount of subcooling. For this reason, the air temperature range 0 °C to 5 °C is often identified as being worst impacted by frosting.

Whilst early ASHP tended to initiate defrost cycles based on fixed time intervals, most modern units attempt to sense frost growth, so that defrost mechanisms are triggerred only when necessary and terminated as soon as frost is melted. One common approach is to monitor the pressure drop across the evaporator coil, which increases from its usual level as frost develops. Another is based on monitoring the temperature difference between ambient air and refrigerant in the evaporator, which is increased by the thermal resistivity of the frost layer. There is some evidence that despite this good control is not always achieved [25].

Although defrost cycles are required less frequently at lower temperature and lower

relative humidity, this is balanced to some extent by a greater time and energy requirement in these conditions. This appears to apply equally to both the reverse cycle method (fig. 2.8) [24] and the hot gas bypass method [14].

In the former method, the refrigerant cycle is temporarily reversed, so that the evaporator and condenser swap roles. This can mean that heat is actually extracted from the building during defrost periods, though in many modern systems a secondary electric resistance heater is employed to avoid this. The hot gas bypass method involves routing hot refrigerant from the compressor directly to the evaporator, skipping the condenser and expansion valve. Heat is not removed from the building, but none is delivered.

At higher water outlet temperatures (50 °C) the two methods consume similar amounts of energy. At lower outlet temperatures (35 °C), the reverse cycle defrost method is slightly more economical [18]. For both methods, power load during defrost seems likely to be influenced by conditions, and may not remain steady throughout the process.

In summary, in certain conditions frost or ice can form on ASHP evaporator surfaces. This harms performance directly, and indirectly by requiring that ASHPs periodically operate defrost mechanisms.

The limits of the conditions under which frosting occurs, along with the frequency, duration and energy consumption of defrost periods are not easy to predict. There is a lack of comprehensive studies into the impact of frosting and defrosting studies on ASHP performance. However it is reported that thermal output may be reduced by over 15%. Both humidity and air temperature will in theory affect frosting rates. The impact on performance is likely to be greatest in the temperature range 0 °C to 5 °C and when humidity is high. It is highly desirable that any ASHP modelling method takes account of the impact of humidity and frosting in performance.

2.5 Fixed and variable output heat pumps

Building heat loads continually evolve due to a large number of factors - such as changing weather conditions and internal gains. ASHP thermal output, just like that of any other heating system, must be modulated in response. There are two methods of achieving modulation: intermittent (or on/off) control, and output variation through use of an inverter

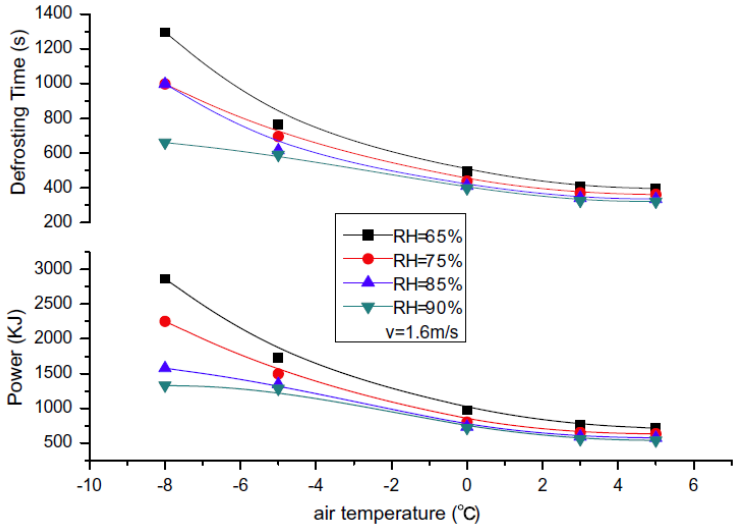

Figure 2.8: Defrost duration and energy consumption (taken from [24])

or other technique.

The first method is used for ASHP which have no way to reduce their output other than to periodically stop the compressor. These are sometimes referred to as fixed output ASHP, though of course this is slightly misleading: ASHP thermal output varies in response to operating conditions such as outdoor air temperature. Indeed thermal output is highest at warm outdoor air temperatures - typically when heat loads are small. Fixed output ASHP can therefore spend a considerable amount of time cycling on and off.

The second method applies to variable output ASHP, which do have the means to modulate their output without resorting to on/off cycling. The most common way to achieve this is to control the speed of the compressor. Inverter-based variable speed drives are perhaps the most frequently mentioned method. Some ASHP may alternatively use stepwise control of compressor speed, achieved through switching the number of active poles in the motor.

A number of potential advantages are ascribed to variable output ASHP. For example average water outlet temperature can be lower than with intermittent control, improving COP; and frosting may be reduced, as at part load evaporator surface temperature will be closer to air temperature [26]. There is some trade-off in terms of increased energy use by circulation pumps, and additional efficiency losses introduced by the inverter.

Currently, the majority of ASHP on the market are fixed output units. Of the 45 heat

pumps for which test data has been published by the Swiss heat pump test centre [1], only 11 are variable output units. Furthermore there does not appear to be widespread testing of variable output ASHPs' part load performance. The main European testing standard, discussed in the following section, requires that all tests must be conducted at maximum output. The main focus of this work is therefore on fixed output ASHPs. Improvements to standard test procedures which would assist in the development of modelling methods for variable output ASHP are considered in chapter 9.

2.6 Chapter summary

In this chapter, the key characteristics of ASHP performance are examined — along with the variables which influence them. This will inform the discussion of modelling methods in later chapters.

The first key characteristic identified is the large variation in steady state thermal output and power load across an ASHP's operating range. The roots of this variation is shown to be changes in evaporator and condenser pressure. Evaporator and condenser pressures are then shown to be influenced by air and heating system water temperatures and flow rates.

Transient behaviour was then discussed. Experimental data suggests that the main factor in large scale transient behaviour is the thermal inertia of the ASHP, rather than the need to re-establish the correct pressure ratio. Studies were cited which found the impact of transient behaviour on long term performance is likely to be just a few percent in well-functioning installations — though potentially more in, for example, oversized insallations.

The conditions under which ASHP evaporators are subject to frost growth was also discussed, alongside the impact this can have on performance both directly and through associated defrost mechanisms. Some authors found thermal output can be reduced by around 15%. The theoretical link between ambient humidity, air temperature and scale of the impact of frosting on performance was discussed, and a lack of comprehensive studies was noted.

Finally, the difference between fixed and variable output ASHP was noted. This work focusses on fixed output ASHP.

Chapter 3

Standard testing of air source heat pumps

This work is concerned with the development of a modelling method which can be informed by standardised performance test data; this data is relatively easy to obtain in comparison to information on an air source heat pump's internal layout and component parameters, and it ensures the wide applicability of the modelling method. Within Europe, independent performance testing of air source heat pumps is often carried out to European Standard EN 14511 [8]. This chapter reviews the EN 14511 test process and its outputs in section 3.1, before presenting analyses carried out by the author on the impact of specific aspects of the test process on example results (section 3.2); and on trends discernible in test results for a large group of ASHPs (section 3.3).

When specifying heat generation equipment for a particular installation, it is vital to know the rate and efficiency at which it can provide heat. As described previously, the thermal output and COP of a heat pump are highly sensitive to the constantly evolving conditions under which it will operate. It is therefore important that reliable information on thermal output and COP is available to customers, installers and suppliers. This information can be useful for the creation of models of heat pump performance.

European Standard BS EN 14511 [8] defines a process for determining output and COP amongst other information. It is not compulsory, though manufacturers wishing their

Table 3.1: EN 14511:2013 test conditions

Application		Air			Water	
Low temperature		$\theta_{a,in,dry}$ (°C)	$\theta_{a,in,wet}$ (°C)	RH (%)	$\theta_{w,in}$ (°C)	$\theta_{w,out}$ (°C)
Standard rating conditions	Outdoor air	7	6	87	30	35
	Exhaust air	20	12	38	30	35
Application rating conditions	Outdoor air	2	1	84	a	35
	Outdoor air	−7	−8	75	a	35
	Outdoor air	−15	—	—	a	35
	Outdoor air	12	11	89	a	35

a: tests are conducted at the water flow rate determined in the test at standard rating conditions for outdoor air ASHP

products to receive MCS accreditation in the UK and be eligible for the Renewable Heat Incentive subsidy scheme must use it [27]. Other standards are in use outside Europe, for example ANSI/ASHRAE Standard 37 [28] and AHRI Standard 550/590 [29] in the USA. However the scope of the performance information which EN 14511 produces is typical.

3.1 Test conditions and process

The EN 14511 process involves the installation of an exemplar unit in a test room, in which a range of environmental conditions can be simulated. In each test the conditions under which the ASHP is operating are maintained at particular values. The conditions for tests of air-water heat pumps designed for low temperature applications are set out in table 3.1. There are further sets of tests for heat pumps intended for medium, high and very high temperature applications. These follow the same pattern, but rather than outlet water temperatures of 35°C, the required water temperatures are 45, 55, and 65°C respectively. Most ASHP are designed to be suitable for a range of applications (commonly low, medium and high temperature applications) and thus are tested across more than one application temperature set.

Prior to the 2011 version of the standard, a more limited number of tests were specified (table 3.2 [30]). At this point, there were no tests at a water outlet temperature of 65 °C: table 3.2 contains the full group of test points required.

The review of theory in the previous chapter described the factors which influence ASHP

Table 3.2: EN 14511:2007 test conditions

		Air			Water	
Low temperature		$\theta_{a,in,dry}$ (°C)	$\theta_{a,in,wet}$ (°C)	RH (%)	$\theta_{w,in}$ (°C)	$\theta_{w,out}$ (°C)
Standard rating conditions	Outdoor air	7	6	87	30	35
	Exhaust air	20	12	38	40	45
	Outdoor air	7	6	87	40	45
Application rating conditions	Outdoor air	2	1	84	a	35
	Outdoor air	−7	−8	75	a	35
	Outdoor air	−15	—	—	a	35
	Outdoor air	2	1	84	b	45
	Outdoor air	−7	−8	75	b	45
	Outdoor air	−15	—	—	b	45
	Outdoor air	7	6	87	b	55
	Outdoor air	−7	−8	75	b	55

a,b: tests are conducted at the water flow rate determined in the test at the corresponding standard rating conditions for outdoor air ASHP

performance. These are air and water temperatures and flow rates, plus air humidity. The EN 14511 standard directly specifies three of these for each test point: air inlet temperature and humidity and water outlet temperature. The water flow rate to be used in tests is not specified directly, but determined during the “standard rating condition” tests. For these test points only, a water inlet temperature as well as an outlet temperature is specified. Prior to the start of the test, the ASHP is fed water at the given inlet temperature, and the flow rate is adjusted until the required outlet temperature is achieved. This flow rate is then used for the tests at the application rating conditions. The only factor influencing ASHP performance not specified by EN 14511 is air flow rate, which is left to the control of the ASHP unit’s inbuilt fan - as it would be in a real installation.

Each test involves operating the heat pump at full output and sampling the thermal output and power load at least every 30 seconds. If after 70 minutes the temperature difference between water inlet and outlet is within 2.5% of the initial value, the test is designated “steady state” and terminated. If there is greater than 2.5% change, this implies frosting of the evaporator is occurring. Tests are continued until either the heat pump completes 3 full defrost cycles, or 3 hours have elapsed. Power load and thermal output are averaged over the test period to obtain integrated performance figures.

3.2 System boundary and power load measurement

The consistent measurement of air-to-water ASHP's power load and thermal output is complicated by the fact that whilst most units include integral water circulation pumps, others do not. Additionally, where a circulation pump is included, the power load will depend to some extent on the resistance to flow of the test rig. This is unlikely to be the same from one test centre to another. Ensuring consistency across different sets of test results is therefore not straightforward.

EN 14511 addresses this by adjusting the power load measured in tests. The adjustment process is different depending on whether or not the circulation pump is integral to the unit.

For ASHP with an integral circulation pump, an amount P_{adjust} (eq. (3.1)) is excluded from the measured power load. P_{adjust} is based on the external static pressure drop Δp between ASHP outlet and inlet — it is an estimate of the proportion of the circulations pump's power load required to drive water through the test rig. Efficiency η is based on benchmark values.

$$P_{adjust} = \frac{\dot{(V)} \times \Delta p}{\eta} \tag{3.1}$$

In the case of ASHP without an integral circulation pump, an adjustment is *added* to the measured power load. The amount is again calculated by eq. (3.1), but this time Δp represents the internal static pressure drop of the ASHP unit. This addition is intended to relate to the power load required to drive water through the ASHP.

It is worth taking a moment to consider what proportion of the circulation pump power load is likely to remain in EN 14511 results. The remainder of this section presents an analysis carried out by the author using as an example a commercially available ASHP with 11.6 kW nominal thermal output and an integrated circulation pump.

The technical specifications for this unit [12, 31] include diagrams which allow the internal and external static pressure difference corresponding to given flow rates to be found. Assuming a flow rate of 0.56 (the rate determined during the ASHP's low temperature application EN 14511 tests) and with the circulation pump at its medium speed setting, these suggest an internal static pressure difference across the condenser of 2.9 kPa and a total external pressure difference across the circulation pump of 43 kPa.

If the efficiency of this unit's circulation pump is the same as the benchmark value assumed by EN 14511, then the adjustment process means that 93% of the circulation pump's power load of 121 W is excluded from EN 14511 results. If the reverse scenario is imagined - a hypothetical ASHP without an integral circulation pump, but with the same internal and external static pressure difference at this flow rate - then the adjustment process means that 7% of the external circulation pump's power load is added to the ASHP's measured total by the adjustment process.

ASHP units will of course have a range of internal static pressure differences, and the efficiency of circulation pumps can also vary. However for this example at least, the proportion of circulation pump power load included in EN 14511 results amounts to only 8.5 W - small relative to overall power consumption of the ASHP which ranges between 2.5 kW and 4 kW across the different test points.

ASHPs do not only draw power when in full operation - a number of ASHP components will also draw power at least part of the time the compressor is off. These may include the controls, a crank case heater, a tray heater and any freeze protection fitted. The crank case heater warms the compressor, to prevent refrigerant condensing and mixing with the oil, as this would cause problems at startup. It may be on at all times, or controlled according to temperature sensors. A tray heater ensures that the drainage pathway for condensation or water released during defrost cycles is not blocked by ice. Tray heaters should only be active at certain temperatures, for example below 4 °C. ASHPs designed for outdoor installation are also likely to include other protection measures to prevent heating system water freezing in the unit.

EN 14511 suggests that the power draw of the unit in standby and off modes is measured and listed as part of the results. This is intended to capture the power load of components which continue to draw power whilst the compressor is off. However the standard offers little information on how this is to be done, and as described above, some of these components may draw power only intermittently or below certain temperatures. Additionally few sources of EN 14511 test results seem to include the measurements. It would appear the test process could benefit from strengthening in this area.

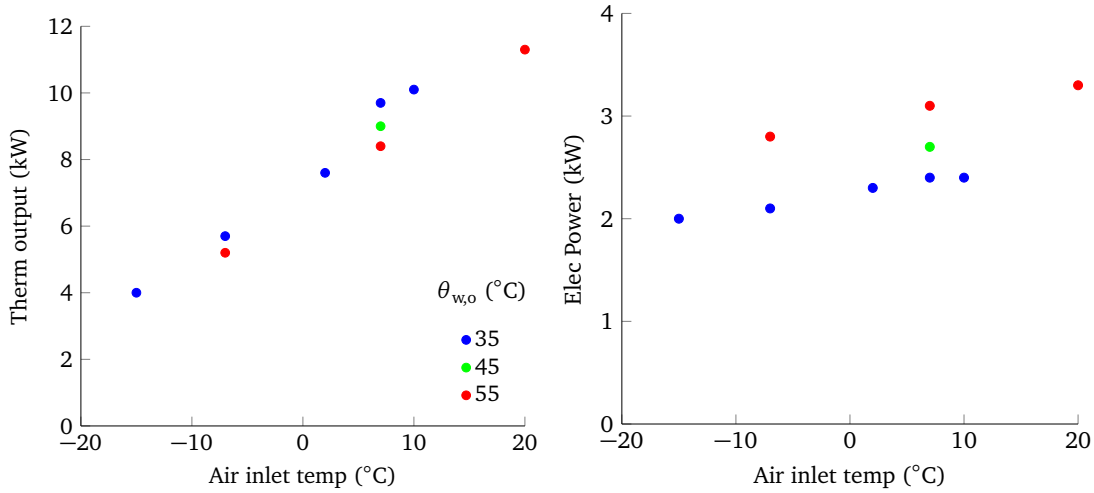

Figure 3.1: Example of EN 14511 test data from WPZ [1]

3.3 Examples of standard test data

A key source for EN 14511 data used in this work is the Wärmepumpen Testzentrum (WPZ) at the Interstaatliche Hochschule für Technik in Buchs, Switzerland (WPZ). Data for 45 different heat pump units was obtained from their publications [1]. Analysis of trends within this data set carried out by the author is presented in this section.

An example of thermal output and power load data for one heat pump tested by WPZ is given in fig. 3.1. Only a subset of the full number of test points are published, however it is shown in chapter 5 that this is generally still sufficient for the creation of some types of models.

Figure 3.2 compares the COP of the ASHP component currently included with standard ESP-r distribution (described further in section 4.2) with the COP of the 45 ASHP units tested by WPZ. The component parameters can be changed by the user to represent different ASHP, however for the purposes of this illustration the default parameters are used. The component takes air inlet and heating system water inlet temperatures as variables, whereas EN 14511 uses air inlet and water *outlet* temperature. The ESP-r component was recreated in MATLAB [32] code and run iteratively to obtain fixed outlet temperature curves which could be plotted on the same graph as EN 14511 data.

There is a considerable spread of performance across the WPZ ASHPs, underlining the need for a modelling method which can be readily tailored to different ASHPs. The ESP-r

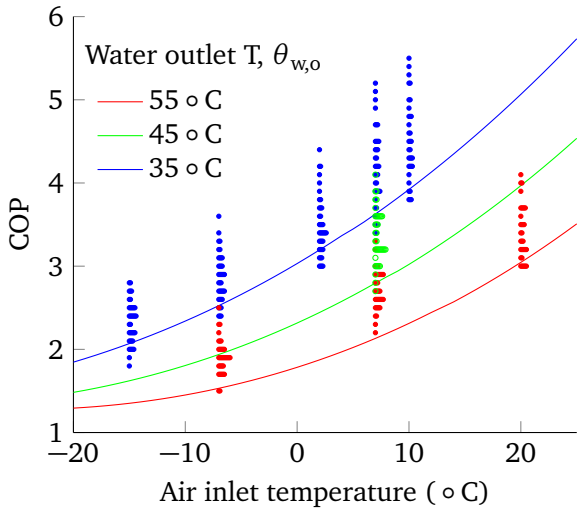

Figure 3.2: ESP-r ASHP component COP (represented by curves) compared to WPZ data (represented by dots)

component with default parameters sits below average in this range, indeed at the very lower limit of the range when water outlet temperature is 55 °C. This is partly due to the surprisingly large heat loss to the environment predicted by the default ESP-r component. For example the rate of heat loss at the air 7 °C, water 55 °C test point is 700 W[1]; without this COP at this point would be 2.38 rather than 2.13 as shown on the figure.

A final set of of graphs (fig. 3.3) were created which, for three different test points, plot the COP of the WPZ heat pumps against the year in which the ASHP was tested by WPZ (assumed to indicate when the ASHP was put into production). It would appear that any improvements in ASHP design over the eight years from 2005 to 2013 has been marginal - though the smaller number of heat pumps tested at each end of the time period makes strong conclusions difficult to draw. In these graphs the refrigerant used by each of the ASHPs is also identified. This suggest that ASHPs using R407C tend to perform better at higher compression ratios than R410A (right hand graph), though the advantage may be switched at lower compression ratios (left hand graph). ASHPs using R404A appear to typically perform less well across the range of points graphed.

[1]This heat loss is calculated on the basis the ASHP is an indoor unit - a reference temperature of 20 °C is used for its environment. Although the heat transfer is contained within the fabric of the building, it is counted as a loss because ESP-r does not add heat losses within a zone to the zone's energy balance equation - they merely disappear from simulations.

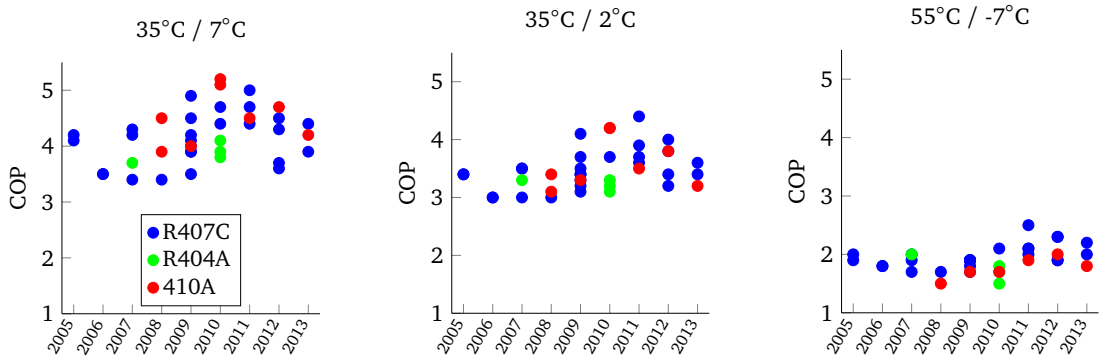

Figure 3.3: COP achieved by ASHPs in WPZ tests against year in which ASHP was tested

3.4 Chapter summary

Standard testing of heat pumps provides a consistent and relatively easily obtained source of data on ASHP performance. This chapter reviews the European Standard for the testing of heat pumps, EN 14511, in order to inform the development and discussion of modelling methods based upon it. The test process for air-to-water heat pumps is focussed on.

The test process involves placing the ASHP being tested in a climate-controlled room, and measuring thermal output and power load at a range of different test points. The key factors influencing ASHP steady state performance - air temperature and humidity, and water temperature and flow rate - are thus fixed at each test point. The only exception is air flow rate, which is left to the control of the ASHP unit's inbuilt fan. The test points are well spread in terms of air and water temperatures, though contain less variation with regard to humidity levels and water flow rates.

A key point is that the test process measures steady state, integrated performance: at each test point average thermal output and power load over the course of an extended period operating at maximum setting is recorded. No information is given as to the transient behaviour of the ASHP being tested. Furthermore, no information on the frequency or energy use of defrost cycles - or even whether any occurred - can be extracted from the results for a particular test point.

The standard's definition of where the system boundary lies with regard to the measurement of power loads was also explored. Only a proportion of the power draw of the circulation pump is included in the results, but this proportion appears likely to be insignifi-

cantly small.

Chapter 4

Approaches to ASHP modelling in dynamic simulation

This chapter reviews air source heat pump modelling methods in the literature. Their ability to represent the key ASHP performance characteristics discussed in chapter 2 is assessed; and their data needs are compared to the data available from standard testing (chapter 3). The grey box methodology emerges as the most suitable method for modelling ASHP performance in dynamic simulation tools using standard test data.

Methods of modelling ASHP in the literature broadly fall in to two categories: the black box approach, and component-based approach. As ever, the boundary between these categories is slightly blurred; a group of models of particular interest in this work fall somewhere in between the two. A third category is therefore useful; for this category the term grey box is used.

Component-based models explicitly model the refrigerant cycle. They consist of sub-models representing each of the main components of the refrigerant cycle. As in real systems, heat pump performance emerges as the net effect of the components' interactions. The sub-models are generally a mix of deterministic and empirically-derived equations, and have been used for detailed studies of ASHP behaviour and aspects of performance. Component-based models require many internal measurements and parameters not generally available for commercial heat pump units, and are therefore of limited relevance here. An exception

to this are “parameter estimation” based models, discussed in section 4.3.

Black box models are wholly empirical representations developed from externally-measured data. As the name suggests, the models can be developed with no knowledge of the internal parameters and physical processes which comprise the system. Methods from this category are therefore an attractive proposition for quickly modelling commercial ASHP using published test data. The resulting models tend to be quasi-steady state, and omit characteristics which in some situations could have a significant impact on model predictions.

In the grey box approach, the model structure is based upon some knowledge of the underlying system, but the form and parameters of equations underlying key performance characteristics are still empirically derived [33, 34]. Grey box models thereby blend elements of component-based and black box models.

4.1 Black box models

Black box models can be categorised as either look-up table models or equation fit models. The former use a look-up table to relate the values of a number of input variables to particular values of thermal output and power load, whereas the latter employs a mathematical expression. Sometimes COP is used in place of either output or power load.

4.1.1 Look-up table models

Look-up table models are the simplest form of model. Here the domain of possible operating conditions is divided into intervals. The examples identified use ambient air temperature, heating system flow temperature, and heating load to define the operating conditions; less important variables such as humidity are ignored. Each interval is associated with a particular value of heat pump maximum thermal output and power load, by reference to the results of performance tests (the intervals are often deliberately chosen so that a test point is at the centre of each). At any time the performance of the heat pump is assumed to be that of the interval in which the current operating conditions fall.

Look-up table models are steady state, and indeed are best suited to use within steady state calculation-based methods for estimating annual building energy use. Ignoring or

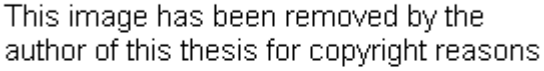

Figure 4.1: Illustration of EN 15316-4-2 method (from [35, p. 2065])

averaging the impact of dynamic effects (thermal mass and internal gains) in both the heating system and building means that the variables which define the operating conditions are then no longer independent: a particular ambient air temperature corresponds to a particular heat load and heating system flow temperature. The domain of possible operating conditions is reduced to 1 dimension, greatly reducing the volume of test data required to create the table. Climate data can also be sorted into bins or represented as a frequency plots , reducing the simulation process to a simple calculation.

Two examples of look-up table models are contained in European standards EN 15316-4-2:2008 *Heating systems in buildings — Method for calculation of system energy requirements and system efficiencies — Part 4-2: Space heating generation systems, heat pump systems* [36] and EN 14825:2013 *Air conditioners, liquid chilling packages and heat pumps, with electrically driven compressors, for space heating and cooling — Testing and rating at part load conditions and calculation of seasonal performance* [37]. These are both calculation-based methods for estimating seasonal COP of a heat pump installation.

EN 15316-4-2 is a general method that can be applied to any building and climate profile, and is intended for use perhaps during the design stage of a construction or refurbishment project. It is intended to work with only EN 14511 test data if necessary, though supplemental performance information can be supplied. In two validation cases the method's predictions were found to be within 6% of actual seasonal performance [35].

EN 14825 estimates the seasonal COP the heat pump would attain in a notional standard

building and climate. It is intended to provide a simpler and more realistic way of comparing one heat pump's performance to another's. It places greater importance on the part load performance of heat pumps than EN 15316-4-2, and indeed began life as a technical standard setting out a method for part load tests.

In both cases the look-up table heat pump model itself is relatively straightforward, and follows the principles already described. The advantages of the look-up table method are broad applicability and transparency. However clearly in omitting the dynamics of the ASHP and heating system some realism is lost. It is difficult to imagine a look-up table model being deployed in a dynamic building energy simulation tool, given the mismatch in approach. Never the less, look up table models face a couple of the same issues as other black box models, and it is worth reviewing how they deal with these issues.

One issue is the representation of part load operation. This is important because the thermal output of an ASHP increases as ambient temperature increases, whereas the heat load they supply will decrease. ASHPs therefore spend much of the year operating at part load. Variable output ASHPs have the capability to match a lower load by reducing the flow rate of refrigerant; however COP is likely to be slightly different to the COP of the heat pump operating at full output in the same conditions. Fixed output units must cycle on and off to match a lower load, potentially resulting in losses.

It is straightforward to conduct performance tests of the COP of variable output heat pumps at part load. EN 14825 requires part load testing of heat pumps to be conducted for use in the look up table model. EN 15316 states that part load test data should be used in the table where it is available.

Fixed output units are more problematic. Dynamic effects related to the thermal mass of the heat pump and heating system, and possibly pressure equalisation in the refrigerant cycle, can result in losses each time the ASHP stops and starts. Furthermore, controls and other components may still draw power when the compressor is not running (whilst also true of variable output ASHP, these will spend less time not running).

As a steady state modelling method, the best a look-up table can do is represent the time-averaged effect of these cyclic losses as degraded performance whenever the heat load of the building is less than the thermal output of the ASHP.

EN 15316-4-2 states that "for adequate system design, losses due to ON/OFF cycling

are small". It requires merely that the residual power load during the off cycle is taken into account. The same approach is prescribed by EN 14825 for fixed output heat pumps with *water-cooled* condensers.

A further interesting aspect of EN 15316-4-2 is that it outlines a method for adjusting heat pump performance test data so that estimates can be made for installations in which the heating system water mass flow rate is different to that which was used in performance tests. The method is referred to as the method of "fixed exergetic efficiency". The mass flow rate is related to the temperature difference $\Delta\theta_w$ between the water inlet and outlet temperatures by equation 4.1.

$$\Delta\theta_w = \frac{\Phi}{\dot{m}.c_{p,w}} \tag{4.1}$$

Equation 4.2 calculates COP at the new flow rate by applying a correction factor to COP obtained in tests (COP_{std}). This is based on the actual difference between water inlet and outlet temperature $\Delta\theta_{w,\Delta}$ and the temperature difference used in tests $\Delta\theta_{w,std}$.

$$COP_\Delta = COP_{std}\left[1 - \frac{\frac{\Delta\theta_{w,std} - \Delta\theta_{w,\Delta}}{2}}{\theta_w - \frac{\Delta\theta_{w,std}}{2} + \Delta\theta_{cond} - \left(\theta_{a,i} - \Delta\theta_{evap}\right)}\right] \tag{4.2}$$

In the above $\Delta\theta_{cond}$ is the average difference between water and refrigerant in the condenser, approximated as 4 °C. $\Delta\theta_{evap}$ is the average difference between air and refrigerant in the evaporator. The default value of $\Delta\theta_{evap}$ given by the standard is unexpectedly high at 15 °C.

In summary, the look-up table approach is a steady state modelling method and as such isn't fully compliant with the aims of this work. There are methods by which transient behaviour can to some extent be accounted for, but in general the approach would not sit well within a dynamic building modelling tool. Its main advantage is that, when paired with steady state, calculation-based building energy modelling, the modelling process is greatly simplified. Finally, EN 15316-4-2 contains an interesting method for adapting test data for the simulation of installations with different heating system water mass flow rates. As described in 2.2, water mass flow rate influences ASHP performance — the modelling method proposed in this work will also require to take account of this. The method presented here however is focused on adapting COP only, rather than thermal output and power load.

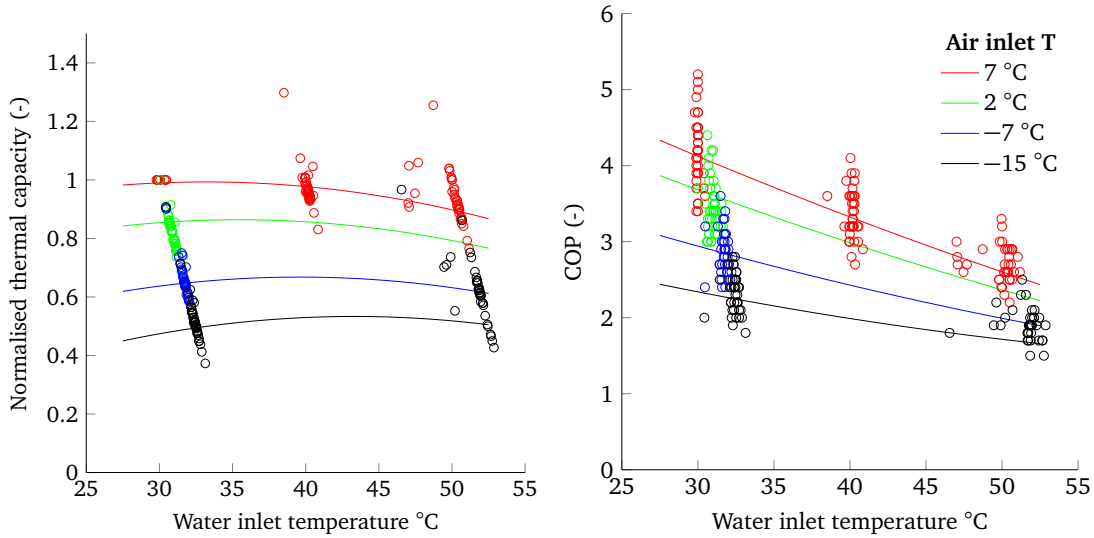

Figure 4.2: Baster et al equation-fitting process: the model curves were calibrated using test data for 30 different ASHP units, represented by dots in the figure.

4.1.2 Equation-fit models

A second approach to black box modelling is the equation-fit method. This involves using regression analysis of test data to generate equations which predict heat pump thermal output and power load based on operating conditions.

As with look-up table models, simplifications are often applied to reduce the number of variables - for example, humidity levels and mass flow rates used in tests are generally omitted from the regression analysis, leaving air temperature and heating system water flow temperature as predictors.

The basic method is most suited to producing steady state models. Defrost cycles and transient behaviour can't easily be encapsulated in a regression model. Some authors have therefore added separate algorithms to enable representation this behaviour, and these are discussed in the second half of this section.

An example of a steady state model produced using the basic method is described by Baster et al. [38][1]. In this study, a least squares fitting technique was used to obtain quadratic equations (4.3 and 4.4) for thermal output and COP from pre-2011 EN 14511 test data. A representation of "average" ASHP was desired, and so test data for 30 ASHP was combined

[1]This model is original work by the author of this thesis: however as it is heavily based on work already presented by the author for the award of a previous degree, it is merely reviewed as part of the literature

(hence the spread of test points in the figures). The inlet air and inlet water temperatures were chosen as the predictor variables. The ASHP model is not validated.

$$\Phi = a_0 + a_1\theta_{a,i} + a_2\theta_{w,i} + a_3\theta_{a,i}^2 + a_4\theta_{w,i}^2 + a_5\theta_{a,i}\theta_{w,i} \tag{4.3}$$

$$COP = b_0 + b_1\theta_{a,i} + b_2\theta_{w,i} + b_3\theta_{a,i}^2 + b_4\theta_{w,i}^2 + b_5\theta_{a,i}\theta_{w,i} \tag{4.4}$$

It was assumed that the ASHP could operate at part load with the same COP as during full load operation. No standby power consumption is included. The model included algorithms reflecting some common features of real heat pumps - such as a cut-out if water inlet temperature exceeded 55 °C, and a back up heater (assumed to be 100% efficient direct electric) which supplied additional heat if the heat demand exceeded ASHP output.

Section 3 described how the humidity levels stipulated in EN 14511 ensure that frosting occurs in some tests, and that the impact of frosting and defrost cycles is averaged over a number of cycles to obtain figures for thermal output, power load and COP. The data and models built from it such as this therefore represent integrated performance, and may only be valid at the humidity levels used in tests.

Jenkins et al. [39] describe a similar, steady state model. Though of an air-to-air heat pump rather than air-to-water, it is included here because of the unusual use of wet bulb rather than dry bulb ambient air temperature as a variable to predict thermal output and COP. Wet bulb temperature was likely to have been chosen because it is proportional to enthalpy - and the more internal energy the air has, the more that can be transferred as it passes through the evaporator at a given rate.

However this may cause problems in the region where frosting occurs. The use of wet bulb temperature means that, for example, the model predicts the same output and COP for a dry bulb temperature of 5 °C and 100% relative humidity as it does for 10 °C and 55% - in both cases the wet bulb temperature is 5 °C, and enthalpy is the same. However, many ASHPs will develop frost on the evaporator at the first of these points, and not at the second. Thermal output and COP at the first would therefore be much reduced from what the enthalpy would suggest.

Using wet bulb temperature in place of dry bulb may offer advantages for simulating climates where frosting is unlikely. However in climates such as that currently experienced

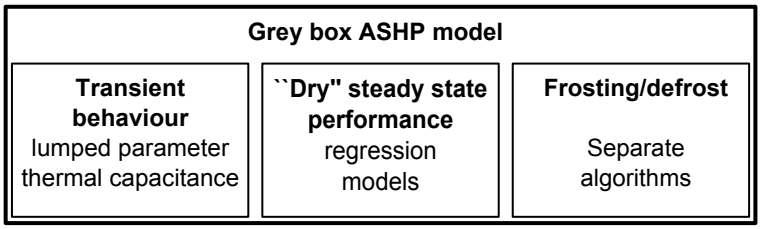

Figure 4.3: Composition of a grey box ASHP model

in the UK, evaporator frosting is common, and the use of wet bulb temperature offers no advantage over dry.

Of the two types of black box model, the equation fit approach would be well suited to use within dynamic building simulation tools. They would add little to computational complexity, and can readily be created from EN 14511 data. However the resulting models are quasi-steady state rather than dynamic, and may give misleading results in simulations in which (for example) frequent on-off cycling of the ASHP occurs.

4.2 Grey box models

A number of other studies make use of steady state equation-fit models as their basis, but include additional algorithms to represent transient behaviour and the impact of frosting. These are occasionally referred to as "grey box" models; aspects of the model structure reflect that of the physical system, but the core of the model makes use of empirical performance maps.

An example is Kelly and Cockroft [33], who described a model of an 8 kW fixed output air-water heat pump. A version of this model is part of the ESP-r standard distribution. The model's structure is depicted in fig. 4.3.

In common with Baster et al., the model is underpinned by equations for thermal output and COP, obtained from regression analysis of laboratory test data. However rather than taking ambient air and heating system water inlet temperatures as separate variables, a new variable Δ_θ was defined as the difference between the temperatures. The equations (4.5 and 4.6) are quadratics in this new variable.

$$\Phi_{ss} = a_0 + a_1\Delta_\theta + a_2\Delta_\theta^2 \tag{4.5}$$

$$COP = b_0 + b_1\Delta_\theta + b_2\Delta_\theta^2 \tag{4.6}$$

This choice of variable is suitable for ASHP whose performance is equally sensitive to changes in either ambient air temperature or water inlet temperature. However for some ASHPs (particularly those using scroll compressors - section 2.1), thermal output in particular is considerably more sensitive to ambient air temperature than it is to water inlet temperature. The ASHP depicted in figure 2.3 (section 2.2) is an example of this. Broader applicability can be assured by taking ambient air and water flow temperatures as separate variables.

In order to represent transient behaviour around startup, two thermal masses were associated with the heat pump model, one (A) representing the "thermal capacitance of the device on the refrigerant side of the condenser" and a second (B) representing the water side. The thermal masses are linked to the rest of the heating system model by eqs. 4.7 and 4.8. A brief description of the solution scheme employed by ESP-r is given in subsection 5.1.

$$M_A c_A \dot{\theta}_A = \Phi_{ss} - UA(\theta_A - \theta_{a,i}) - K_{AB}(\theta_A - \theta_B) \tag{4.7}$$

$$M_B c_B \dot{\theta}_B = K_{AB}(\theta_A - \theta_B) - \dot{m}_w c_{p,w}(\theta_B - \theta_{w,i}) \tag{4.8}$$

The values for the masses and specific heat capacities are found through a calibration process using high-resolution thermal output and power load data recorded during startup and shutdown of the heat pump. The masses therefore compensate not just for the impact of the heat pump's actual thermal capacitance on thermal output at start-up, but also for any measurable re-pressurisation effect.

As is apparent from equation 4.7, there is also a term representing heat loss to the environment. The value of *UA* was found through another calibration process, using data recorded during the period following shut down.

The calibration process for determining these parameters is based on a method created for IEA Annex 42 [34], as part of a project which developed a grey box modelling method for small scale cogeneration devices. These models actually involved two linked thermal masses, due to the underlying physics of some types of cogeneration device. The calibration process involves using an optimisation tool which runs multiple simulations of the model

whilst varying the values of the parameters until a satisfactory fit with measured data is obtained.

Kelly and Cockroft compared the predicted COP of the ASHP model at different air inlet temperatures to "snapshot" measurements taken from a real installation. Whilst there was a degree of spread in the measured values, they found that the mode of measurements at a particular air temperature tended to correspond closely with the model's prediction. It was conclude that the model is suitably realistic to, for example, draw conclusions regarding the relative performance of the ASHP compared to a gas boiler over a year.

The ASHP component included with the general ESP-r distribution [10] is based on the model Kelly and Cockroft describe, albeit with a few differences. Firstly, it is represented as a single thermal mass, rather than two distinct thermal masses as described in the paper.

Secondly the ESP-r component is based on regression models for power load and COP, rather than thermal output and COP. The same quadratic form and combined variable Δ_θ as before can be used for COP, or alternatively an equation based on Carnot's theory or a cubic in $\theta_{a,i}$ can be selected. The power load regression model takes $\theta_{a,i}$ and $\theta_{w,i}$ as distinct variables and has the form of an equation of a flat plane.

Finally the ESP-r component also contains optional algorithms to represent the impact of defrost cycles on thermal output. If in a simulation the temperature falls below 5 °C, the defrost mode is triggered. In this mode the thermal output is set to zero whilst the power load remains as it would be in normal operation. After a period t_{df} the component returns to normal operation. Defrost duration t_{df} is calculated by an empirically-derived relation based on relative humidity Φ (eq. 4.9). Assuming the temperature remains below 5 °C, subsequent defrost periods are triggered after 40 minutes of normal operation. No adjustment is made to performance between defrost periods to account for any deterioration due to frost growth.

$$t_{df} = a_0 + a_1\Phi \tag{4.9}$$

The parameters of the ESP-r component are all accessible to the user, with the intention that the component should be able to represent a wide range of ASHP types. However the availability of data in the form required to inform the model is an issue.

Another ASHP grey box modelling method is set out by Afjei and Wetter [40]. The method uses the basic structure introduced at the start of this section (fig. 4.3): its core consists of regression models of "dry" (unfrosted) performance; another part modifies the regression model outputs to account for transient behaviour at start-up and shutdown; and a third part applies another adjustment to account for the impact of frosting. Each part of the model takes a different approach to that used by the corresponding part of Kelly and Cockroft's, however.

The regression models describe thermal output and power load, and are based on the variables ambient air temperature and heating system water outlet temperature. They are of quadratic form, with an interaction term.

$$\Phi_{ss} = a_0 + a_1\theta_{a,i} + a_2\theta_{a,i}^2 + a_3\theta_{w,o} + a_4\theta_{w,o}^2 + a_5\theta_{a,i}\theta_{w,o} \tag{4.10}$$

$$P = b_0 + b_1\theta_{a,i} + b_2\theta_{a,i}^2 + b_3\theta_{w,o} + b_4\theta_{w,o}^2 + b_5\theta_{a,i}\theta_{w,o} \tag{4.11}$$

In order to account for the temporary reduction in output following start up, the steady state thermal output determined by the regression model is multiplied by an additional term which increases from 0 to 1 as the time since start up t_{on} increases (in the following, Φ_d denotes heat delivered by the ASHP).

$$\Phi_d = \Phi_{ss}\left(1 - e^{-\frac{t_f + t_{on}}{\tau_{on}}}\right) \tag{4.12}$$

A similar expression accounts for residual heat after the ASHP shuts off:

$$\Phi_d = \Phi_{ss} e^{-\frac{t_f + t_{off}}{\tau_{off}}} \tag{4.13}$$

The variables t_{on} and t_{off} represent time since startup and shutdown respectively, and τ_{on} and τ_{off} are the time constants of the transients. The variable t_f accounts for occasions when the ASHP restarts before fully cooling, or switches off before reaching its full steady state output, and its value is set by an additional algorithm.

This approach to representing transient behaviour will provide a similar gradual increase in thermal output at start up and decrease at shutdown as Kelly and Cockroft, but unlike

Kelly and Cockroft there is no means to represent transient behaviour related to a change in operating conditions - for example a change in water inlet temperature when an ASHP providing both space heating and DHW switches between the two modes. Also, implicit in the approach is an assumption that water continues to flow after the ASHP compressor stops running, but this may not be the case for all heat pump systems. It is therefore less flexible.

Afjei and Wetter's approach to account for the impact of frost and defrost cycles in essence involves applying an adjustment to dry thermal output, to represent the time-averaged reduction in output due to frost growth and periodic defrost cycles. It is assumed that power load is unaffected by frost and defrost cycles - or at least that any effects cancel out. It is also assumed that the size of the adjustment depends only on air temperature. Whilst the method has interesting similarities with the EN 14511 test method, the neglection of the influence of humidity on frost growth and defrost cycles is a limiting factor.

In implementation the method becomes rather complicated. The adjustment is actually applied to COP, rather than thermal output directly. At each timestep an unadjusted COP (COP_d) is calculated:

$$COP_d = \frac{\Phi_d}{P} \tag{4.14}$$

To this an adjustment term $\Delta COP(\theta_{a,i})$ is applied:

$$COP = COP_d(1 - \Delta COP) \tag{4.15}$$

Finally thermal output is recalculated using the new adjusted COP, leaving power load unchanged.

COP correction factor $\Delta COP(\theta_{a,i})$ is obtained by fitting a curve to test data. Afjei and Wetter assume that the adjustment term depends only on air temperature, and that its shape is a superposition of a straight line and a Gauss curve .

$$\Delta COP = c_0 + c_1\theta_{a,i} + c_2 \exp^{-\frac{(\theta_{a,i}-c_3)^2}{c_4}} \tag{4.16}$$

for $\theta_{a,i} > -\frac{c_0}{c_1}$. If $\theta_{a,i} \leq -\frac{c_0}{c_1}$, the first two terms are omitted.

As with Kelly and Cockroft, the key conclusion is that the data requirements of this

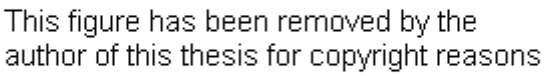

Figure 4.4: COP frosting adjustment term ΔCOP (from [40, p. 5])

modelling method could not be supplied by standard test results. Neither the algorithm representing the integrated impact of defrost periods nor the exponential curves representing transient behaviour could be calibrated. The implication is that the aim of this project to produce a dynamic model from standard test data need to be revisited.

Aspects of the method are none the less interesting. It is intended the model can be used to represent a wide range of ASHP units. The core of the method — the quadratic regression models — would be satisfactory for this aim. The modification of thermal output with an exponential curve to represent transient behaviour at startup and shutdown will result in curves of the same shape as the method used by Kelly and Cockroft, but is more limited. It also requires fewer variables to be determined, though the implementation in computer code is more complex.

The approach to modelling the impact of frosting is pragmatic. For simulations where the focus is on performance over extended periods rather than minute-to-minute behaviour, the approach of modelling "integrated" performance rather than explicitly representing defrost cycles seems likely to be sufficient. However for a study looking into ASHP or heating system control for example, more detail may be required. The particular implementation of this approach — specifically the assumption that the integrated impact of frosting depends only on air temperature and not also on humidity level — contradicts the studies of frosting discussed in section 2.4.

A final equation-fit model of interest is that described by Petinot [14]. The method is a

development of the ESP-r ASHP component, which in turn resulted from Kelly and Cockroft's work. The focus of the work is on representing a particular ASHP model (one using CO_2 as the refrigerant). Petinot drew on extensive data from real installations in order to give a more detailed representation of defrost cycles. The model is also implemented in ESP-r.

The ASHP unit represented displayed unusual behaviour in that thermal output of the ASHP appeared to be constant at 9 kW. This allowed Petinot to base his model around a single regression model, representing COP. The COP equation takes air temperature and return water temperature as the variables, and is of quadratic form with a interaction term. Petinot reasoned that the ASHP must have some output control capability, and an internal control system which was set to maintain a constant output. This seems valid: a thermal output which does not change with air inlet temperature is inconsistent with the underlying physics, and furthermore, such a control approach is likely to decrease cycling thereby improving performance.

Like the ESP-r ASHP component, Petinot's model has thermal mass to represent the transient behaviour of the ASHP. Additionally Petinot found that the ASHP studied did not instantly reach full power at start up. The component was modified so that at start up power load increases linearly to reach full power at the end of first minute.

The main development to the ESP-r component is an extension of the frosting code. Like Kelly and Cockroft, Petinot found that the ASHP initiated defrosts before performance degradation was significant, hence all that was required was to model defrost periods.

Rather than a fixed time period between defrosts, it was found that the period varied - as did the length of the defrost periods themselves. A regression model for the time between defrosts t_{ff} was obtained. This takes average air temperature and relative humidity since the preceding defrost period as the basic variables. It has an R^2 value of 0.79, suggesting that additional variables may also play a role.

$$t_{ff} = a_0 + a_1\theta_{a,i} + a_2 RH + a_3\theta_{a,i}^2 + a_4 RH^2 + a_5\theta_{a,i} \times RH + a_6\theta_{a,i}^3 \tag{4.17}$$

The component assumes that power load during defrost is constant at 2.4 kW. This contrasts with the ESP-r component, in which it was assumed that power load during defrost is the same as it would be in normal operation in the current conditions. Both methods are

likely to be approximations.

The defrost model is completed by a final regression model linking the energy required to defrost E_{df} to air temperature and the time between defrosts (eq. 4.18). This combined with the assumption of a fixed power load during defrost gives the duration of defrost periods. A further algorithm is used to estimate the natural defrosting which occurs whilst the heat pump is off and air temperature is above 0 °C.

$$E_{df} = a_0 + a_1\theta_{a,i} + a_2 t_{ff} + a_3\theta_{a,i}^2 + a_4 t_{ff}^2 + a_5 t_{ff}^3 \tag{4.18}$$

Whilst the overall precision of the defrost algorithms is not perfect, the method certainly offers greater detail than those described by other authors. However it was made possible by access to extensive field measurements, beyond the scope of a standard performance testing process such as EN 14511.

Petinot used ESP-r to simulate an actual house fitted with an example of the modelled ASHP, and compared the model's predictions to measured data over one day in March and another in July. Simplifications inherent in the building and plant models as a whole mean that the match between predicted and measured values for heat delivered was relatively poor, with discrepancies of approximately 20% for the March day and up to 40% for July. COP values on the other hand were very close for the March day, with a difference of 1% for March, and behaviour with regard to defrost cycle frequency and duration was similar. The model over-estimated COP over the July day by 22%. Again, some of the discrepancy at least is due to the overall building and plant model: the return flow to the heat pump is lower in the model than in the real system, and Petinot identifies the representation of stratification in the hot water tank as a key factor. It is difficult to draw firm conclusions regarding the ASHP model's validity given the differences between building and plant model and the actual system, but the COP results for the March day show some merit.

In general, the grey box approach appears well suited to dynamic building simulation tools - of course, the examples identified in this review were designed precisely for this purpose. Grey box models such as these can be integrated within such building simulation software relatively easily, as they don't require bespoke solvers or greatly extended simulation times. They have the potential to encapsulate the major characteristics of heat

pump behaviour, though some of the smaller details may be lost. The close matches between predicted and measured COP found by Petinot and Kelly and Cockroft suggest the equation fit approach has strong merit.

However, a further key conclusion from this review is that existing grey box methods require input data beyond what is currently provided by standard performance testing of heat pumps. A new grey box method is required in order to make best use of the data produced by test procedures such as EN 14511.

A particular difficulty with current models is the representation of the impact of frosting on performance. They all start by modelling peak ("unfrosted") performance, and then modifying that to account for frosting. EN 14511 in contrast records only integrated performance - that is, performance averaged across a number of frosting/defrost cycles. Peak performance is not given in results (although frustratingly, it would be obtainable with access to the raw data recorded by test centres).

Kelly and Cockroft and Petinot explicitly modelled defrost cycles. This approach perhaps has the highest data requirements, well beyond the scope of standard performance testing. Afjei and Wetter instead applies a variable adjustment term to modelled peak performance, which represents the averaged impact of defrost cycles over a whole cycle. Afjei and Wetter's method therefore predicts integrated performance, the same as is recorded by EN 14511 testing - however it still requires information on peak performance first in order to get there, and thus can't be informed by EN 14511 test results.

All three grey box methods reviewed also make adjustments to the output of peak performance regression models to account for transient behaviour. Different approaches are taken, but all assume that the modeller has access to high resolution data on ASHP performance in order to calibrate relevant parameters. Again, such data is not part of EN 14511 testing.

4.3 Component-based models

Component-based (or refrigerant cycle) models of heat pumps consist of sub-models representing each of the major components of the refrigerant cycle. Model outputs - thermal output, power load - arise from the interactions between the component sub-models. The

component sub-models are generally a mix of deterministic and empirical equations, and the overall model can be quasi-steady state or dynamic.

The overall aim of this work is to identify a method of modelling ASHP performance which can be informed by standard performance test data. Component-based modelling methods in general are of limited relevance to this aim: they are almost all based on internal measurements and parameters not found in standard test data. An exception are parameter estimation methods such as those described by Jin and Spitler [6, 41]. Here typical performance test data is used in a multi-variable optimisation technique to arrive at estimated values of internal parameters. The methods described are for brine-to-water heat pumps, but none the less merit discussion here.

Alongside the works of Jin and Spitler, a large variety of component-based vapour compression cycle models can be found in the literature. A brief outline is included in this section to give context. The reviews of Bendapudi and Braun [42] and Afjei and Dott [43] proved valuable.

Jin and Spitler's method is amongst the simplest type of component based models. These are quasi-steady state models in which the heat exchangers are modelled as single cohesive units using the ϵ-NTU method, and the compressor model is based on the rate of work for isentropic compression adjusted by efficiency and standing loss factors. Refrigerant mass flow rate is calculated from compressor speed, geometry and refrigerant states at entry and discharge. The approach used avoids the need to explicitly model the expansion valve. An iterative solution method is employed. A large number of assumptions and simplifications are required, for example that refrigerant mass flow rate is uniform throughout the cycle; UA for each the heat exchangers can be approximated by a fixed value; the degree of superheating at the evaporator outlet is fixed; and that there is zero leakage across the compressor.

The main feature of this model is that the relatively small number of parameters it requires (8) can be estimated from EN 14511-type performance test using an iterative process. The authors intend for the model to be used in building energy simulation tools and it has been implemented in EnergyPlus [44]. In validation tests of the reciprocating compressor version [6], the authors found relative errors were significantly lower than for an equation fit model of the same GSHP. A later study [45] compared the scroll compressor version [41] with an equation fit model and found the latter provided a slightly better

fit to test data, but the parameter estimation model still offers more confidence when extrapolating.

Jin and Spitler note some caution is required in the interpretation of the model. The values of internal parameters estimated by the optimisation process are the values which result in the closest match between the model's global outputs and performance test data. However as the model contains many assumptions and simplifications, these values are not necessarily the same as would be obtained were the parameters to be directly measured. Similarly, though the model involves internal variables such as evaporating and condensing pressures, it is not designed to accurately predict these quantities. This would cause difficulties were an attempt to be made to adapt the method to ASHP and add a model of frost growth, as this would depend on evaporator temperature.

There are a number of variations on this type of quasi-steady state model in the literature. These assume parameters can be found either from identifying individual components and obtaining their technical specifications, or through direct measurement. This enables greater freedom in terms of the complexity of the model. Bertsch and Groll [46] considered the approach sufficiently detailed to make a comparison of the steady state performance of various configurations of two-stage ASHP. In order to study the performance of variable output compressors, Madani et al. [47] extended the approach by splitting the heat exchangers into sections according to process the refrigerant is undergoing: the two-phase and superheating portions of the evaporator are treated separately, and the condenser is split into de-superheating, condensation and subcooling sections. This is because the heat transfer coefficient between the refrigerant and the inner surface of the heat exchanger is different depending on the state of the refrigerant. Performance maps of UA for each exchanger (which varies as operating conditions change) for each section are derived from testing.

The component-based approach lends itself well to the creation of dynamic models of the vapour compression cycle. Recent examples are described by Uhlmann and Bertsch [13] and Lepore et al. [48]. These take account not only of thermal storage within the heat exchangers, but also mass storage effects. Like Madani et al., these studies split the heat exchangers into sections, but the boundaries between sections are explicitly allowed to move to reflect variation in refrigerant distribution as operating conditions change.

Other approaches are described in Bendapudi and Braun's review. These methods enable detailed representation of the transient behaviour of ASHP, and potentially the inclusion of explicit frost growth and defrost models. As with the steady-state component based methods, these assume parameters can be found either from identifying individual components and obtaining their technical specifications, or through direct measurement. Therefore their relevance to this work is limited.

Broadly then, component based models are not well matched to the aims of this work because their data needs are too great. The parameter estimation technique can reduce these data needs to something close to that provided by EN 14511 testing. However the resulting models appear to have little benefit over the much simpler equation fit black box approach - at least where the conditions being simulated are close to the range covered by EN 14511 testing.

Furthermore they have only been applied to ground source heat pumps so far, which do not require defrost mechanisms. Whilst it may be possible to add representation of defrost cycles to the method, much more extensive data than provided by EN 14511 would be required. Alternatively defrost cycles occur could be ignored, and EN 14511 data merely "plugged-in" to the current model - but then the model structure would be one step removed from what is happening in reality, and the theoretical basis for the parameter estimation process would be undermined.

4.3.1 Frost growth models

Chapter 2 discussed evaporator frost growth and defrosting, and the associated impact on performance. It is highly desirable for ASHP models to represent this behaviour. In addition to the methods described as part of the grey box methods in 4.2, a number of frost-focussed or stand-alone frost-growth models have been described in the literature. These are of varying complexity, though all require to some extent measurements and parameters not included in standard testing. A brief description is included here for completeness

Vocale et al. [19] present a highly simplified, first-principles approach which can be applied to ASHP with reverse cycle defrost mechanisms. The method is to a large extent compatible with the type of data produced by standard tests. However evaporator surface temperature and air mass flow rate, quantities not measured in EN 14511 tests, are required.

When conditions are such that evaporator surface temperate is less than −3 °C, a rate of frost formation is calculated based on the rate of energy extracted from the airstream, along with its mass flow rate and psychrometric properties. The energy extracted is assumed to be given by subtracting the ASHP's power load from it thermal output. These quantities can of course be obtained from equation fit models based on defrost-free performance data.

The method employs an pair of equations empirically derived by ASHRAE which relate air enthalpy to dry bulb temperature and moisture content, and moisture content to relative humidity and saturation and total pressures. The rate of energy extracted from the airstream is subtracted from the enthalpy of incoming air to obtain the enthalpy of air exiting the evaporator. The article explains that this can be used with the ASHRAE equations to determine whether the air has been cooled past the dew point, and if so, the difference in moisture content between entering and leaving states. This is combined with the mass flow rate of air to give a rate of frost formation.

Once the rate of frost formation is obtained, it is used to calculate the energy required to melt the frost formed over one hour. This involves a sensible heat transfer to raise the frost layer (assumed to be at evaporator surface temperature) to melting point, plus the latent heat required for melting. As the latter will dominate, a precise value for evaporator surface temperature is unlikely to be necessary. The time required to defrost is calculated by considering the cooling capacity of the ASHP. Data on cooling capacity would be available for ASHP with a cooling function.

The method is limited in applicability to ASHP with reverse cycle defrost mechanisms for which cooling performance data and air flow rate information is available. There are some aspects which give rise to concerns about the accuracy of results. Chief amongst these is the assumption that no heat is wasted during defrost cycles, though this could be improved by the application of an efficiency factor to defrost energy. Further potential oversimplifications are the assumptions that there is no degree of supersaturation as the air passes through the evaporator; that all condensation occurs on the surface of the evaporator rather than in the airstream; and that all water condensed freezes without running off.

A number of much more detailed frost growth models exist, for example those described by da Silva et al. [49] and Getu and Bansal [50]. All require a considerably larger number of parameters (mostly related to evaporator geometry and fan power curves), and are therefore

beyond the scope of this work. The models mix deterministic and empirical relations, and make use of the Lewis Analogy of heat and mass transfer.

Of note are the group of articles emerging from the Swiss Government-funded LOREF project [16, 23]. The models of frosting and defrost advanced not only appear to be the most comprehensive, but the driver for their development was an assessment of the natural defrosting approach. This is where, rather than stopping the fan and supplying heat to the evaporator using the compressor, the compressor is stopped and the fan allowed to run. Where air temperature is 2 °C and relative humidity levels 85%, the heat delivered to the frost layer is comparable to conventional defrost methods (largely due to the latent heat flow provided by moisture from the air condensing on the frost layer). The power load however is considerably lower. These conditions neatly coincide with the region in which frost growth is fastest. To what extent the method has been adopted by manufacturers is unknown.

4.4 Chapter summary

Of the methods of modelling ASHP reviewed in this chapter, the grey box method emerges as the best aligned with the aims of this work - though there are issues with its application when using only EN 14511 data.

The equation-fit black box approach is easy to implement within dynamic simulation tools, and can be informed using EN 14511 data. However the resulting models are quasi-steady state rather than dynamic, and may give misleading results in (for example) simulations which involve frequent on-off cycling of the ASHP - such as sizing studies.

Most component-based models require extensive knowledge of the internals of the heat pump being modelled, and must therefore be ruled out for this work. Parameter estimation methods could potentially be informed by EN 14511 data, however model structures described in the literature relate to ground source heat pumps hence do not need to take account of the impact of defrost cycles. In terms of predicting ground source heat pump performance, they have an advantage over equation fit models when extrapolating to operating conditions outside of the range of test data. However it is doubtful that this advantage would fully apply to ASHP models without alterations to take account of the

impact of defrost cycles. This would require more data than is available from EN 14511 tests. Further the model requires to be solved iteratively every timestep, adding to simulation times.

Like equation fit methods, grey box models can be readily integrated within dynamic building simulation tools, and do not (necessarily) require bespoke solvers. They are widely applicable to different ASHP designs. A key advantage over both black box and parameter estimation models is that they are dynamic rather than quasi-steady state. They are able to represent large scale transient behaviour, such as that around start up and shut down, and can explicitly or implicitly account for the impact of frosting on performance.

A disadvantage in terms of the aims of this work is that those grey box models reviewed all require additional data to that provided by EN 14511 tests. They require peak (unfrosted) performance data, as well as the integrated performance data provided by EN 14511. They also make use of high resolution data on performance immediately following start up and shut down. The grey box approach is therefore adapted in the next chapter, to produce a modelling method that has lower data requirements whilst retaining some of the advantages of existing models over those produced by other approaches.

4.5 Problem Statement, research questions and methodology

The core problem which emerges from this review is that existing air source heat pump modelling methods which can be informed by standard test data have weaknesses: they are quasi-steady state, omitting important transient aspects of ASHP performance. More comprehensive, dynamic modelling methods exist, but these require additional input data.

This work was initiated with the aim of establishing whether an improved modelling method can be developed - one which remains capable of being informed using only standard performance test data, but which includes transient aspects of performance and is better suited to dynamic simulation tools.

The theory and literature review sections of this work have shown that this aim cannot be fully achieved. Dynamic approaches to ASHP modelling require information with which to inform their representation of transient behaviour which is not provided by the standard test process.

A dynamic method is proposed which can be partially calibrated using standard test data, but which would also require a minimal amount of additional data to calibrate parameters governing transient behaviour. The potential value of this approach is examined, and it is used to identify the extensions that would be required to standard testing to aid the production of dynamic models.

The methodology used is as follows:

- A new, grey box method is proposed;
- The method is developed and tested;
- A process for others to make use of the method is described;
- Validation tests are applied, including some investigation of the importance of transient behaviour to the prediction of performance over extended periods;
- Conclusions are presented, and limitations and future enhancements and uses are discussed; and
- Recommendations are made for extensions to standard testing to better support dynamic modelling.

Chapter 5

Proposed ASHP modelling method

This chapter sets out the ASHP modelling method developed during the project. The overall aim was that this method should be suitable for use in building modelling tools, and should require only performance test data provided by European Standard EN 14511 for calibration. The review of theory and literature presented in previous chapters found that this aim could not be fulfilled: Standard test data isn't sufficient to calibrate parameters related to transient behaviour, and no established relationships capable of bridging the gap were found.

Rather than resort to a steady state model, a dynamic method is proposed in this chapter which would require some data additional to that produced standard testing. This is based on the grey box approaches described in the previous chapter, and is tailored as far as possible to the data produced by standard testing.

The method as set out is therefore incomplete – a process to calibrate transient parameters is identified, but could not be applied and tested here due to insufficient data. In subsequent chapters, the value of the approach is tested using transient parameter based on those determined in a different author's study, the importance of transient behaviour to long term performance is explored, and extensions to standard testing which would support dynamic modelling proposed.

This chapter first justifies the choice of approach, then introduces the modelling environment ESP-r. The method is then set out. Key aspects of it are tested by application to 41 sets of EN 14511 test data. A calculation method used to adapt models produced under the method to different heating system water flow rates is also introduced.

It has been said that the art of mathematical modelling lies in the selection of appropriate assumptions and simplifications. Chapter 2 showed that the behaviour of ASHPs, like that of many real systems, is complex. A mathematical representation will necessarily make various simplifications.

This chapter sets out a method for the production of dynamic ASHP models based as far as possible on standard performance test data provided by European Standard EN 14511 — the revised aim of this work. EN 1411 data already contains a large amount of simplification. The approach is to identify the best that can be done with the limited information available, and to assess the impact of the enforced simplifications on the realism of model produced under the method.

The grey box approach to modelling ASHP emerged from chapter 4 as the most appropriate for this purpose. Grey box models are based on the equation fit approach, but include algorithms which represent the impact of frosting on performance, and empirical factors intended to characterise the heat pump's transient response to major changes in operating conditions. These methods are well suited to building energy simulation tools: they do not require bespoke and computationally intensive solution methods like component-based methods. Whilst they inevitably simplify some aspects of the behaviour of ASHP and their internal controls it seems likely that they have merit across a wide range of types of simulation studies.

There are however issues with replicating the grey box methods reviewed in section 4.1.2 here.

The first is that an explicit representation of defrost cycles is not possible. Kelly and Cockroft and Petinot show that this is possible within the grey box approach, but EN 14511 data does not provide the necessary information such as frequency and duration of defrost cycles. An alternative approach is offered by Afjei and Wetter and Jenkins et al., in which

the averaged impact of periodic defrost cycles is included in the model. This tallies well with the EN 41511 test process, and is used here in an form similar to that employed by Jenkins et al. (the averaged impact of frosting is included implicitly in the regression models at the core of the method; there is no separate algorithm). This has repercussions for the use of the model: its minute-to-minute outputs are no longer representative of an actual heat pump's in conditions where evaporator frosting occurs. The impact of this on the use and interpretation of simulation outputs is discussed in subsequent chapters.

A second difficulty is that it was not possible to overcome the lack of information on transient behaviour in EN 14511 test results. The transient parameters of the modelling method cannot be calibrated directly using the test data. No established relationship between test data and dynamic behaviour was identified which could be used.

A dynamic modelling method is seen as important in order to retain realism across as wide a range of simulations as possible. In particular it is important for simulations where short cycling is a possibility – e.g. in sizing studies or control system development.

It was therefore decided to relax the aims for the work to enable a dynamic model to be produced: rather than strictly limiting calibration data to only that provided by EN 14511 testing, it is assumed a small amount of non-standard data will be available for the calibration of a lumped parameter thermal mass term.

An added difficulty is that no data of this type was available during this project. Values for the transient parameters from the study by Kelly and Cockroft are used instead. In section 6.2, the proposed modelling method is applied to an ASHP with a nominal thermal output larger than that of the ASHP modelled by Kelly and Cockroft. As a stop gap measure, values of the transient parameters for this larger ASHP are estimated by scaling by nominal thermal output. No evidence is put forward to support this process, and it is not seen as part of the proposed method. The best way for this gap to be overcome is for the EN 14511 test process to be extended. This is discussed further in chapter 7. Sensitivity of model's predictions to the value of transient parameters is also explored in the following chapter.

In summary, a partial modelling approach is put forward in this chapter, representing the closest it is possible to come to the project aims. This approach is a new grey box method adapted to suit EN 14511 test data, and with an implicit rather than explicit treatment of defrost cycles. The structure of such a model is depicted in fig. 5.1; this contrasts for

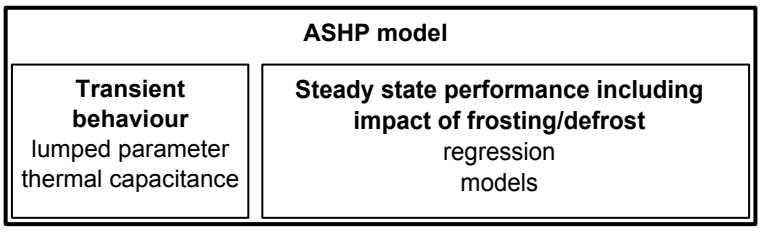

Figure 5.1: Structure of proposed ASHP model

example with fig. 4.3 which shows the structure of Kelly and Cockroft's model.

The chapter proceeds by briefly introducing the ESP-r building modelling software, which is used to demonstrate the modelling method, before the different aspects of the method are set out in detail.

5.1 Plant modelling in ESP-r

Though the modelling method proposed in this work could be used within a variety of building energy simulation tools, it is illustrated here through implementation in ESP-r. The methodology employed by ESP-r to simulate plant systems is briefly introduced, in order that aspects of the modelling method may be better understood. Further information on ESP-r can be found in the work of Clarke [51] and Hensen [52].

ESP-r employs a control volume approach to building modelling. In this method, plant systems are represented as a series of control volumes. A volume may represent a length of pipe or ducting, a radiator, an ASHP - or a small portion of one of these components if a more detailed representation of the component's behaviour is required. It is assumed each control volume can be treated as being homogeneous, and thus can be approximated as a node described by a single temperature, pressure etc. A plant system thereby becomes a network of interconnected nodes.

During simulations mass and energy balance equations for each node are established every timestep. These form notional matrices representing the the whole plant system. One matrix relates to the energy; each row contains an energy balance for a particular node. A second relates to mass flow, and has rows comprising of mass balances for each node (if a two-phase fluid flow is present, there may be a third matrix containing mass balances for the other phase). Once the matrices are established, a simultaneous solution technique is

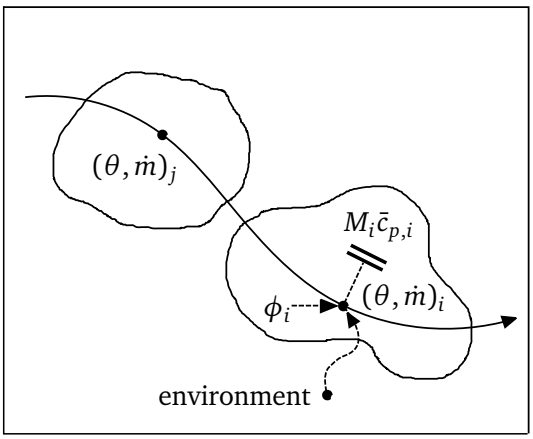

Figure 5.2: ESP-r nodal method

applied to each in turn. In the case that there is a strong thermodynamic coupling between balance equations in different matrices, an iterative process can be activated to ensure that overall the solution is truly simultaneous.

A portion of a simple plant network model, consisting of two control volumes, is depicted in figure 5.2. Node i receives a fluid flow from node j; heat is generated internally at rate Φ_i; and heat is lost to the environment at rate $U_i A_i(\theta_i - \theta_\infty)$. The general form of the energy balance equation for node i is:

$$\bar{c}_i M_i \frac{\partial \theta_i}{\partial t} = \dot{m}_{w,j} c_{pw}(\theta_i - \theta_j) + UA(\theta_e - \theta_i) + \Phi_i \tag{5.1}$$

By convention only flows received by a node are included. Outward flow is accounted for in the balance equations for the subsequent node. The mass balance equation in this example is elementary, $\dot{m}_{w,i} = \dot{m}_{w,j}$: the fluid flow is single phase and there is no leakage or diversion.

Each plant component in ESP-r has a piece of associated code, known as a "coefficient generator", which calculates at each timestep the parameters for the nodes comprising the component. The coefficient generator is essentially the component model translated into code: in the case of the ASHP component, it is here that the regression models for thermal output and power load and the associated algorithms as described in section 4.1.2 are implemented, along with code which represents internal controls and establishes additional parameters such as the heat loss coefficient and mass flow rate.

The process used by ESP-r software to solve the mass and energy balance matrices is based on a weighted summation of the implicit and explicit finite difference formulations of the balance equations for each node. The energy summation for node i (in which α is the weighting factor) is:

$$\begin{aligned}
&[\alpha(-\dot{m}_{w,j}c_{pw} - U_iA_i) - \frac{\bar{c}_iM_i}{\Delta t}]\theta_i + \alpha\dot{m}_{w,j}c_{pw}\theta_j = \\
&\quad [(1-\alpha)(-\dot{m}^*_{w,j}c_{pw} - U^*_iA^*_i) - \frac{\bar{c}_iM_i}{\Delta t}]\theta^*_i + \\
&\quad (1-\alpha)\dot{m}^*_{w,j}c_{pw}\theta^*_j - \alpha U_iA_i\theta_e - (1-\alpha)U^*_iA^*_i\theta^*_e - \alpha\Phi_i - (1-\alpha)\Phi^*_i
\end{aligned} \tag{5.2}$$

The summation has been rearranged so that quantities relating to the current (known) timestep - denoted by * - are on the right hand side.

At each timestep of a simulation, the coefficients of the summation equations are established by the relevant coefficient generator. In the solution process the “future time row” temperatures (the temperatures for the subsequent timestep, which appear on the left hand side of the summation equations) for all nodes are determined simultaneously. For the ASHP component (or any ESP-r plant component which involves heat generation), this means the water inlet and outlet temperatures for the forthcoming timestep are calculated simultaneously, based on a thermal output which is assumed to be known in advance. Note that Φ_i as well as Φ^*_i appears on the “known” side of equation 5.2.

This raises a common issue when modelling heat pumps, which is that the thermal output and flow temperatures are interdependent. The thermal output for the future timerow can’t be calculated until the future timerow temperatures are known - and vice versa.

Authors such as Afjei and Wetter overcame this by employing an iterative solution technique. As mentioned above, an iterative process can be activated within ESP-r during the solution of the plant matrices. The nodal temperatures determined during each iteration are temporarily stored, and can be accessed by the ASHP component’s coefficient generator code. Kelly and Cockroft made use of this in their ASHP model; the regression equations for power load and COP use the most recently stored value for water inlet temperature. This is the value from the penultimate iteration before a satisfactory solution is achieved. Close examination of simulations shows that when the system is evolving slowly this is

indistinguishable from the final future timerow temperature. When it is evolving quickly (mainly, directly after the ASHP starts up) there can be a discrepancy of a few °C, however this persists only for two to three timesteps and is unlikely to affect the model outputs unduly.

As stated, Kelly and Cockroft made use of the inlet water temperature estimate to calculate thermal output. EN 14511 tests, however, treat outlet temperature as the primary quantity of interest. A result of ESP-r's combination of simultaneous and iterative solution methods is that estimates of both water inlet and outlet temperature are available prior to the final solution of each timestep. Though it is less intuitive, the proposed modelling method can therefore easily make use of water outlet rather than inlet temperature.

5.2 Regression models of steady state performance including impact of frosting/defrost

This section outlines the creation of regression models representing steady state ASHP performance. These represent the core of the grey box ASHP modelling method set out in this chapter, and comprise the first of the two model components in the visualisation in fig. 5.1. The second component, which modifies the output of the steady state regression models to represent transient behaviour, is described in the following section alongside remaining aspects such as internal controls and parasitic power loads.

Two regression models are employed within the model, one to calculate a value for steady state thermal output for each timestep, and another to calculate power load. Two regression models are required as ASHPs' thermal output and power load vary independently as operating conditions change. As noted in the literature review, some authors have substituted a regression model of COP for either the thermal output or power load regression model. So long as two of thermal output, power load and COP are represented by separate regression models the accuracy and generality of the heat pump model is not compromised. The choice here of thermal output and power load reflects an assumption that these are generally the main outputs of interest when modelling ASHP performance.

$$\Phi_{ss} = a_0 + a_1\theta_{w,o} + a_2\theta_{a,i} + a_3\theta_{w,o}\theta_{a,i} + a_4\theta_{w,o}^2 + a_5\theta_{a,i}^2 \tag{5.3}$$

$$P_{ss} = b_0 + b_1\theta_{w,o} + b_2\theta_{a,i} + b_3\theta_{w,o}\theta_{a,i} + b_4\theta_{w,o}^2 + b_5\theta_{a,i}^2 \tag{5.4}$$

In common with several of the models in the literature, the input variables are restricted to ambient air and water outlet temperature. The reasons for the use of these variables will be discussed first, then the choice of equation form is considered.

Outlet rather than inlet water temperature was chosen here because only outlet temperature is specified in (most) EN 14511 tests. Though it appears straightforward to calculate the inlet water temperature for each test point using equation 5.5, this is based on a false assumption that heat pump thermal output is remains steady throughout tests. It is of course an average value which may include periods of zero or negative output when the heat pump is in defrost. For test points subject to frosting, the actual inlet temperature will for the most part be less than that given by equation 5.5.

$$\theta_{w,i} = \theta_{w,o} - \frac{\Phi_{ss}}{\dot{m}_w c_{p,w}} \tag{5.5}$$

Although the choice of ambient air and water outlet (or inlet) temperature is common to most ASHP modelling method reviewed in the previous chapter, chapter 2 described how humidity, water and air flow rate also have an effect on ASHP performance. Due to the limited nature of EN 14511 test points, it is not possible to include these as variables in regression analysis.

In the case of air mass flow rate, this omission is not seen as problematic. Air flow rate in EN 14511 tests is left to the control of the unit, and not recorded. Assuming for a given ASHP model that the rate is likely to be more or less unaffected by the characteristics of a particular installation, there would be little merit in incorporating it as a variable in any case.

Water mass flow rate in contrast is dependent on the characteristics of a particular installation. As discussed in section 2.2, changes in water flow rate can in theory affect

performance by changing the rate of heat transfer in the condenser, with the result that a given water outlet temperature then corresponds to a different condensing pressure. Ideally therefore, the proposed ASHP modelling method would include mass flow rate as a variable.

Unhelpfully from a modeller's perspective, although EN 14511 specifies different water flow rates for different tests, the flow rate used is tied to the water output temperature of the test (chapter 3). This means that water flow rate can't be included as a variable in the thermal output and power load regression models, as regression analysis cannot separate the impact of water flow rate from the more significant impact of water outlet temperature.

To test the impact of flow rate on simulation results, a calculation process has been devised (section 5.5) which takes actual EN 14511 performance test data and predicts how different it would be if a single, user-specified water mass flow rate had been used across all the tests. Applying this process prior to undertaking the regression analysis of the proposed modelling method results in a model whose predictions are tailored to a specific, constant water mass flow rate. Tests described in the following chapter compared the results of pairs of simulations, one using a model adjusted to a particular flow rate and another using a model based on unadjusted EN 14511 data. For the ASHP modelled, across the flow rate operating range specified by the manufacturer, the difference in performance between the pairs of models was never more than a few percent.

A further factor which affects ASHP performance but is not included as a variable in the modelling method is humidity. The humidity level experienced by an ASHP will vary constantly, and it may have a significant influence on performance through influencing the frequency and duration of defrost cycles. This issue is distinct from the fact that defrost cycles are not explicitly represented in the modelling method, as mentioned in this chapter's introduction. EN 14511 tests are designed such that defrost cycles occur and their averaged impact on performance at the conditions specified in testing is included. However the issue is similar to that of water flow rate - the humidity levels specified for tests are tied to air temperature, and it is impossible for regression analysis to separate the impact of humidity from that of air temperature, therefore humidity is not included. Both issues are discussed further in subsequent chapters.

The quadratic form of the regression models is a compromise: it has been found to be complex enough to give a good fit to test data, but not so complex that models become

Table 5.1: Regression model parameters for figures 5.3 and 5.4

	Quadratic		4th Order	
	Φ_{ss}	P	Φ_{ss}	P
a_0 (constant)	11.61	0.7682	451.6	−292.4
a_1 ($\theta_{w,o}$)	−0.07190	0.03999	−41.96	26.15
a_2 ($\theta_{a,i}$)	0.2992	−0.005914	0.3293	−0.02080
a_3 ($\theta_{w,o} \times \theta_{a,i}$)	-1.816×10^{-3}	8.165×10^{-5}	-2.089×10^{-3}	4.061×10^{-4}
a_4 ($\theta^2_{w,o}$)	3.088×10^{-4}	2.823×10^{-4}	1.481	−0.8652
a_5 ($\theta^2_{a,i}$)	-5.564×10^{-4}	-1.459×10^{-4}	1.574×10^{-3}	-9.583×10^{-5}
a_6 ($\theta^3_{w,o}$)	0	0	−0.02300	0.01266
a_7 ($\theta^3_{a,i}$)	0	0	-6.366×10^{-5}	-5.229×10^{-6}
a_8 ($\theta^4_{w,o}$)	0	0	1.325×10^{-4}	-6.893×10^{-5}
a_9 ($\theta^4_{a,i}$)	0	0	-4.605×10^{-6}	6.501×10^{-8}
R^2	0.991	0.997	0.994	0.999

unstable. Though one might expect that an equation of higher order in $\theta_{a,i}$ might better represent the dip in performance due to frosting around 0 °C, the benefit was found to be limited. The fourth order model shown in fig. 5.4 shows little inflexion at this point, and indeed there is little difference to a quadratic model of the same ASHP (fig. 5.3, parameters for both given in table 5.1). Additionally attempts to implement even third order models in ESP-r were found to lead to instability. In terms of the regression analysis method itself, the conventional least-squares fitting process has been found adequate.

The data [12] provided by the manufacturer of this unit includes additional test points to those specified by EN 14511 (indicated by crosses on the figure). These additional points were excluded from the fitting process. In the case of the quadratic model, the fit to data is good if not perfect, particularly when the water output temperature is 35 °C. The R^2 value[1] for the thermal output regression model is 0.991, and for the power load regression model is 0.997. The model tends to overestimate thermal output when air inlet temperature is 2 °C, and underestimate at 7 °C. The reason is that the upper boundary of the frosting region lies between these two points. The greatest relative error in the thermal output regression model is 5.2% (water 35 °C, air 7 °C), and the greatest in the power model is 1.6% (water 55 °C, air 7 °C). The 4th order model only improves on these metrics by 0.2 to 0.3% - not enough to justify the added complexity.

The approach described has also been applied to EN 14511 data for 41 different ASHPs,

[1] Calculated using all data points, not just those included in EN 14511.

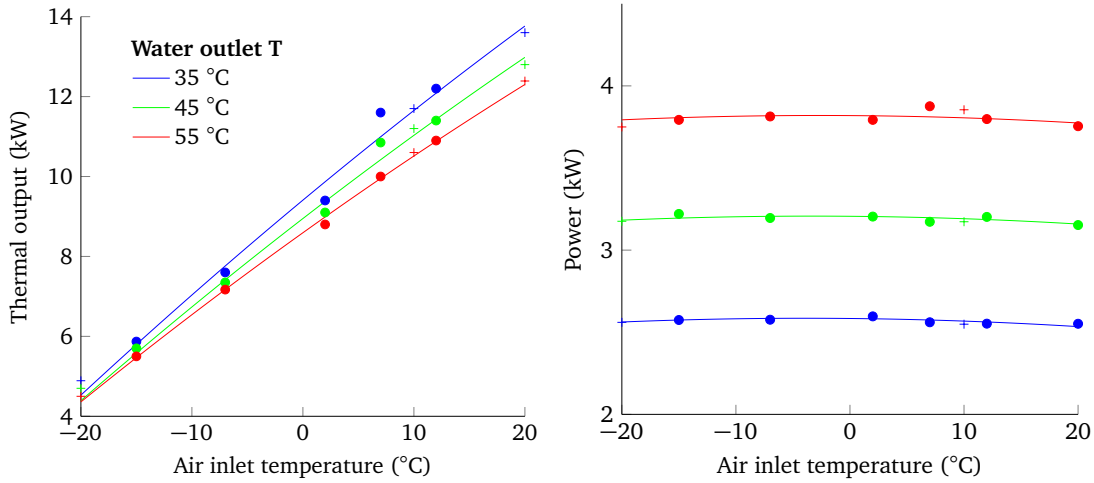

Figure 5.3: Example of application of proposed method to test data [12], quadratic equation form. Curves represent model, dots represent test points ("+" is a non-EN14511 test point included by manufacturer)

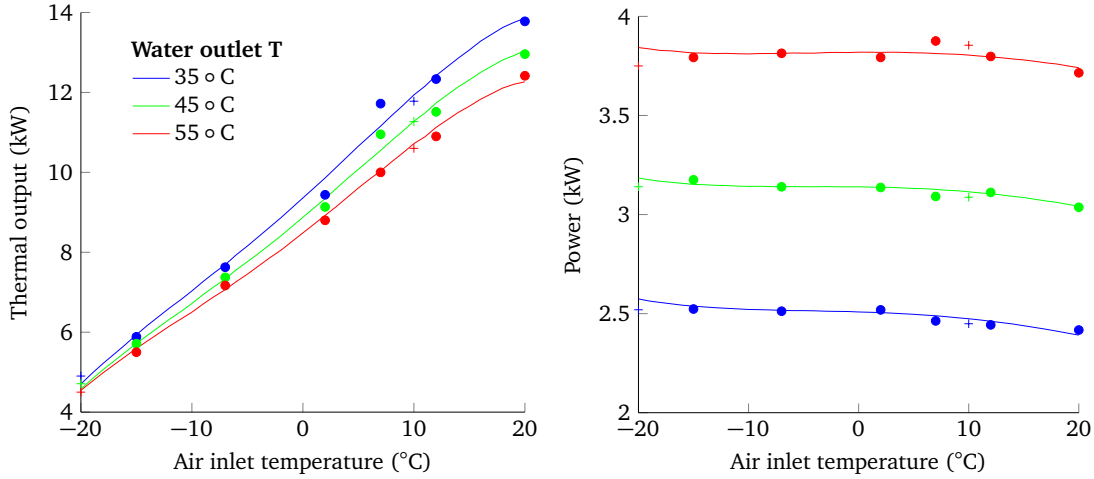

Figure 5.4: Example of application of proposed method to test data [12], showing little benefit from 4th order equation form

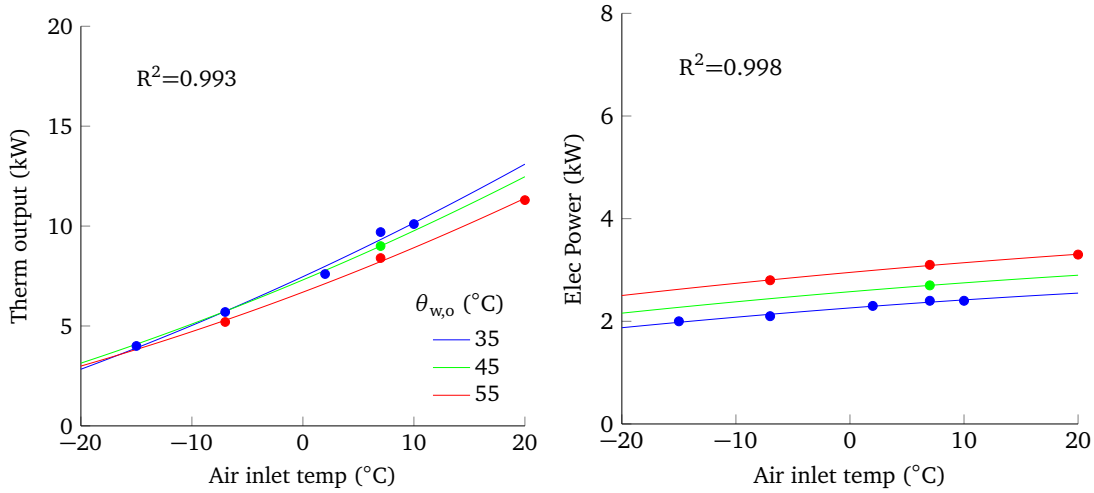

Figure 5.5: Application of method to WPZ ASHP 102 (parameters given inappendix A)

obtained from a Swiss independent test centre [1]. Graphs of the fit achieved in each case are given in appendix A. It should be noted that these results sets do not include the full number of test points. None the less, for the most part a good fit is achieved — in 24 of the cases, both the thermal output and power load regression models have R^2 values of at least 0.98. In total, regression model fit was found to be satisfactory in 25 of the 41 cases. Fit in seven of the cases was judged to be unsatisfactory, and the remaining nine were judged to be usable with caution. It should be noted that most data sets had only 8 or 9 data points - typically 18 would be expected.Further information on the grading criteria used is given in appendix A.

An example appears in fig. 5.5. Although a good fit to the few data points that there are, it is difficult to be certain that actual performance is well reflected in areas without data points - for example, the area with water temperature around 45 °C and an air temperature of less than 0 °C.

Whilst missing data points were the key to failures, ASHP with unsatisfatory fits had some common features which may contribute. Firstly, all seven had strongly reduced performance at the test point with air temperature 2 °C, suggesting inefficient or poorly controlled defrost mechanisms. Three further features made it more likely fit would be unsatisfactory, though there was not a clear causal link: a ‘split’ rather than monoblock construction type; the use of R410A as a refrigerant; and output control. Whilst it seems logical that output control would reduce predictability, in all except one case there was no visible sign of the capability

being used.

A number of guidelines emerge from the examination of these regression models. Firstly, a visual check of any model created is a wise precaution. However those with an R^2 value greater than 0.98 are very likely to be satisfactory. Where only a subset of EN 14511 test points are available:

- To determine the coefficients of the quadratic equation form recommended here, a minimum of 6 data points are required.
- If there are fewer, it may be possible to use a linear equation form instead.
- A least two of the data points within a set should have a different water outlet temperature to the others. Where this isn't the case, failure to achieve a satisfactory fit is likely.

5.3 Proposed model structure and approach to representing transient behaviour

The previous section described the first component of the proposed ASHP modelling method - the regression models representing steady state performance. This section completes the presentation of the modelling method by describing the second component, which modifies the output of the regression models to account for transient behaviour. It also describes in more detail the model structure, along with other important aspects such as the representation of internal controls and parasitic power loads.

The ASHP model is based around the following energy balance equation. The reader may notice the form of this equation is identical to the general ESP-r nodal energy balance equation (5.1) stated in the previous section.

$$\bar{c}M\frac{\partial\theta_{w,o}}{\partial t} = \dot{m}_w c_{p,w}(\theta_{w,o} - \theta_{w,i}) + UA(\theta_e - \theta_{w,o}) + \Phi \tag{5.6}$$

The first two terms on the right hand side represent actual heat output to the heating system and heat loss to the environment respectively. When the ASHP compressor is on,

$\Phi = \Phi_{ss}$, the output of a regression model of steady state thermal output, based on EN 14511 data.

Transient behaviour is accounted for by the inclusion of a lumped parameter thermal mass term (in conjunction with the environmental heat loss term). This mirrors the approach of Kelly and Cockroft and [14] (section 4.2), and is justified by analysis of start up data in section 2.3 which suggested thermal inertia is far more significant to start up performance than re-pressurisation effects.

This approach to representing transient behaviour requires three parameters: ASHP mass-weighted average heat capacity $\bar{c}$, mass M and heat loss parameter UA. Care should be taken in interpreting these parameters: for example, M is not the actual mass which would be be determined by weighing the ASHP, it is merely the value which in calibration enables the closest match between model output and calibration data. All three are simply calibration parameters, rather than physically measurable actual quantities.

UA is used a little differently to the other two transient parameters in that it changes value: it has fixed value UA_{off} whilst the ASHP compressor is off, but is set to zero whilst it is on. This is because heat loss to the environment whilst the compressor is running is effectively accounted for in Φ_{ss}. The regression model is based on the measured output of an ASHP unit during standard tests. Heat loss to the environment was occurring in these tests just as it would be in normal operation, and therefore were UA not set to zero when the ASHP is on heat loss would be double-counted.

Kelly and Cockroft were able to derive values for $\bar{c}$, M and UA_{off} using measurements carried out on a real ASHP unit during startup and shutdown. Such detailed data is not available under EN 14511 tests, which only record average performance over extended time periods at full load.

This currently represents a gap in the modelling method. Chapter 7 discusses how the EN 14511 test method could be expanded, so that it would provide the type of data required to calibrate the transient parameters. A calibration process is also outlined.

Calibration data of the sort used by Kelly and Cockroft was not available during this project. The value for the transient parameters that they determined during their study were, however. The testing of the proposed modelling method in the following chapter makes use of these values.

Two models are created using the proposed method in this chapter. The first is of the same ASHP that Kelly and Cockroft modelled. Kelly and Cockroft's transient parameter values are used directly in this model. The second model is of an ASHP with a larger nominal[2] thermal output. The transient parameter values are modified for use in this version. This is done based on the untested assumption that $\bar{c}$ is the same for all ASHP units, and that M and UA_{off} for all ASHP are directly proportional to nominal thermal output. This means that the value of $\bar{c}$ determined by Kelly and Cockroft is used for all ASHP modelled under the method; and that the values of M and UA_{off} to be used are calculated by scaling the values found by Kelly and Cockroft. The ASHP unit modelled by Kelly and Cockroft had a nominal thermal output of 8 kW. If, for example, the proposed method was being applied to an ASHP with a nominal thermal output of 16 kW, the value of $\bar{c}$ would remain the same - but the values of M and UA_{off} would be multiplied by two. This scaling process is a stop gap measure, and is not seen as part of the proposed modelling method.

The proposed method effectively incorporates a very simple circulation pump model, which assumes a fixed water mass flow rate $\dot{m}_{cp}$ and power load P_{cp}. Analysis of the EN 14511 test process in section 3.2 revealed that the large majority of circulation pump power is effectively excluded from the electrical power measured in tests, and therefore P_{cp} is added to the output of power load regression model. In use, the values of $\dot{m}_{cp}$ and power load P_{cp} can be set by the modeller to suit the particular system being modelled. This approach does not preclude the modelling of ASHP units which require an external circulation pump - rather than including a specific circulation pump component in the plant system model, its parameters would just be entered in the ASHP component model.

The reader may recall from section 3.2 that a number of components continue to draw power even when the ASHP is not generating heat. The ability to assign a constant parasitic power load P_{par} within the model, active only when the compressor is not running, is provided for (when it is running, these components' power loads are already accounted for in the power load regression model). This is consistent with EN 14511, which requires only a single measurement of parasitic power load. It is worth noting that in a real ASHP, this power load may not actually be constant, as some of the relevant components are may

[2] that is, thermal output determined at the EN 14511 standard rating condition test point for low temperature applications. This has an air temperature of 7 °C and a water outlet temperature of 35 °C.

only be active intermittently or within certain temperature ranges. EN 14511's provisions for parasitic load measurement don't appear to take account of this and could usefully be clarified.

The provisions for controls included in the implementation of the modelling method in ESP-r are intended to be sufficient to model a wide range of fixed output ASHP. Though information on a particular ASHP's precise internal controls is unlikely to be available, it is difficult to imagine any control approach radically different to that outlined below being used in fixed output heat pump units.

First, the model requires an external on/off control signal. In the simulations reported in this work, this is generated by the standard ESP-r room thermostat component. This control loop does not form part of the modelling method and can be set by model users.

When this external signal is on, both the ASHP model's circulation pump sub-model its own internal control are activated. The internal control loop - a key part of the modelling method - switches the compressor on and off to maintain the ASHP inlet water flow temperature at a user-selectable set point (within a deadband, also user-selectable).

The model contains code representing the effect of weather compensation: this is taken from the model described by Kelly and Cockroft [33], and adjusts the inlet water temperature set point based on external air temperature. To simplify analysis however, the adjustment is set to zero in the simulations reported in this work.

The aspects of the model presented in this section - the approach to representing transient behaviour and the process for estimating relevant parameters; the circulation and parasitic power submodels; and the ASHP internal controls - complete the description of the proposed modelling method. The following section breifly describes implementation and demonstration of the modelling method in ESP-r, after which the calculation method used to assess the sensitivity of ASHP performance to heating system water flow rate is presented.

5.4 Implementation of the method in ESP-r

The modelling method is implemented in ESP-r, in order that it could be tested. A "proof of concept" approach was taken to the implementation; this focusses on functionality rather than usability aspects such as the user interface. Changes have been restricted to the

"coefficient generator" portion of the code referred to in section 5.1, and the code for the existing ASHP component, which was the outcome of Kelly and Cockroft's work, was used as a starting point. The new code is included in appendix B.

The implementation approach taken means that some variables had to be hard-wired in the model code rather than being accessible via the user interface, and elements of the existing component such as its options for representing defrost cycles are rendered unusable as they should not be applied in this model. Multiple installations of the ESP-r software have to be used in order to retain access to the original ASHP model. However it would be entirely possible with a number of further code changes to have the new ASHP model as a user selectable option alongside the existing model.

The production of models using the proposed method would have three main steps - the second of these is currently a gap in the method:

- Regression models for thermal capacity and power load are derived according to the process in 5.2.
- Transient parameters are derived. The lack of suitable data means that a process for this is not tested in this work. Validation work in the following chapter relies on values determined in the study by Kelly and Cockroft.
- Finally set points and other parameters can be chosen as appropriate for the system being modelled.

5.5 Adjusting EN 14511 data to the required water mass flow rate

The flow rate of water through a ASHP's condenser can influence its thermal output and power load. This is why test standard EN 14511 is careful to specify a process for determining the flow rate to be used in a particular test.

During development of the proposed ASHP modelling method, it was found it was not possible to include water flow rate as a variable: the rate used in EN 14511 tests is tied to the water output temperature of the test, and its influence can't be disentangled.

This section sets out a process for investigating the level of uncertainty introduced by using ASHP models calibrated at particular water flow rates in simulations with different flow rates.

5.5.1 Motivation

Chapter 2 established that the thermal output and power load of a given heat pump depends on the condensing and evaporating temperatures of the refrigerant cycle. In steady state operating conditions these temperatures settle at equilibrium values such that the rate of heat transfer at the heat pump condenser is balanced by the heat transfer at the evaporator plus the heat added by the compressor motor. A change in operating conditions would disrupt the balance of heat transfer rates. This drives changes in the condensing and evaporating temperatures until a new equilibrium is reached, with a new thermal output and power load.

"Operating conditions" in the above means the flow rate and temperature of air moving through the evaporator, and the flow rate and temperature of water moving through the condenser. Changes in any of these four quantities will change heat transfer rates and alter thermal output and power load.

The proposed modelling method uses only two quantities as predictor variables, air inlet temperature and water outlet temperature. Whilst it is argued earlier in this chapter that the omission of air flow rate is unimportant (it is completely under the control of the heat pump during tests and will be the same wherever the heat pump is installed), the omission of water flow rate is more problematic.

Water flow rate is not under the control of the ASHP during tests – it is set to values dictated by the test method. In real installations, water flow rate will be heavily influenced by the characteristics of the connected heat distribution system, and could easily be different to the flow rates used in tests.

It is therefore important to ask, how much difference would water flow rate variations make to model predictions? Consider a model calibrated using EN 14511 data in which tests at 55 °C water output temperature were run with a water flow rate of 0.3 litres per second. This is used to in simulations where the mass flow rate is 0.6 litres per second. How much uncertainty would this introduce into predictions?

This could be answered by comparing the predictions to those of a model calibrated with data from tests which were run at the simulation flow rate of 0.6 litres per second. Such an analysis is carried out in the following chapter.

Data from tests at water flow rates different to those specified by the EN 14511 method were not available. The required data are instead created by a calculation method which uses a simple heat exchanger model and the theoretical principles from chapter 2 which were summarised above.

5.5.2 Calculation method

The aim of this calculation process is to adjust a set of EN 14511 test points so that it is as if the tests were carried out at a different flow rate. A method for adjusting the thermal output and power load results was not found: instead an adjusted water output temperature for each test point is obtained.

The process draws on two key principles described in 2. The first is that evaporating and condensing temperature are the real determiners of a heat pump's thermal output and power load. The second is that changes in these temperatures are driven by change in the rates of the heat transfer across the evaporator and condenser.

Consider an ASHP in the process of undergoing an EN 14511 test, in operation at a particular test point. The above principles suggest that if the flow rate and temperature of water passing through the condenser are simultaneously changed by carefully calculated amounts *such that the rate of heat transfer across the condenser stays the same*, then the heat output and power load of the ASHP will be unaffected.

Figure 5.6 is an illustration of refrigerant and water temperatures as they pass through the condenser in opposite directions. The solid lines indicate the flow and temperature conditions stipulated by the test process. The dotted lines indicate a new water mass flow rate and temperature which achieves the same rate of heat transfer, and thus refrigerant condensing temperature is unaltered.

The calculation process proposed uses the data for one EN 14511 test point (alongside one additional piece of information) to calibrate a simple model of the heat transfer process in an ASHP's condenser. Mass flow rate is a variable in this model. Once the model is calibrated, the mass flow rate variable can be changed whilst holding the rate of heat transfer constant

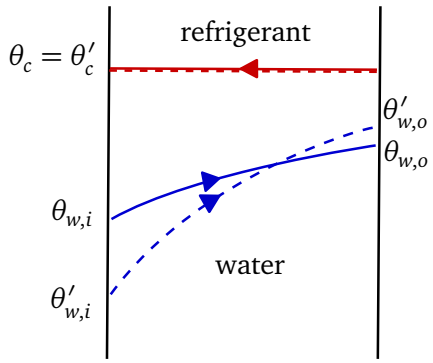

Figure 5.6: Temperatures in the condenser under different water flow rates

and the required corresponding change in water outlet temperature calculated.

The model used to represent the heat transfer in the condenser is the effectiveness-NTU method. This is a standard method of modelling heat exchanger processes, and can be applied to situations where one fluid is undergoing a phase change.

The effectiveness-NTU method describes the heat transfer across a heat exchanger as a fraction ϵ of the maximum possible heat transfer.

$$\epsilon = \frac{\Phi}{\Phi_{max}} = \frac{1 - e^{-NTU(1-R)}}{1 - Re^{-NTU(1-R)}} \tag{5.7}$$

$$R = \frac{\dot{c}_{min}}{\dot{c}_{max}} \tag{5.8}$$

$$NTU = \frac{UA_c}{\dot{c}_{min}} \tag{5.9}$$

$$\Phi_{max} = \dot{c}_w \left(\theta_c - \theta_{w,in}\right) \tag{5.10}$$

In the above, θ_c denotes the temperature of the condensing refrigerant, and specific heat rate $\dot{c}$ is the product of specific heat and mass flow rate for each of the two fluids passing through the heat exchanger. The larger of the two values is given the suffix max. In this case, as the refrigerant is undergoing a phase change, its $\dot{c}$ is very large in comparison to that of the water flow and their ratio R is approximately zero. This enables eq. (5.7) to be simplified to the following:

$$\epsilon = \frac{\Phi}{\Phi_{max}} = 1 - e^{-NTU} \tag{5.11}$$

The method proceeds by first estimating UA_c - the heat transfer coefficient across the condenser. This is done by combining equations 5.9 and 5.10 into 5.11, and solving for UA_c:

$$UA_c = -\dot{c}_w ln\left(1 - \frac{\Phi}{\dot{c}_w\left(\theta_c - \theta_{w,i}\right)}\right) \tag{5.12}$$

Inserting values for the variables on the right hand side gives a value for UA_c. Any of the EN 14511 test points from the set to which the process is being applied will provide the required values (for all but one of the variables). Implicit in the method is the assumption that UA_c is constant across the range of water and (and refrigerant) mass flow rates encountered. In reality flow effects will mean this is not strictly the case, therefore it is helpful if the test point chosen is close to the centre of the range of operating points covered by tests.

The value of one required variable is not included in EN 14511 test results: condensing temperature θ_c. Where this method is applied in section 6.2, an estimate is made based on data from the study by Uhlmann and Bertsch [53]. As part of this study two ASHP were operated in conditions close to the EN 14511 test point with $\theta_{w,o}$ of 45 °C and $\theta_{a,i}$ of 2 °C. Under these conditions, θ_c in each ASHP was on average 9 °C greater than the water inlet temperature. Thus, in order to estimate AU_c for the ASHP modelled in section 6.2, it was assumed that at the test point with $\theta_{w,o}$ of 45 °C and $\theta_{a,i}$ of 2 °C, θ_c is also 9 °C greater than $\theta_{w,i}$ - in other words, 49 °C.

Once UA_c is obtained, Equation (5.12) is then rearranged and the estimate for UA_c is used to calculate θ_c for all the other EN 14511 test points in the set to which the adjustment is being applied.

$$\theta_c = \theta_{w,i} + \frac{\Phi}{\dot{c}_w\left(1 - e^{-\frac{UA_c}{\dot{c}_w}}\right)} \tag{5.13}$$

Now recalculating $\dot{c}\prime_w = c_p\dot{m}\prime_w$ using the new mass flow rate to be used in simulations, new water inlet and outlet temperature for each test point are found.

$$\theta'_{w,i} = \theta_c - \frac{\Phi}{\dot{c}\prime_w \left(1 - e^{-\frac{UA_c}{\dot{c}\prime_w}}\right)} \tag{5.14}$$

$$\theta'_{w,o} = \theta'_{w,i} + \frac{\Phi}{\dot{c}\prime_w} \tag{5.15}$$

Water outlet temperatures adjusted using this method can be used in place of the EN 14511 temperatures when developing a model. This will result in a model which more accurately reflects performance under the particular flow rate of the simulated system. As mentioned above, the method is used in **??** to assess the sensitivity of ASHP performance to different water mass flow rates.

5.6 Chapter summary

This chapter addresses the main aim of the work by setting out a method of modelling ASHP based on standard performance test data for use in dynamic simulation tools. The method is adapted from grey box approaches described in the previous chapter.

The structure of the model is comprised of two parts - regression models of steady state thermal output and power load including the averaged impact of defrost cycles; and parameters governing transient behaviour. No method is developed to determine the value of the transient parameters, as EN 14511 does not contain the necessary data.

The process of producing regression models is described in 5.2, and applied to test data for 41 heat pumps. A satisfactory fit was achieved in 26 cases, despite the fact that most data sets included only eight or nine points - half the number that would normally be expected. In seven cases the fit was unsatisfactory, and the remaining 9 could be used with caution. A common feature of all the unsatisfactory cases was a pronounced dip in thermal output at test points with air temperatures of 2 °C and/or 7 °C, most likely related to an inefficient defrost mechanism. Issues are likely to be reduced with full EN 14511 data sets.

Section 5.3 described the approach to representing transient behaviour, as well as aspects of the model structure. As transient behaviour can't be derived from EN 14511 test data, there is currently a gap in the method regarding the calibration of transient parameters: as a stop gap measure in the following chapter, values are borrowed from a study by another

author.

Finally section 5.5 set out a calculation which can be applied to test data prior to the creation of regression models, which adapts test data to different heating system water flow rates. This will be used to assess the sensitivity of ASHP performance to heating system water flow rate.

The following chapter describes validation testing applied to the proposed modelling method.

Chapter 6

Validation tests

This chapter describes the validation tests applied to the ASHP modelling method set out in the previous chapter. Comparative testing is carried out against a known grey box dynamic modelling method, and also a steady state method based on elements from two published methods. Sensitivity analysis is also carried out, to determine the influence the values of transient parameters have on predictions, and to determine whether the water flow rate adjustment process proposed in the last chapter is worthwhile.

Validation is an essential part of the process of simulation software development. It was recognised early in the history of building energy simulation that rigorous validation methods were required in order for the new sector to achieve its full potential. International efforts to establish and maintain agreed testing procedures have been underway since at least the 1980s. A notable strand is the work carried out under IEA SHC Task 8 and later Task 12, which established an overall validation methodology of which the Building Energy Simulation Test (BESTEST) and Diagnostic Method forms a part.

Building energy simulation programmes are complex pieces of software, and it is not possible to test every possible path a simulation may take. The approach arrived at under the IEA tasks aims to provide a sufficiently thorough examination of software through the application of 3 types of testing. These types are analytical, empirical and comparative.

Analytical verification is a test of the numerical solution of the model. It involves comparing outputs from a programme to a known analytical solution. Generally testing

needs to be carried out at the level of subroutines or algorithms, and use simple and highly defined boundary conditions, for analytical solutions to be obtainable.

Comparative testing involves comparing a new modelling method to existing modelling methods. These methods may be better known to the researcher, and would generally have been chosen as they have been subject to validation themselves. This tests both the model and the solution process, and can be applied to models of any level of complexity. It is quick and inexpensive, and generally avoids input uncertainty issues. However, there is no truth standard.

Empirical validation refers to the comparison of simulation outputs to data from physical systems. Again this tests both model and solution process, and can be applied to models of any complexity. There is a real truth standard. Drawbacks are that acquiring appropriate data can be expensive and time-consuming, and there will also be some measurement uncertainty with regard to the input data.

Hensen [52], the originator of plant network modelling within ESP-r, wrote at length on the validation. He described the use of a five stage validation process developed by Bloomfield [54] and Irving [55]. This precedes the three types of test above with an initial examination of model theory and source code; and also adds a parametric sensitivity analysis.

Of these five stages of testing, three are addressed to some degree in this work; one is deemed to be unnecessary; and the final one is desirable but sufficient data could not be obtained.

An examination of model theory and code is to a large extent represented by this thesis; a thorough examination of theory was undertaken in the early chapters, and key simplifications and issues in the proposed modelling method (around frosting and determination of transient parameters) highlighted. The additions to the ESPr source code made for this work are extensively 'marked-up' and appear in appendix B. Hensen refers to examples of formal processes for checking and cross-referencing of code that have been used by large, team-based research projects, however these are less appropriate for a PhD project.

Analytical validation of the numerical solution method is deemed to be unnecessary, as the proposed model follows the standard structure for ESP-r components and makes use of the inbuilt solver: this has been subjected to extensive testing, some of which is documented by Hensen in his thesis [52].

Empirical testing was omitted due to appropriate data not being found. It was not possible to carry out practical testing or monitoring of an ASHP as part of the project. Some data was obtained from other researchers' projects, however this had been collected for other purposes and did not record some important categories of data point.

Comparative testing has been carried out, using methods reviewed in chapter 4. The process and outcomes are described in the following subsection. The methods employed for comparison are the grey box dynamic method and model developed by Kelly and Cockroft [33], as well as a steady state approach based on elements of the black box methods used by Jenkins et al. [39] and Wemhoener et al. [35]. Comparison of the proposed method with the steady state approach shows that the dynamics of the heating distribution system at least are important; comparison with the grey box dynamic method shows problems with the representation of performance during part load operation in weather conditions where defrost cycles occur, though better agreement elsewhere.

Finally, a parametric sensitivity analysis is carried out, and is presented in section 6.2. First, given the gap in the proposed method around the determination of suitable values for transient parameters, sensitivity of predictions to these values is investigated. Sensitivity is found to be low. Secondly, the impact of water flow rate on model predictions is explored, using the water flow rate adjustment process described in section 5.5. It is found that sensitivity to water flow rate is also low, suggesting it can be safely neglected by grey box ASHP modelling methods.

6.1 Comparative testing

Comparative testing involves calibrating a new modelling method alongside some known existing modelling methods using the same data set, and then comparing their simulation outputs.

In this section the proposed modelling method is compared to two others: the method of Kelly and Cockroft, and a steady-state approach borrowing elements from the black box methods used by Jenkins et al. and Wemhoener et al..

The calibration of the models is undertaken differently to the normal approach. This is largely due to difficulties obtaining suitable data for calibrating the Kelly model. However, a

ready-calibrated and tested implementation of the Kelly and Cockroft model *is* available. This model was subjected to a virtual EN 14511 test within ESP-r using a plant-only simulation, and a set of EN 14511-like results extracted. The proposed modelling method and the steady state method were then applied to these results to obtain two further models.

The impact of this necessary approach is taken account of in the analysis of simulation results.

6.1.1 Model preparation

Kelly and Cockroft applied their modelling method to data for an 8 kW Heat King ASHP. The original input data was no longer available. However the resulting model is.To extract EN 14511-type results, the model was subjected to a virtual EN 14511 test process. It should be remarked that the results for test points with air temperature 7 °C and 12 °C would be straightforward to obtain without simulating: the regression equations underlying the model can be easily evaluated, and the main model equation eq. (5.1) (70) then solved as the tests are steady state and the differential term on the left hand side can be set to zero. This is not true for the remaining test points however: the occurrence of defrost cycles means that they are not steady state, and it is easier to simulate than solve.

The EN 14511 test process was reviewed in chapter 3. The essential elements of the test are that the ASHP receives a flow of water at a constant temperature; and that the ASHP unit experiences fixed climate conditions (temperature and humidity). The latter was easily achieved using ESP-r's ability to create climate files. Five were created, with constant climate conditions relating to the EN 14511 test points.

The constant water flow was achieved by creating a simple plant network of two components, the ASHP and a pipe component acting as the inlet water supply. By making using of the ESP-r connection type "from known temperature", the temperature of the flow of water into ASHP could be set to the required constant value. Mass flow rate in the network is determined by setting the appropriate parameter of the ASHP component.

Using this virtual test chamber, a simulation was run for each of the test points in the EN 14511 process. [1] In accordance with the test process, thermal output was taken to be

[1]The reader may recall that for tests at air temperatures other than 7 °C, no input water temperature is specified, only an output temperature; prior to each test the input water temperature is adjusted (maintaining flow rate at the level determined in the 7 °C test) until the specified output temperature is achieved. Whilst

the average over a test period of three hours or three complete heating/defrosting cycles, whichever occurred soonest. It is calculated using the water flow rate and the inlet and outlet temperatures for the ASHP component. A 70 minute equilibrium period precedes the test period. In tests where defrost cycles occur, an additional 10 minute recovery period follows the first defrost period in the simulation results file.

A graphical depiction of the test process can be seen in fig. 6.1. It is worth noting for later that between defrost periods, each heating period lasts 40 minutes as determined by the model's code and parameters.

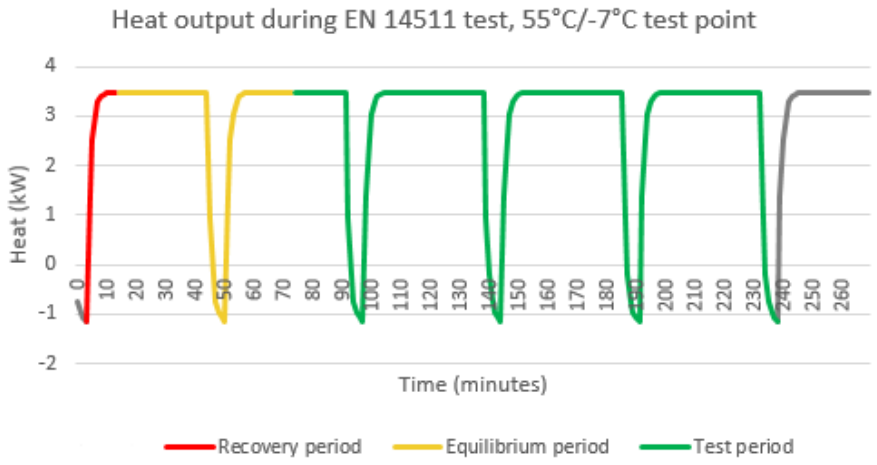

Figure 6.1: Simulated EN 14511 test example

The outputs of the tests appear in table 6.1[2]. As in the EN 14511 process, circulation pump power is subtracted from the measured power load to obtain the test results.

The proposed modelling method as outlined in chapter 5 was applied to the data from the virtual EN 14511 test. The curve fit obtained is depicted in section 6.1.1, and the parameters are given in table 6.2.

this process could have been mirrored in ESP-r by running multiple simulations using an iterative script, a shortcut could be taken given that the equations and parameters of the model are known: the input water temperature required to achieve the specified output temperature was merely calculated. In this case, solution of the model equation was straightforward even for those tests in which defrost cycles occur; the differential term could still be set to zero as it is during the stable period following recovery from a defrost cycle that water inlet temperature is determined.

[2]It may be noted that Φ_{ss} at the test point water 35 °C air 7 °C is 7.15 kW rather than the 8 kW nominal output claimed for the ASHP. It is thought that this is due to an oversight in the modelling method: the heat loss term in the model equation applies both when the ASHP is running and when it is not. In the original test data, however, it is likely that heat loss when the ASHP is running is already implicit in the measured thermal output with which the model was calibrated. Heat loss is therefore double counted whilst the ASHP is running. None the less, the model is used as is.

Table 6.1: Virtual EN 124511 test results for the Kelly and Cockroft model

$\theta_{w,o}$	$\theta_{a,i}$	Φ_{ss}	P	COP
35	−15	3.01	1.936	1.56
35	−7	3.66	1.99	1.84
35	2	4.99	2.04	2.45
35	7	7.15	2.07	3.46
35	12	8.396	2.08	4.02
45	−15	2.73	2.26	1.21
45	−7	3.23	2.32	1.39
45	2	4.42	2.37	1.87
45	7	6.43	2.39	2.68
45	12	7.60	2.42	3.14
55	−15	2.58	2.60	0.99
55	−7	2.83	2.68	1.06
55	2	3.80	2.72	1.40
55	7	5.59	2.74	2.04
55	12	6.59	2.78	2.37

Table 6.2: Regression model parameters for the proposed method

	Φ_{ss}	P
a_0	6.4719	1.0286
a_1	-3.8685×10^{-2}	2.4752×10^{-2}
a_2	3.1506×10^{-1}	3.8750×10^{-3}
a_3	-2.5212×10^{-3}	4.0093×10^{-5}
a_4	-2.2134×10^{-4}	1.0310×10^{-4}
a_5	6.7900×10^{-3}	-6.6398×10^{-5}

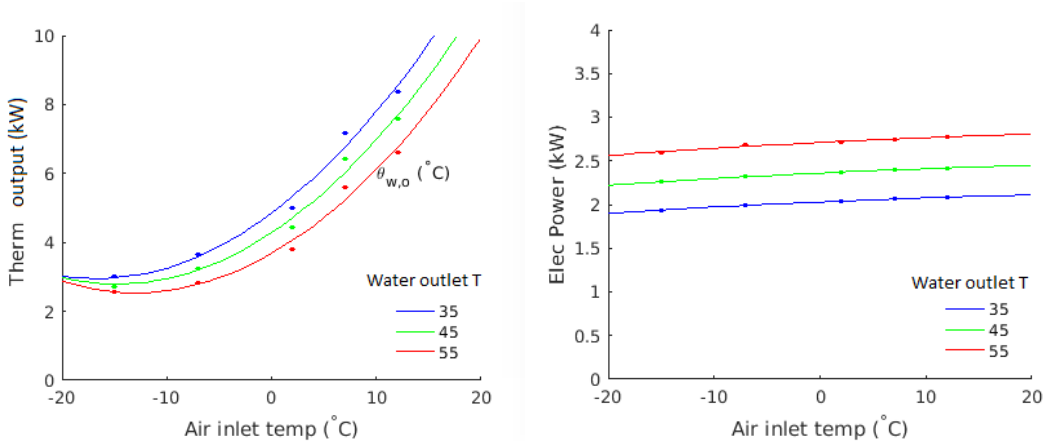

Figure 6.2: Regression models for the proposed method

Comparison will also be made with a steady state plant system model. This is based primarily on EN 15316-4-2:2008 *Method for calculation of system energy requirements and system efficiencies — Part 4-2* [36]. This is a calculation-based approach: for this analysis the building portion of the calculation is replaced with ESP-r simulation, to arrive at a method similar to that of Jenkins et al. [39]. The approach of Jenkins et al. is not used directly as it was applied only to an air-to-air ASHP system.

The basis of both the above methods is that the heat load of the building is modelled first. The electrical demand of the ASHP at any particular timestep is given by dividing this idealised heat demand by the COP of the heat pump at the current operating conditions.

The steady state method to be deployed here will follow exactly the same process: a heat demand profile is determined by running building-only simulation in ESP-r; The electrical load of the ASHP is then obtained by dividing the heat demand at each timestep by COP, the value of which is determined by a regression model obtained using EN 14511 data.

Further details of the method:

- In accordance with EN 15316-4-2, the output temperature of the ASHP is taken to be the flow temperature of the heating system as determined by control settings - in the simulations that follow, the ASHP's internal thermostat is set to 55 °C, and so this value is used.

- The COP regression model is quadratic in $\theta_{w,o}$, and parameters are determined based on the 5 EN 14511 test points with $\theta_{w,o} = 55$ °C.

Table 6.3: Regression model parameters for the steady state method

a_0	a_1	a_0
1.312	0.60408	0.0023646

- No allowance is made for part load performance. In EN 15316-4-2, part load performance is only taken into account if part load test results are available: commentary suggests this is considered unlikely, and that EN 14511's full-load tests are the expected source of COP data.

- ESP-r requires the maximum heat demand that can be delivered to the building to be set by the modeller - in this case it was set equal to the heat output of the ASHP at design heat load conditions.

The fit of the regression model obtained for COP is shown in section 6.1.1 and the parameters are given in table 6.3.

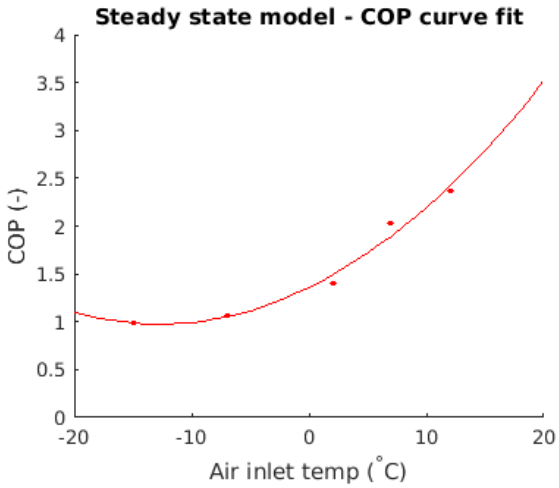

Figure 6.3: Regression model for the steady state method

6.1.2 Simulation scenarios

The use of an existing instance of the Kelly and Cockroft modelling method means that a building model had to be used whose design heat load matched the ASHP, rather than the other way round. Typical UK design parameters are chosen: and internal temperature of 21 °C, an ambient temperature of −5 °C, and a heating system designed for a flow temperature of 55 °C. Under these conditions the ASHP has a thermal output of 3.05 kW.

A detached house was determined to be the most appropriate type to model, based on a review of the *Scottish House Condition Survey: Key Findings 2014* [56].

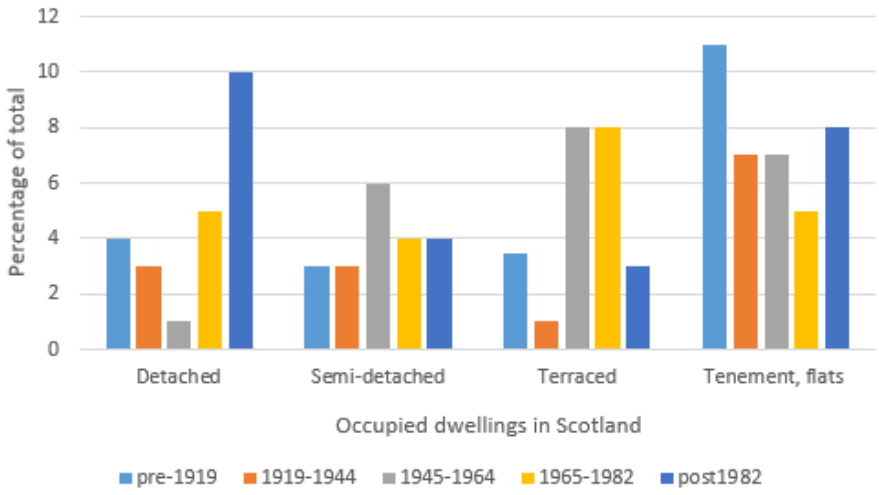

Figure 6.4: Types of housing in Scotland (Scottish Government [56])

Figure 6.4 shows the proportion of Scotland's housing falling into different categories. Pre-1919 tenements and other flats are the most common (11%), however these are unlikely to be suitable for ASHP installations: few will have outdoor space in which to position the evaporator unit; and most will be in urban locations on the gas mains, where the current economic case for ASHP is weaker.

The next most numerous category, post-1982 detached housing, was therefore selected. Detached housing is the category least likely to have a mains gas supply. It is also the most likely category to be found in a rural location – over 50% of rural houses are detached. Many will have the outdoor space necessary for an ASHP installation, and they are less likely to have noise-related planning restrictions.

It was recognised that a small house would be required in order to meet the target design heat loss. The two zone, single storey model depicted in fig. 6.5 was arrived at based on common features from small house plans available online. This has a floor area of 83.25 m^2.

Table 6.4: Element U-values of the building model

Element	Construction	U-value $W\,m^{-2}\,K^{-1}$
Floor	Solid, insulated 200mm glasswool	0.176
External walls	Block cavity, insulated 75mm Mineral fibre	0.420
Roof	Pitched, cold loft, 150mm fibreglass quilt	0.253
Windows	Double glazed	0.280

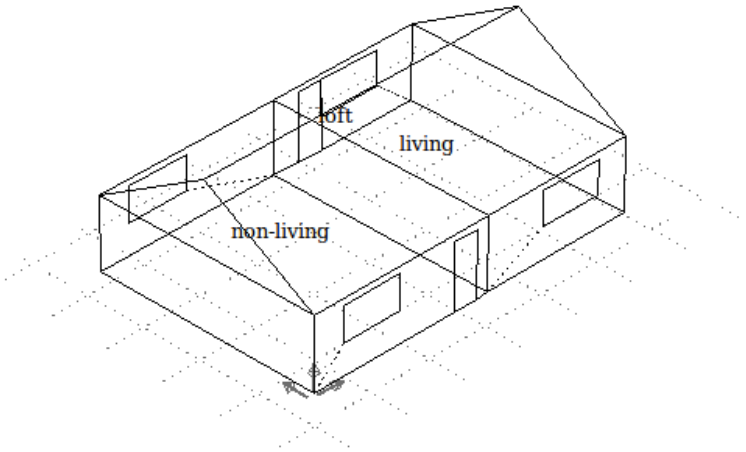

Figure 6.5: Wireframe diagram of house model

A number of combinations of envelope constructions were trialled. The following, combined with an infiltration rate of 0.5 air changes per hour, gave a design heat loss of 3.02 kW, very slightly less than the ASHP's 3.02 kW thermal output at design conditions.

The U values of the various elements (table 6.4) are approximately equivalent to those required from 1990 until 2002 in the *Technical Standards for Compliance with the Building Standards (Scotland) Regulations 1990* [57]. An exception is the floor construction, which has a U value closer to that required by current regulations. This is due to the process of matching model design heat load to ASHP output.

The plant system model consists of the ASHP component, two radiator components (radiators in the living and non-living zones respectively are lumped together into single entities), two TRV components and a number of pipes and merging components to complete the circuits.

The radiator components are sized to meet the heat load of their respective zones at the design parameters mentioned previously (internal/ambient/flow temperatures 21 °C/−5 °C/ 55 °C).

Two control files were created, so that simulations could be run with continuous and intermittent heating patterns. Both consist of a control loop with the ASHP as the actuator, responding to a temperature sensor located in the Living zone. The setpoint temperature is 21 °C, with a deadband of ±1 °C. In the case of the intermittent heating file, heating is on from 06:00 to 08:00 and 17:00 to 22:00 weekdays and from 07:00 to 22:00 at weekends.

A simple causal gains schedule was created based on two occupants working standard office hours. This is slightly incongruous with the use of a continuous heating pattern, but will be unimportant for the purposes of a comparative test.

It was decided to run simulations with three UK climate files which form part of the ESP-r standard distribution: these are for Aberdeen, Birmingham, and Oban. ESP-r's "find typical weeks" tool was used to determine representative Winter and Spring weeks for each.

6.1.3 Simulation results and analysis

The results of winter simulations using the three models are presented in figs. 6.6 and 6.7. It should be noted that heat delivered is calculated by summing the ASHP's thermal output to the heating system over the period of the simulation. Thermal output is the first term on the right hand side of the energy balance equation (eq. (5.1), 70) which underlies the models. It is different to Φ, the value of which is determined by the thermal output regression model. Φ is the notional thermal output of the ASHP when operating in steady state conditions; actual thermal output to the heating system must take account of transient effects.

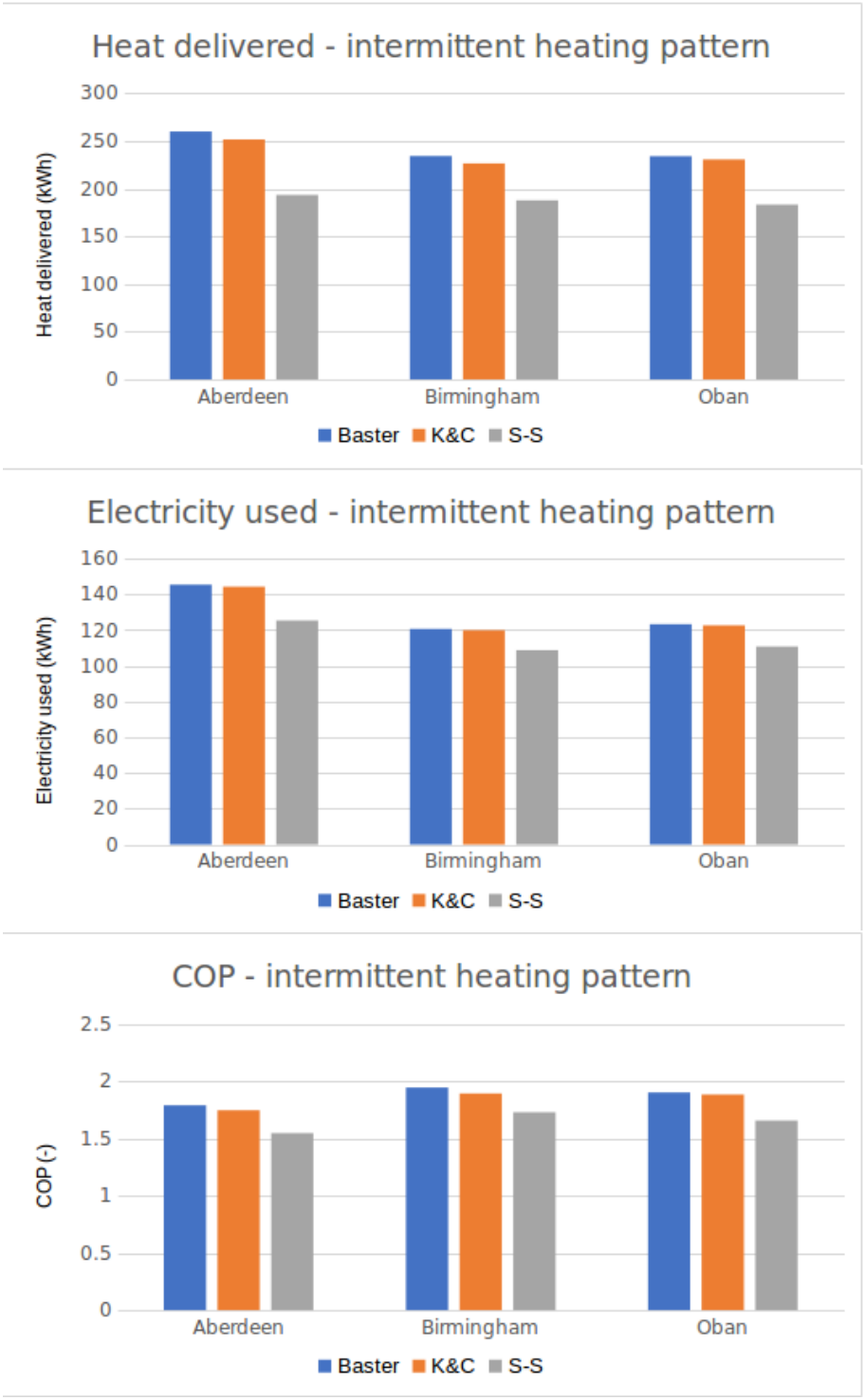

Figure 6.6: Typical winter week simulation results, intermittent heating

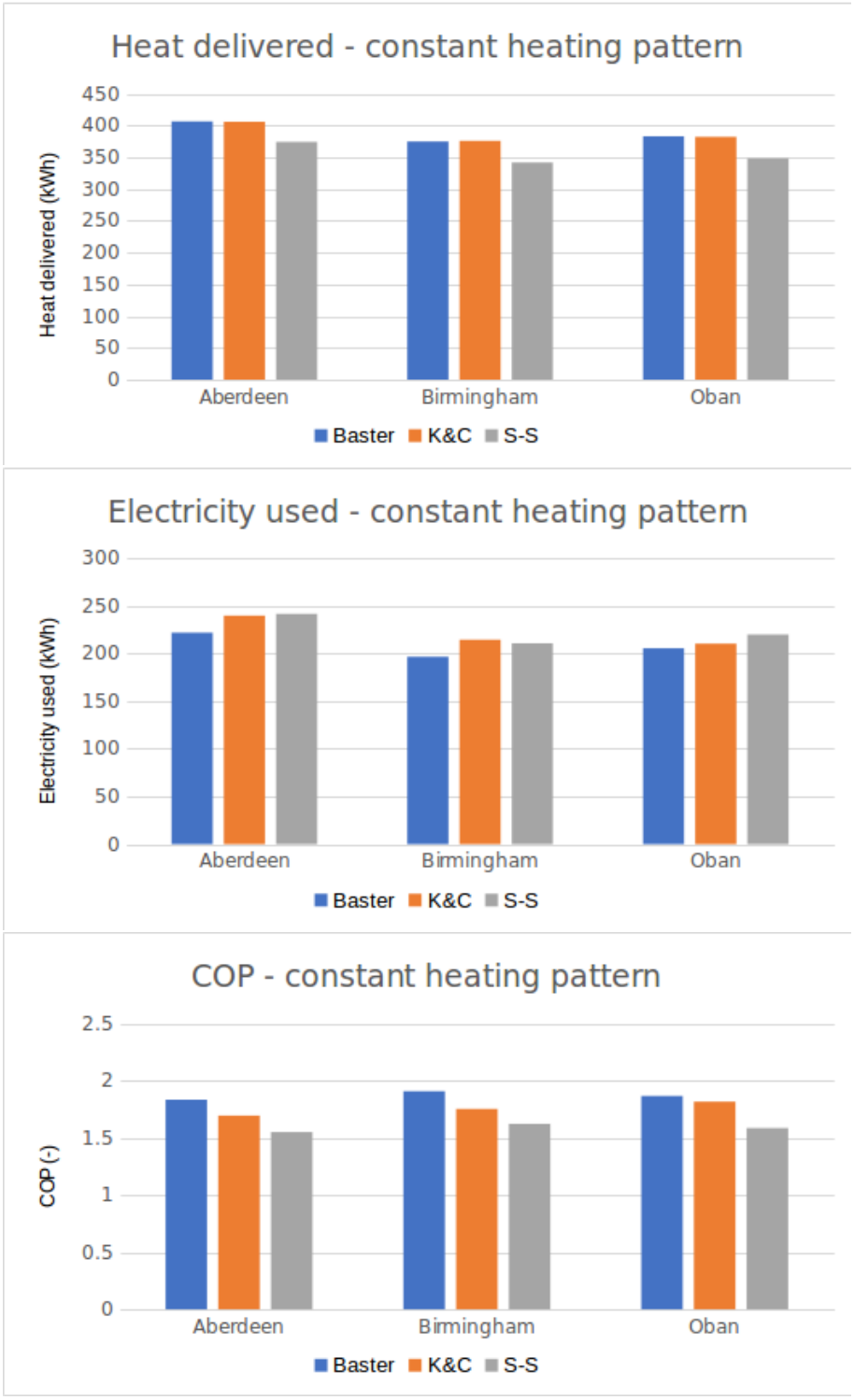

Figure 6.7: Typical winter week simulation results, constant heating

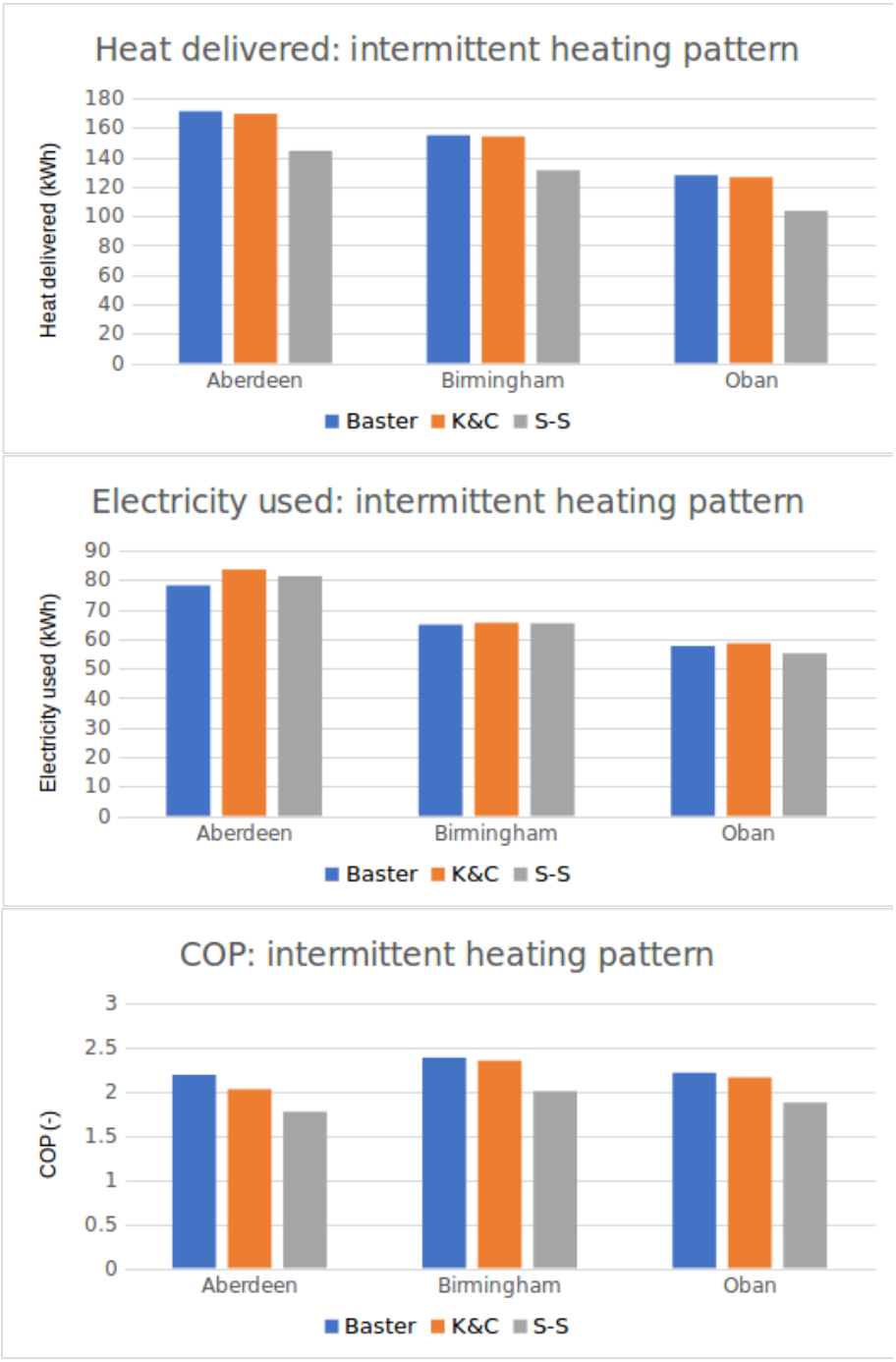

Figure 6.8: Typical spring week simulation results, intermittent heating

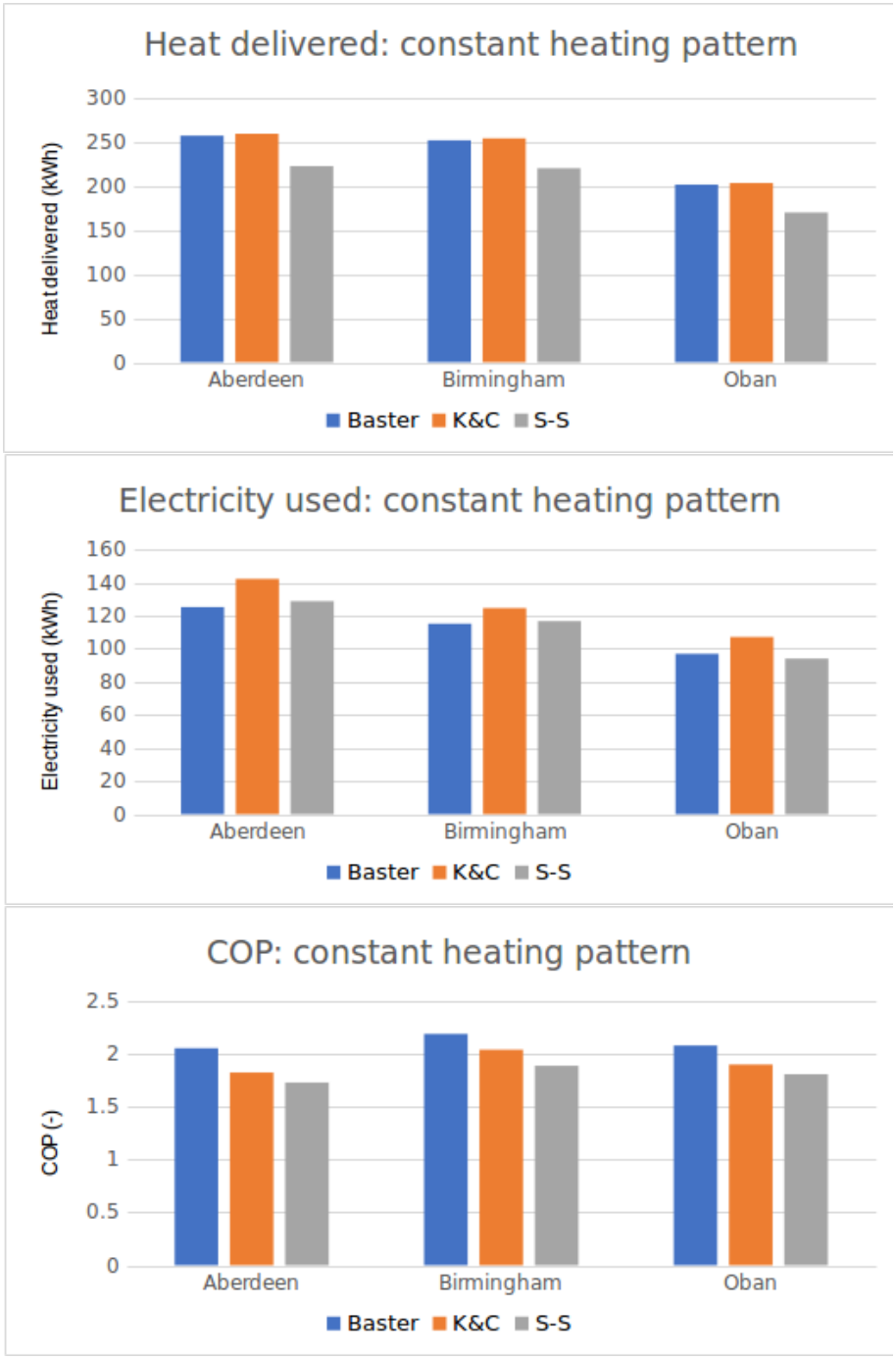

Figure 6.9: Typical spring week simulation results, constant heating

A clear pattern emerges from the simulation results: the proposed modelling method predicts a higher COP across all scenarios simulated (though in some the differences between the proposed method and that of Kelly and Cockroft is small).

A comparison with the steady state model is considered first. It was anticipated that the dynamic methods would be required to produce more heat to satisfy building demand than

the steady state method, as the steady state method does not take account of the inefficiencies inherent in a wet central heating system. There are also pronounced differences in COP over the simulation periods however. This can be understood by considering output temperatures of ASHP models during simulations.

In the steady state model, it is assumed the ASHP is constantly operating at the output temperature the heating system is sized for: 55 °C. The dynamic ASHP models in contrast only ever achieve this temperature momentarily. Both feature internal thermostats which switch off the compressor as soon as an output of 55 °C is achieved. Across the winter simulations presented here, the average output temperatures of the two dynamic models whilst the compressors are all within the range 44 °C to 47 °C.

In warmer periods in spring simulations, the discrepancy between the predicted COPs of steady state model and the dynamic models is even more pronounced. In simulations for this period using the dynamic models, generally the room thermostat is satisfied before the ASHP's internal thermostat: output temperature rarely reaches 55 °C, and average output temperature is even lower than in winter. It is inevitable therefore that the COPs predicted by the steady state model are low.

Due to these issues with the steady state model's predictions, there is little that can be concluded with regard to the usefulness of the proposed ASHP modelling method. The importance of the dynamics of the wet, radiator-based heat distribution system to performance prediction have been demonstrated, at least for the case where weather or load compensation is not employed. It is not possible to draw conclusions concerning the importance of the ASHP model itself being dynamic. This issue is addressed later in the chapter.

The comparison between the proposed method and that of Kelly and Cockroft offers more insight into the proposed method's usefulness.

There is reasonable agreement between the proposed method and that of Kelly and Cockroft in winter week simulations with an intermittent heating pattern. The proposed method predicts heat delivered to be 3.7% higher for the Birmingham climate than the Kelly and Cockroft model, but this is the largest discrepancy encountered across the three metrics. When the heating pattern is changed to continuous, however, greater discrepancies are seen. Discrepancies continue to grow when the simulations of typical Spring weeks are considered.

The proposed method over-predicts COP by as much as 12.6% (though intermittent heating pattern simulations using Birmingham and Oban climates still achieve good agreement).

In order to gain a better understanding of the source of the differences, three 24 hour periods were identified within the simulated weeks: these feature cold, moderate and warm ambient temperatures (approx 0 °C, 4 °C and 8 °C respectively). Results can be seen in fig. 6.10.

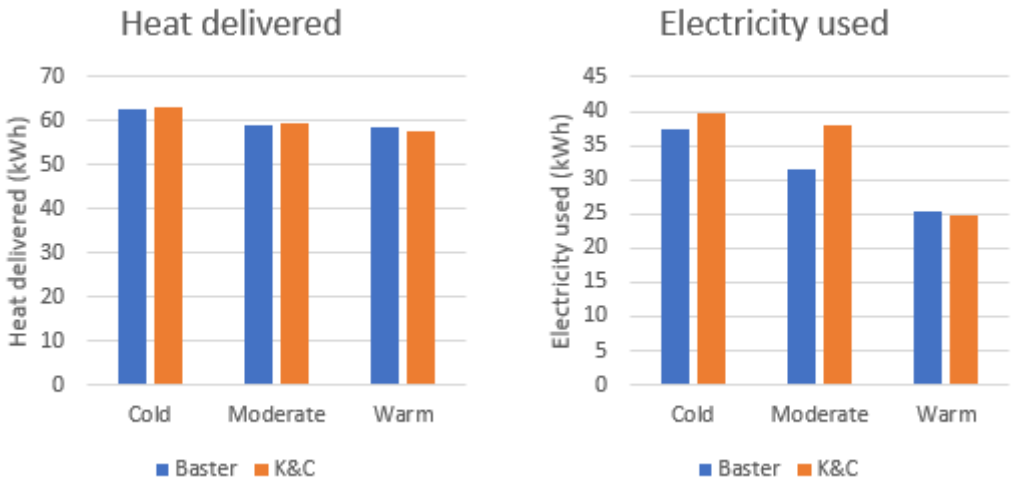

Figure 6.10: Extracted results for cold, moderate and warm days

It is clear that the proposed modelling method has severe difficulty matching the original model in the moderate temperature period. It offers a better match in cold temperatures, and a much better match in warm temperatures.

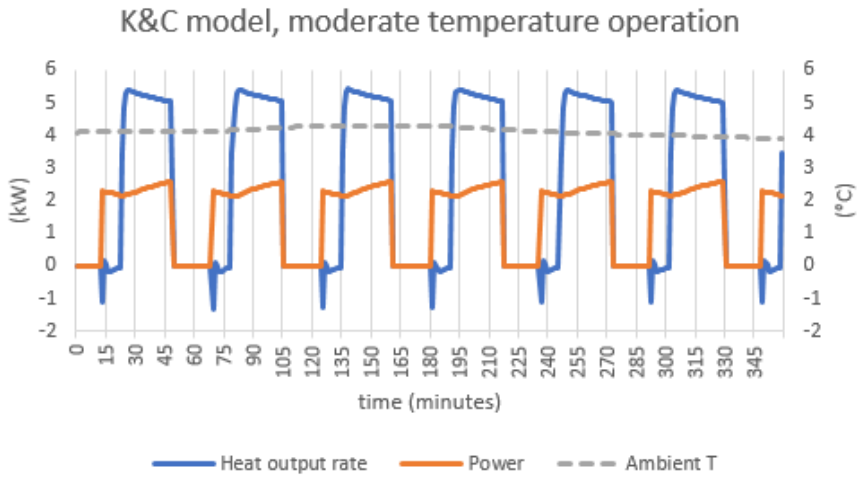

Figure 6.11: Moderate temperature operation, Kelly and Cockroft model

Figure 6.11 shows a 6-hour excerpt of moderate temperature operation from the simulation using the Kelly and Cockroft model. It can be seen that the heat demand of the building is well below the heat output of the heat pump, as it only needs to heat for brief periods before one of the thermostats in the system is satisfied. The key issue is that the ASHP model initiates a defrost cycle at the start of every heating period. During full load operation, such as occurs in the EN 14511 test process, the ASHP model enters defrost after every 40 minutes of heating (as shown in fig. 6.1). Here, the heating portion of the cycle is approximately 20 minutes, so there is one defrost period for every 20 minutes of heating.

Essentially, the Kelly and Cockroft ASHP model's performance will be reduced when operating in frosting conditions at part load such that heating cycle length is less than 40 minutes, due to a decrease in the ratio of time spent heating to time spent defrosting. The proposed modelling method implicitly assumes the ratio of heating to defrosting time is the same as in the EN 14511 tests which are conducted at full load: it will not predict the same performance reduction.

This is borne out by the pattern of the differences in the two models' predictions: cycle length decreases the warmer the temperature, so the maximum difference would be expected close to the 5 °C frosting limit. This is precisely what was seen during the moderate temperature 24-hour period. Cycle length is also shorter with continuous heating than with intermittent, and the greatest differences were seen with the former. It is worth noting that all the spring typical weeks contain significant periods during which ambient temperature is in the "frosting zone", and the same root cause is behind the differences in these simulations too.

It is not known how closely the defrost cycle aspect of the Kelly and Cockroft model represents the actual ASHP studied. The behaviour described above is consistent with how an ASHP which relies on the time-and-temperature method of controlling defrost cycles might operate section 2.4. Under this method, defrost cycles are initiated based on fixed time intervals whenever the temperature is below some predefined value. One can imagine such a controller being set to start each heating period with a defrost cycle, to ensure the evaporator is clear. Clearly, the performance of such ASHP when operating at part load in frosting conditions is not captured by the EN 14511 test process - and therefore is not reflected in the proposed modelling method, giving rise to the differences seen in the

methods' predictions.

Most modern ASHP however are thought to use a demand-based defrost control approach, which use sensors to detect frost build up. It is expected that performance of these heat pumps in frosting conditions is less affected by part load operation. There is likely to still be some difference between part load and full load operation, but it will be opposite to that detailed above. At temperatures above freezing, the ice formed during heating periods will partially melt during off periods, reducing the need for defrost.

In summary, the proposed ASHP modelling method can provide a good match to the Kelly and Cockroft ASHP model in conditions where the ASHP is operating at full load or where frosting is not occurring. However, the performance of the Kelly and Cockroft model at part load in frosting conditions, which is likely to be representative of at least some ASHPs, is different to the full load performance captured by the EN 14511 tests on which the model is based. The proposed method is therefore not adequate for representing the performance of such ASHP in typical UK climates. It is anticipated that it will offer better results for ASHP with demand-based defrost control, however this is not tested.

6.2 Sensitivity analysis

Parametric sensitivity analysis is often employed during model validation. A common motivation is to determine whether model predictions lie within the uncertainty band associated with the input data. There are uncertainty bands associated with EN 14511 test results, due to the measurement tolerances set by the standard. A sensitivity analysis looking at the impact of these on predictions may in time be of interest. However, two further areas were considered more important to investigate at this stage. These are the sensitivity of the method's predictions to variation in the values of the "transient parameters" governing dynamic behaviour, and the sensitivity of model predictions to the use of the proposed water flow rate adjustment process.

Sensitivity of predictions to the values of the transient parameters (active thermal mass M, mass weighted average specific heat $\bar{C}$, and heat loss parameter UA) is of interest due to the lack of calibration information provided by the steady-state EN 14511 test method. This is investigated by running multiple simulations using a model prepared using the proposed

method, and separately varying M and UA. It is not necessary to vary $\bar{C}$ also, due to the fact that when it appears in the equations which underlie the modelling method, $\bar{C}$ always multiplies M; thus varying $\bar{C}$ has the same effect as varying M.

EN 14511 is also lacking with regard to information on the importance of water flow rate to a performance prediction method which uses water outlet temperature as a variable. The potential importance is investigated by comparing the predictions of models created using the proposed water flow rate adjustment process to that of a model created without it.

Building, plant and ASHP models are introduced in the next two subsections; different models to those described in the preceding comparative testing section are used. Following this, simulations and results are presented.

6.2.1 Model preparation

The ASHP model versions used in this sensitivity analysis are based on test data for a commercially produced ASHP unit [12] with nominal thermal output of 11.6 kW (this data was previously used to test regression model forms in section 5.2). It is of "monoblock" design - all components are housed in a single unit installed outdoors.

The proposed method was applied to the test data as set out in chapter 5. The parameters of the quadratic regression models in add table and reference, and the fit achieved can be seen on page 76. Transient parameters have been determined by scaling those for the Kelly and Cockroft model according to thermal output at the 35 °C/7 °C test point, in accordance with the stop-gap measure described in chapter 5.

For the investigation of water flow rate, several other versions of the model were produced, this time with the application of the water flow rate adjustment process. This is described in section 6.2.4.

6.2.2 Simulation scenarios

The building model used in simulations represents a two story detached house. The building has a footprint of 70 m^2, and is modelled as two zones. Constructions corresponding to approximately 1990 building standards - the U-values of main elements are set out in table 6.6. As with the smaller housing model described in the previous section, this is a type

Table 6.5: Regression model parameters for the 11.6 kW model

Parameter	Φ_{ss}	P
a_0	11.518	0.37383
a_1	−0.071389	0.064011
a_2	0.27608	-3.2616×10^{-3}
a_3	-1.4316×10^{-3}	6.5171×10^{-5}
a_4	3.250×10^{-4}	-2.3738×10^{-5}
a_5	-3.751×10^{-4}	-1.1008×10^{-4}
Transient parameters		
Parameter	K and C model	11.6 kW model
M (kg)	110	165
$\bar{C}$ ($\mathrm{J\,kg^{-1}\,K^{-1}}$)	600	600
UA ($\mathrm{W\,K^{-1}}$)	20	30

Table 6.6: Element U-values of the building model

Element	Construction	U-value $\mathrm{W\,m^{-2}\,K^{-1}}$
Ground floor	Solid, minimal insulation	0.620
External walls	Block, insulated cavity	0.450
Roof	Pitched, cold loft, 150mm fibreglass quilt	0.253
Windows	Double glazed	3.304

and age of house which is very common in Scotland, and which has several characteristics which improve the likely viability of an ASHP installation.

The building's design heat load is 7.4 kW (ambient temperature −5 °C, indoor temperature 21 °C). The plant network uses the same design principles as that of the single story building used in comparative testing. Radiator components are sized to meet the design heat load with a heating system flow temperature of 55 °C. The thermal output of the heat pump model at design conditions is 7.5 kW.

Two heating patterns are again used, intermittent and continuous. The times of the two daily heating periods in the intermittent heating pattern are from 05:00 to 08:00 and from 14:00 to 22:00. The ASHP is switched on and off by a thermostat in the main zone, with a setpoint of 21 °C and a deadband of ±1 °C.

A gains file is defined based on 3 occupants, with the house vacant during the working day. Simulations are run using the climate file for Oban, UK, included in the standard ESP-r distribution.

6.2.3 Transient parameters

To assess the impact of variation in the transient parameters on the proposed modelling method's predictions, two sets of simulations were run.

In the first set, the value of M is varied. Given that a calibrated value for mass of the ASHP modelled is not known, it was considered important to include a wide range of values in the sensitivity analysis. The range to be tested was set to be from 0% to 200% of the value estimated by scaling, in steps of 25% (41.25 kg). The results of these simulations can be seen in fig. 6.12.

In the second set of simulations, the value of UA is varied. Again the values used range from 0 to 200% of the value estimated by scaling, in steps of 25% ($7.5\,\mathrm{J\,kg^{-1}\,K^{-1}}$). Results can be seen in fig. 6.13.

The results for variation in M are considered first. There is a surprisingly small variation in the weekly metrics in fig. 6.12[3], despite such a wide range of variation. The simulation using a constant heating pattern is most affected. This suggests that M has most impact when the ASHP is cycling on and off frequently.

Turning to the results for variation in UA, it is clear that sensitivity of the weekly metrics is low. In this case it is the spring climate simulation which shows the most variation. This is consistent with the ASHP spending less time heating: recall that the modelling method only applies the heat loss term when the ASHP is not running.

[3]Note that the central simulation with the sring climate was found during analysis to contain an error, and is therefore omitted

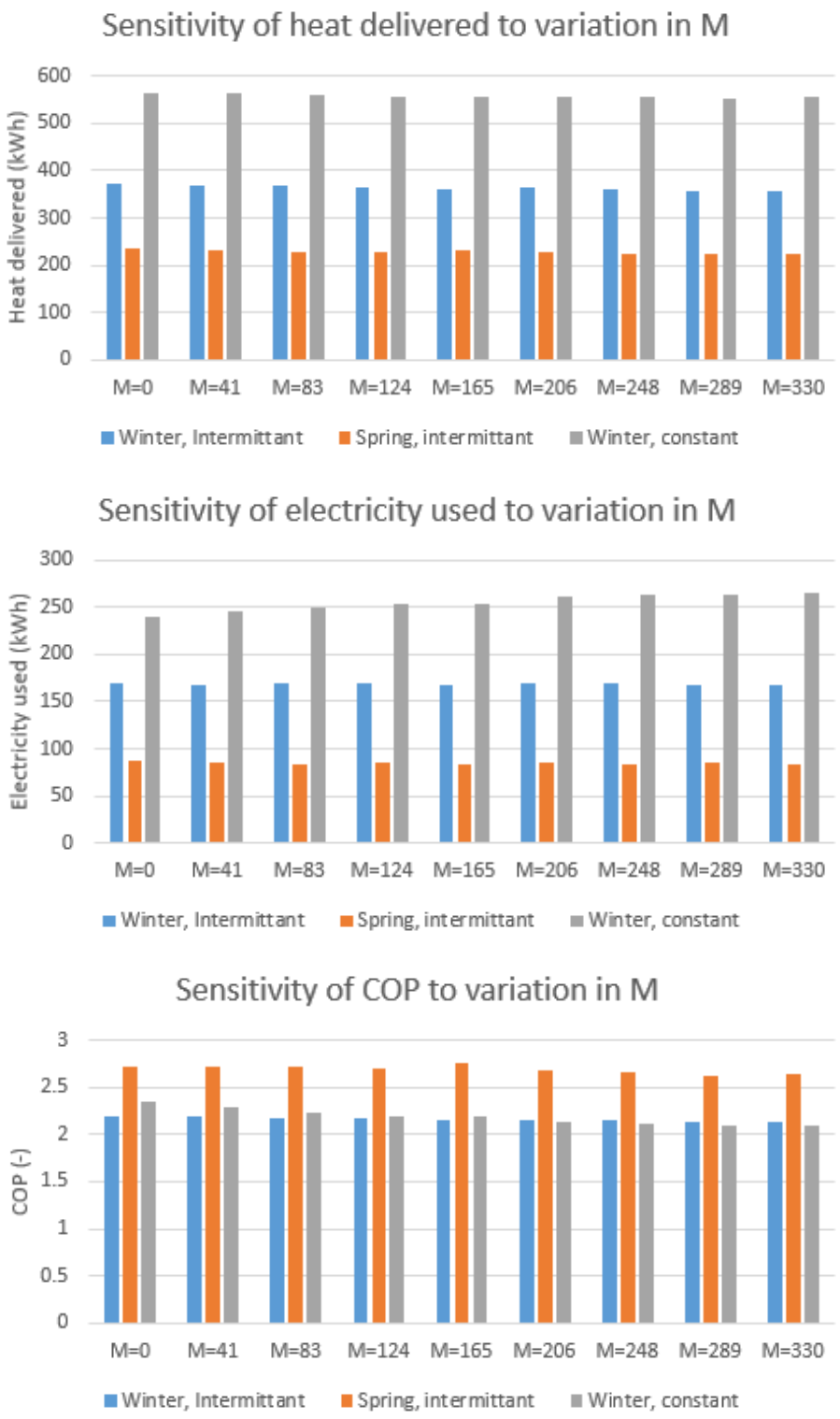

Figure 6.12: Sensitivity of weekly predictions to variation in M

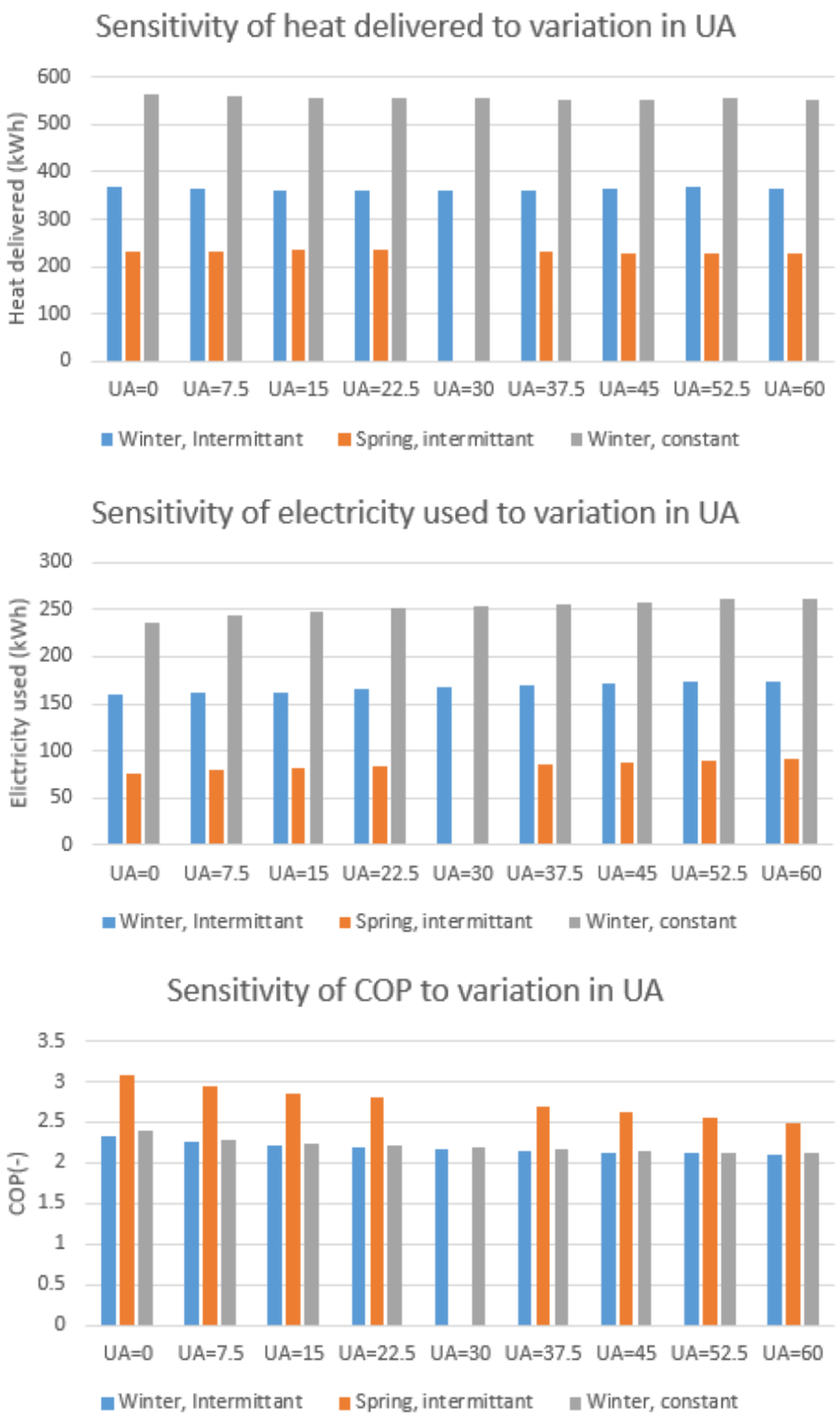

Figure 6.13: Sensitivity of weekly predictions to variation in UA

This low sensitivity to variation in transient parameters, particularly in the case of M, raises the possibility that the proposed modelling method does not need to account for

transient behaviour at all.

To gain further insight cool (average temperature 0.3 °C)and warm (6.4 °C) 24-hour periods were identified within the weekly simulations. The results from simulations using the constant heating pattern over these periods for the M=0 and M=165 model versions are compared in table 6.7. The differences between the M=0 and M=165 case are similar for both cool and warm periods: COP is approximately 7% higher when M=0.

Figures representing heat output over a 6 hour excerpt from the cool and warm periods were also created. As described in the previous chapter, the fact that the proposed method does not explicitly represent defrost cycles means that care must be taken in interpreting profiles: the results at minutely timesteps are not representative of a real ASHP. For this reason, fig. 6.15 depicts the average heat output over the course of each hour of the period. A figure showing minutely profiles (fig. 6.14) has also been included, but only to help understand the workings of the model under the two M values.

The average heat output for each hour during the cool period is similar for both the M=0 and M=165 case, with the exception of the last two hours: though even here average heat output over the two hours together is similar. Substantial hour-to-hour variation between the M=0 and M=165 case is apparent during the warm period.

Looking at the minutely profiles, there is a fairly strong difference 'under the bonnet', however. Considering the warm period first, as would be anticipated, cycles are more frequent when M=0. It is also clear that the ASHP mode's internal flow temperature thermostat is the cause of the cycling: during off periods, water continues to flow through the heating system as there is still a call for heat from the room thermostat. This effectively turns the heat pump into an outdoor radiator, sucking heat out of the building. The circulating water cools within a few minutes to the point where the point where the ASHP's internal thermostat begins another heating cycle. It is only at around 250 minutes that the room thermostat is finally satisfied, and the circulation pump stops running for a period. The fact that the circulating water is cooled rapidly inbetween heating cycles is also the explanation for the peak in output in the M=0 case at the start of heating periods. In the M=165 case in contrast, cycles are longer and there is no negative flow of heat.

There is less variation between the M=0 and M=165 cases in the warm period - it is clearly the slight mismatch in the times of heating periods which leads to variation in hourly

Table 6.7: Warm and cold 24 hour periods

	Cold 24 hrs (0.3 °C)			Warm 24 hrs (6.4 °C)		
	$M = 165$	$M = 0$	difference	$M = 165$	$M = 0$	difference
Heat (kWh)	87.5	88.8	1.5%	73.1	73.5	0.5%
Electricity (kWh)	42.0	40.0	−4.9%	31.4	29.6	−5.7%
COP (-)	2.08	2.22	6.8%	2.33	2.49	6.7%

results.

These simulations raise the prospect that it may be possible to obtain predictions over extended periods using a model with values of M and UA set to zero. Unfortunately they are not conclusive - largely because M and UA were varied one at a time rather than simultaneously. Whilst minute-to-minute performance is not intended to be representative of that of a real performance, the negative heat flows caused by non-zero UA in conjunction with the relative settings of the room and ASHP internal thermostats gives rise to concerns that results may not be replicable in different simulation scenarios. Additional simulations would be desirable to confirm findings, using another building and plant model - and varying M and UA parameters simultaneously as well as one at a time.

What can be concluded from the sensitivity analysis, however, is that when applying the proposed method, a lack of precision when determining the values of UA and M is highly unlikely to have a significant impact on performance over extended periods.

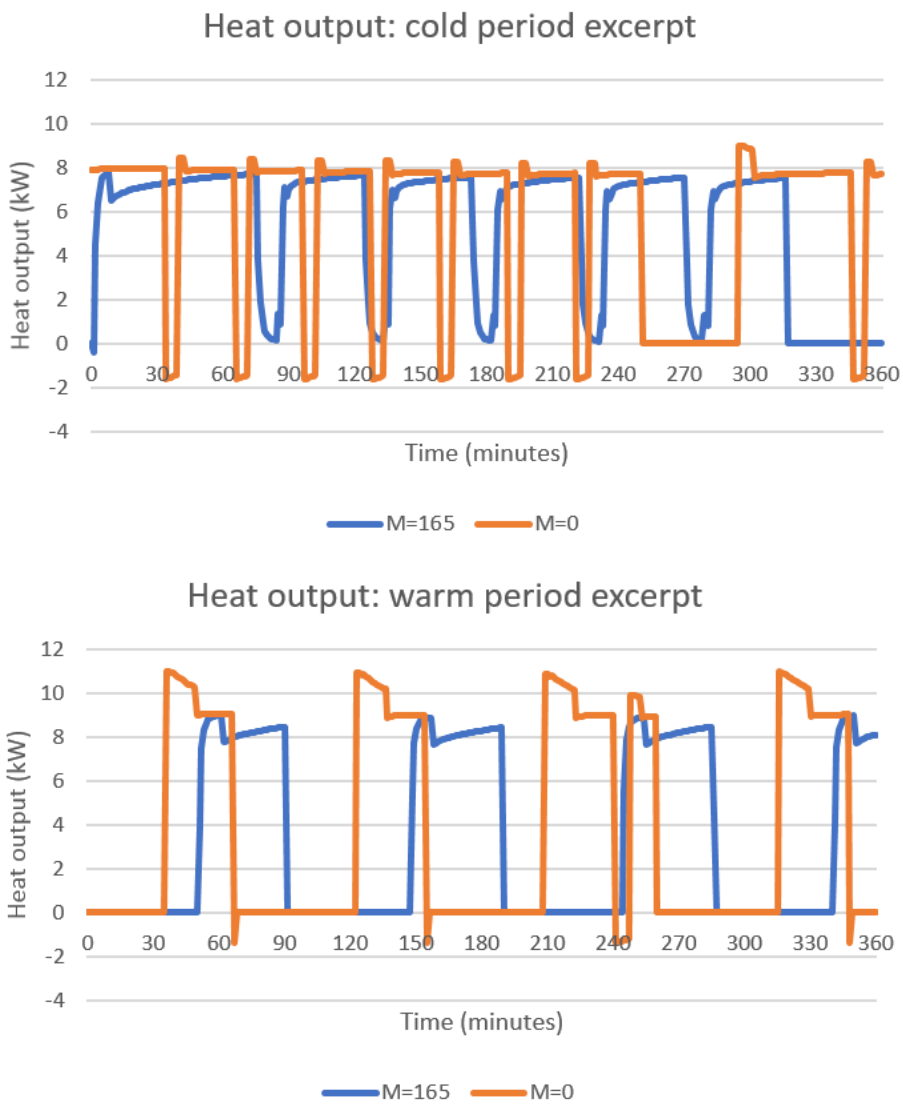

Figure 6.14: Heat output during warm and cold periods

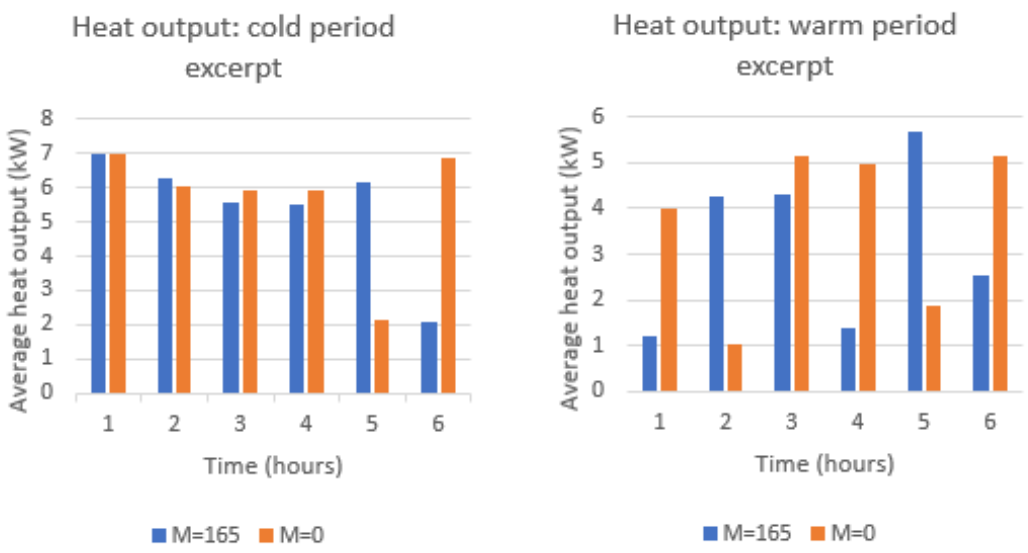

Figure 6.15: Heat output during warm and cold periods

6.2.4 Water flow rate

Previous sections of this thesis have established that the mass flow rate of water through an ASHP has an impact on its performance (by changing the rate of heat transfer in the condenser, which in turn changes the parameters of the refrigerant cycle); and, that there is not enough information in EN 14511 test results to include water mass flow rate as a variable in the proposed modelling method.

A calculation method was proposed in section 5.5, which makes use of the widely known Effectiveness-NTU method to make a simple model of the heat exchange taking place in an ASHP's condenser. The method estimates, for a mass flow rate chosen by the modeller, the water inlet and outlet temperatures giving the same condensing temperature and heat transfer as occurred at a given EN 14511 test point with the mass flow rate specified by the test method.

Recall that chapter 2 concluded that, for a heat pump in steady operation, the condensing and evaporating temperatures of the refrigerant cycle determines the heat output and power load: and that changes in these temperatures are driven by changes in heat transfer at either heat exchanger. The calculation method can thus be used by a modeller to adjust the water outlet temperatures in a set of EN 14511 data to what they would have been under a different water flow rate of their choosing - whilst the remaining data for the test

point, such as power load and heat output remain valid. This adjusted set of water outlet temperatures can then be used in the proposed ASHP modelling method. It is hypothesised that this will result in ASHP models which are more accurate for simulations at the chosen water mass flow rate than a model created using raw EN 14511 data.

The complete testing and validation of this calculation method and hypothesis is beyond the scope of this thesis. However, the impact of the method can be explored, to indicate whether it is worth pursuing further. This is done by comparing the results of pairs of simulations using flow-rate-adjusted and 'raw' model versions across a range of flow rates. The size of the variation between the model versions will indicate whether water flow rate is likely to be an important factor for performance prediction.

The same ASHP model, house model and climate file as were used in the transient parameter sensitivity analysis is used here. Five different flow rates were selected for testing, covering the range 0.2 to 0.6 litres per second. This range was chosen to encompass the minimum and maximum permissible flow rates given by the unit's manufacturer (0.25 to 0.56 l/s); and the minimum and maximum flow rates required by EN 14511 testing of the unit (0.30 to 0.56 l/s).

For each flow rate, a new version of the ASHP model was created using EN14511 data which had been subject to the adjustment procedure. At each flow rate, two simulations were initially run. The first used the version of the ASHP model created using raw, unadjusted EN14511 data. The second used a version of the ASHP model created using adjusted EN14511 data.

In the first set of simulations, the intermittent heating pattern was used, the return temperature set point was 50 °C, and the simulation was for the Winter week.

	Flow rate (l/s)	0.2	0.3	0.4	0.5	0.6
Heat (kWh)	Unadjusted	359.3	360.7	361.3	356.2	343.3
	Adjusted	358.1	361.0	360.3	356.0	345.5

	Flow rate (l/s)	0.2	0.3	0.4	0.5	0.6
Power (kWh)	Unadjusted	173.6	167.2	165.6	162.0	158.6
	Adjusted	169.5	167.1	166.6	165.3	163.4

	Flow rate (l/s)	0.2	0.3	0.4	0.5	0.6
COP	Unadjusted	2.07	2.16	2.18	2.20	2.16
	Adjusted	2.11	2.16	2.16	2.15	2.11

	Flow rate (l/s)	0.2	0.3	0.4	0.5	0.6
Number of cycles	Unadjusted	68	81	84	87	96
	Adjusted	73	81	84	87	94

Figure 6.16: Comparison of flow adjusted and unadjusted model versions - Winter, intermittent heating, 50°C

It can be seen in fig. 6.16 that, at each flow rate, there is little difference between the outputs of the pair of model versions. There is less than 3% difference between any pair of heat, power or COP results. There is a 7% difference between the numbers of cycles in the 0.2 l/s flow rate case, however for the modelling method as it currently stands this is not relevant; the minute to minute output is not of concern, only the cumulative results over extended simulations.

A similar set of simulations was run for the Spring week (fig. 6.17), using the intermittent heating pattern as before but now with a 40 °C return temperature set point. Differences between the adjusted and unadjusted model versions were generally slightly more pronounced. The gap was still less than 3%, except in the case of COP in the 0.2 l/s flow rate simulations where it was 6%.

	Flow rate (l/s)	0.2	0.3	0.4	0.5	0.6
Heat (kWh)	Unadjusted	212.8	231.1	239.3	245.8	254.6
	Adjusted	218.2	231.2	238.2	245.9	255.7

	Flow rate (l/s)	0.2	0.3	0.4	0.5	0.6
Power (kWh)	Unadjusted	84.3	83.6	85.7	85.7	87.3
	Adjusted	81.5	81.4	84.3	85.7	88.3

	Flow rate (l/s)	0.2	0.3	0.4	0.5	0.6
COP	Unadjusted	2.52	2.76	2.79	2.87	2.92
	Adjusted	2.68	2.84	2.82	2.87	2.90

	Flow rate (l/s)	0.2	0.3	0.4	0.5	0.6
Number of cycles	Unadjusted	84	94	109	117	126
	Adjusted	86	94	110	117	126

Figure 6.17: Comparison of flow adjusted and unadjusted model versions - Spring, intermittent heating, 40°C

A third set of simulations were run (fig. 6.18), using the Winter week and a 50 Celsius set point as with the first; but this time the heating was set to be on continually.

Similar to the first set of simulations, differences within simulation pairs are less than 3.5% for heat, power and COP. The difference in the number of cycles for the two simulations at a flow rate of 0.2 l/s is 3.9%.

	Flow rate (l/s)	0.2	0.3	0.4	0.5	0.6
Heat (kWh)	Unadjusted	551.1	554.6	553.5	552.6	529.2
	Adjusted	551.8	554.5	554.4	551.4	529.3

	Flow rate (l/s)	0.2	0.3	0.4	0.5	0.6
Power (kWh)	Unadjusted	262.9	253.9	251.4	251.0	246.3
	Adjusted	254.4	252.0	253.1	254.7	251.5

	Flow rate (l/s)	0.2	0.3	0.4	0.5	0.6
COP	Unadjusted	2.10	2.18	2.20	2.20	2.15
	Adjusted	2.17	2.20	2.19	2.17	2.10

	Flow rate (l/s)	0.2	0.3	0.4	0.5	0.6
Number of cycles	Unadjusted	98	112	122	130	141
	Adjusted	102	112	119	126	139

Figure 6.18: Comparison of flow adjusted and unadjusted model versions - Winter, constant heating, 50°C

For the ASHP modelled here at least, the application of the water flow rate adjustment to EN 14511 data is unlikely to make a significant difference to the output of models produced

– provided it is used within the flow rate limits specified by the manufacturer, which happen to match well with the range of flow rates used in its EN 14511 test.

Recall that the flow rates used in EN 14511 tests are set uniquely for each ASHP tested, to achieve a temperature difference across the ASHP of between 5 °C and 7 °C when the outdoor temperature is 7 °C. It would appear that the manufacturer of this ASHP has designed their ASHP to work with a similar temperature difference between output and return temperatures.

It seems likely that the above conclusion could be extended to other ASHP which have been designed to operate with a similar temperature difference between output and return. Furthermore, this is likely to represent the majority of the systems available: the EN 14511 testing regime would not have been designed around a 5 °C to 7 °C temperature difference if most ASHP manufacturers were designing for a 10 °C difference. A minor exception may be ASHPs using CO_2 as a refrigerant. The use of a transcritical vapour compression cycle in these units means that low return temperatures are preferred, an this can be promoted by a low flow rate. This type of ASHP is as yet rare, however.

In summary, it is concluded that for the ASHP unit simulated here, the application of the water flow rate adjustment is unnecessary assuming that the flow rate of the simulations it is intended to be used in are within the range specified by the manufacturer. This range matches closely the range of flow rates used in EN 14511 tests of the AHSP unit, because like EN 14511 it has been designed to operate with a temperature difference between output and return of 5 °C to 7 °C. For other ASHP which have been designed for this temperature difference, the water flow rate adjustment is also unlikely to be necessary. For ASHP designed for a greater temperature difference the water flow rate adjustment could still be useful.

6.3 Summary

This chapter set out the validation tests applied to the proposed ASHP modelling method.

Comparative testing against a known grey box dynamic modelling method produced similar results in warm conditions where the known model carried out few defrost cycles, and also in cold conditions where the models were operating close to full load. However the proposed method failed to match the known method in moderate conditions where ASHP

were operating at part load and defrost cycles were occuring.

Sets of simulations were carried out in which the values of transient parameters were varied one at a time. The performance predictions of the proposed method for extended periods showed very little sensitivity to the transient parameter values. This hints that where long term performance is of interest, a steady state ASHP models within a dynamic plant model may be similar to a dynamic ASHP mode. Results do not allow this to be firmly concluded however.

Finally, sensitivity analysis was also carried out to determine whether the water flow rate adjustment process proposed in the last chapter is worthwhile. It was found to have limited impact on model predictions.

These results and their implications are discussed further in the following Chapter.

Chapter 7

Discussion

It was noted in the introduction that there is no broadly-accepted method for the creation of dynamic ASHP performance models based on results of standard testing. It was argued that such a method would be useful to aid understanding of how current ASHP installation practices can lead to poor performance and to facilitate research into the integration of ASHP into future energy network scenarios characterised by thermal storage and flexibility of electrical demand. Additionally, as National Calculation Methods begin to make use of dynamic simulation (for non-domestic buildings at least), the need for such methods - and for adaptations to standard testing to better support them - becomes more pressing.

Chapter 5 presented a ASHP performance modelling method which partially addresses this knowledge gap, though the method requires additional calibration data to that provided by current standard testing. Aspects of the method were subjected to validation tests in chapter 6. This chapter reviews the merits and limitations of the method, and discusses findings relevant to the wider field.

The achievements of the project and the applicability of the modelling method are considered first in the following section. Key limitations are then discussed. Potential extensions to the EN 14511 test process are suggested which would allow these limitations to be addressed. Finally, the future uses of dynamic modelling are discussed in the light of the findings of this work.

7.1 Applicability and achievements of method

It was recognised during the course of this work that some compromise was required on the initial aims. The EN 14511 standard for the testing of ASHP provides data only on the average performance over an extended period; it provides no information on transient behaviour which could be used to inform a model. An examination of theory and literature suggested no further data sources or methods which could be used to fill the gap.

Transient behaviour is more significant to the performance of fixed output ASHPs than it is to other heating systems. Their increase in thermal output in warmer conditions - precisely when heating loads are lower - means that much of their lives is spent cycling on and off. Whilst there is some evidence that such behaviour has limited impact on ASHP performance, this relates to run times above a minimum duration of 8 to 15 minutes. It seems likely that this minimum duration is sometimes breached - especially in the UK, where national installation guidelines recommend sizing ASHP to meet 100% of the heating load during the coldest expected conditions.

It was therefore seen as important for an ASHP modelling method to include this dynamic aspect of performance. This resulted in the approach taken: the development of a dynamic method which can be calibrated using EN 14511 test results plus a minimal amount of additional data.

The grey box modelling approach was adapted to suit these aims. This couples regression models of steady state performance to a lumped parameter thermal mass in order to represent transient behaviour. Analysis in section 2.3 of a sample of high-resolution data covering start-up of an ASHP showed that thermal inertia dominates transient behaviour, and re-pressurising effects are likely to be minimal.

The grey box approach has sound empirical justification. It has been deployed by others, in particular Kelly and Cockroft [33], Petinot [14] and Afjei and Wetter [40]. The former two of these compared model predictions to measured data and found the representation to be satisfactory. It has been used to model other plant components, notably micro CHP units as part of IEA Annex 42 [34].

All the above methods were designed around the availability of more extensive performance data than is obtained from standard testing of ASHP. The contribution of this work

has been to adapt the approach to make best use of standard test data, test its application to a wide range of ASHPs, and to subject it to validation processes.

Key features which enable the use of EN 14511 data are the variables chosen for regression models; the inclusion in regression models of the averaged impact of defrost cycles on performance; the alignment of the treatment of heat losses and circulation pump and parasitic power loads to test processes; and the development of a calculation process to adapt test data to a single, user-selectable heating system water flow rate.

The change in regression model variable from to water inlet to water outlet temperature aligns the method better with EN 14511 test processes. The form selected for regression models includes both water outlet and air inlet temperatures as separate variables - rather than using the difference between them. This allows a more accurate representation of more recent ASHPs using scroll compressors. The treatment of heat losses and circulation pump and parasitic power loads are often an afterthought, but are a none the less vital to simulation results.

7.1.1 Testing outcomes

The application of the new regression modelling approach was demonstrated using partial sets of EN 14511 data for 41 ASHP units (section 5.2), obtained from a Swiss test centre. Regression model fit was judged to be satisfactory in 25 of the cases. Fit in seven of the cases was judged to be unsatisfactory, and the remaining nine were judged to be usable with caution.

It should be noted that most data sets had only eight or nine data points - typically 18 would be expected. The proportion of succesful results achieved is therefore seen as positive. Additional data points are likely to have raised many of the ASHP graded ‘caution’ or unsatisfactory to a higher category.

Whilst missing data points were the key to failures, ASHP with unsatisfatory fits had some common features which may contribute. Firstly, all seven had strongly reduced performance at the test point with air temperature 2 °C, suggesting inefficient or poorly controlled defrost mechanisms. Three further features made it more likely fit would be unsatisfactory, though there was not a clear causal link: a ‘split’ rather than monoblock construction type; the use of R410A as a refrigerant; and output control. Whilst it seems logical that output control

would reduce predictability, in all except one case there was no visible sign of the capability being used.

Two key types of validation testing were applied to the model: comparative testing against two other models, and a sensitivity analysis for selected parameters.

Comparative testing with the steady state modelling method did not yield any strong conclusions about the validity of the proposed method. It did show that in some circumstances at least, the dynamics of the heat distribution system as a whole are important to determining ASHP performance. This adds weight to the argument for increased used of dynamic modelling in NCMs.

Comparison to the Kelly and Cockroft model showed close matches in terms of performance over warmer periods where defrost did not occur, and in cooler periods when the ASHP was operating close to full load. The reasons for the discrepancies elsewhere were identified, and are discussed further in the following section. It is concluded that no major errors were made in the code for the model.

Although water flow rate is identified as a factor which can influence ASHP performance, it was found that the variation in flow rates in EN 14511 data is insufficient for it to be included as a variable in regression models. However in many heating systems, water flow rate through the heat pump is in any case fixed. A calculation method is therefore proposed in section 5.5 to adjust test data to a single, user-selected flow rate. This would be applied before the regression modelling is carried out, resulting in a model that is valid for a particular flow rate. Investigation using this method found that the impact of flow rate is likely to be limited. None the less the method may be beneficial in simulations using water flow rates outside the range of those specified in EN 14511 tests.

The values of parameters governing transient behaviour used in this thesis were based on values found in the study by Kelly and Cockroft. It is recognised that the inclusion of a lumped parameter thermal capacitance term in the proposed method, when data is not available with which to calibrate the parameters, means there is a gap in the method. For this reason, a sensitivity analysis was conducted in section 6.2 to assess the impact of the parameters on predicted performance over extended periods. Results showed sensitivity is surprisingly low, and simulations with M set to zero produced results which were not far off those with values of M greater than is likely in reality. Results were not conclusive enough

to say that transient behaviour can be ignored, however.

A key aim of the work is that the resulting method should be suitable for implementation in dynamic building simulation tools. This is illustrated through the implementation of an example of the model in building simulation tool ESP-r.

The selection of ESP-r as the environment for demonstrating the proposed modelling method has influenced the design of the model in a number of ways. A control volume approach to modelling is adopted, and the method is tailored to make use of ESP-r's inbuilt plant solver. The portability of the approach to other simulation environments is discussed later in this chapter.

7.2 Limitations of the method

The main aim of this work is the development of a method of modelling ASHP which can be informed by standard test data. Whilst EN 14511 standard testing offers a relatively easily obtained, reliable source of data for informing models, it does not fully represent all the aspects of ASHP behaviour discussed in chapter 2.

A key limitation is that the EN 14511 only measures steady state performance, meaning that it provides no information on transient behaviour whether at the start and end of heating periods or related to defrost cycles. Secondly, the standard offers no process for testing ASHPs at part load conditions. If the process is applied to variable output ASHPs, they must be always be at maximum setting. Finally, there is limited information on the impact of humidity on performance. These factors result in limitations on the modelling method itself.

7.2.1 Representation of transient behaviour

The lack of part load testing means that the modelling method is restricted to simulating fixed output ASHP. Section 7.3 considers how extensions to standard testing could might enable the method to be extended to variable output units. However, as noted in section 2.5, variable output units are currently less common than fixed.

Transient behaviour is more significant to the performance of fixed output ASHPs than it is to other heating systems. Their increase in thermal output in warmer conditions - precisely

when heating loads are lower - means that much of their lives is spent cycling on and off. Whilst there is some evidence that such behaviour has limited impact on ASHP performance, this relates to run times above a minimum duration of 8 to 15 minutes. It seems likely that this minimum duration is sometimes breached - especially in the UK, where national installation guidelines recommend sizing ASHP to meet 100% of the heating load during the coldest expected conditions.

It was therefore seen as important for an ASHP modelling method to include this dynamic aspect of performance. In the proposed methodology, this is accomplished by a lumped parameter thermal capacitance term, despite the fact that EN 14511 data does not allow the calibration of its parameters. Indeed, no suitable data from any source was obtained during the course of the project.

the approach to representing dynamic behaviour is the same as that used by Kelly and Cockroft for their ASHP model. This enabled investigation of the method to proceed; parameters for a version of the Kelly and Cockroft model were available, and in the comparative testing of the two methods presented in the previous chapter the values of the transient parameters were 'borrowed' for the proposed method.

It is recognised that the lack of any application and testing of a calibration process for determining transient parameters represents a gap in this work. The data requirements for calibrating these parameters, and how standard testing could be expanded to provide it, is discussed later in the following section.

7.2.2 Representation of defrost cycles

The steady state nature of EN 14511 test process has a further significant impact on the model. Defrost cycles cannot be explicitly modelled, as there is no information on their frequency, duration or whether power load changes when one is in progress. The proposed modelling method is forced to include the averaged impact of defrost cycles on performance in its underlying regression models, as the EN 14511 test process measures performance across a number of defrost cycles (in tests where these occur).

The initial impact is that the model's minute-to-minute output can no longer be seen as representative of the physical ASHP's, at least in conditions where defrost cycles occur; the proposed method is a slightly uncomfortable hybrid of dynamic and steady state. This

approach has been used by others, namely Jenkins et al. [39] and Afjei and Wetter [40]. It was hypothesised that predicted performance over extended periods will still be similar.

The comparative testing of the proposed method against the Kelly and Cockroft model (which models defrost cycles explicitly), suggests that this hypothesis may not always hold true. Large differences were encountered during simulations of periods in which frosting was occuring and the ASHP was operating at part load. This was because the defrost control implemented in the Kelly and Cockroft model means that the ratio of time in defrost to time heating was much greater in these conditions than at full load. This has a negative impact on performance which is not captured by the full load EN 14511 test method, and therefore is not reflected in the proposed method.

The defrost control method employed in the Kelly and Cockroft may be a fair representation of an ASHP with time-based defrost controls. however, industry sources [58] state that demand-based defrost control is the most common approach in modern ASHP units, and it was also far more frequently encountered in the studies of frosting in the literature. ASHP with demand-based defrost controls are likely to show less difference between full and part load operation. In subzero temperatures, the ratio of time in defrost to time heating is unlikely to change between full and part load operation. In temperatures above freezing, the off-cycles of part load operation will allow some of the ice formed to melt, meaning that the ratio of time in defrost to time heating is actually slightly increased rather than reduced.

7.2.3 Impact of humidity

A further limitation of the proposed method also concerns frosting. As section 2.4 discussed, the average performance at any given air temperature is highly likely to vary as humidity level changes. Below approximately 5 °C, the frequency of defrost periods increases as humidity increases (in ASHPs with demand-based defrost) - and at lower levels of humidity, no defrost cycles may be required at all. Secondly, it appears that increasing humidity also reduces the time required to defrost. Whilst the effect of these two trends on average performance is opposite, it is unlikely they cancel each other out.

Furthermore, whilst at temperatures above approximately 5 °C no frost growth occurs, the latent heat transfer associated with condensation on the evaporator surface leads to a small increase in performance. Though smaller than the impact of frosting at low temperatures,

this effect is also dependent on humidity levels.

Unfortunately the EN 14511 test process specifies that the same humidity level is used in tests at a given air temperature. For example, all tests with an air temperature of 2 °C are run with 84% relative humidity. This means that is not possible to include humidity as a variable in the regression models for Φ_{ss} and P. There is not enough variation in humidity levels for regression analysis to correctly identify its impact on average performance.

In simulations using climates in which the humidity levels are close to those used in EN 14511 tests, there can be little issue with using the described modelling method. Conversely if humidity levels for the location or time period being simulated are significantly different to EN 14511 levels, there could well be a significant discrepancy between simulation results and actual performance.

Two key questions are therefore, how much might performance vary at different humidity levels, and how do humidity levels compare to those used in EN 14511 tests?

As stated in section 2.4, no work was found which comprehensively assessed the overall relationship between humidity and ASHP cyclic performance. However an indication of the size of the variation in performance caused by humidity can be seen in some manufacturer's test data. The ASHP test results in figure 2.6 show that at an air temperature of 2 °C, thermal output including defrost cycles is 17% lower than peak or "unfrosted" output (a smaller decrease in power load means that COP drops by 14%). Peak output is likely to be similar to ASHP output at 55% relative humidity. Whilst it is not known what relative humidity was used in the cyclic test, it seems unlikely the manufacturer would publish the worst case scenario, which would be 100% relative humidity. There is thus substantial space for variation in performance.

The histograms in figure 7.1 give an idea of common climate conditions for a sample of UK locations, and were produced using climate data from the USA Department of Energy [59]. Focussing on the zone in which frosting can occur (approximately 5 °C and below), it can be seen that the most frequently occurring relative humidity levels in Aberdeen are spread fairly evenly above and below EN 14511 humidity levels (represented by grey dots). It seems likely therefore that when simulating a ASHP located in Aberdeen over a full heating season, reasonable results would be obtained. Care would still need to be taken if simulating over a shorter period, as relative humidity may not be so well spread.

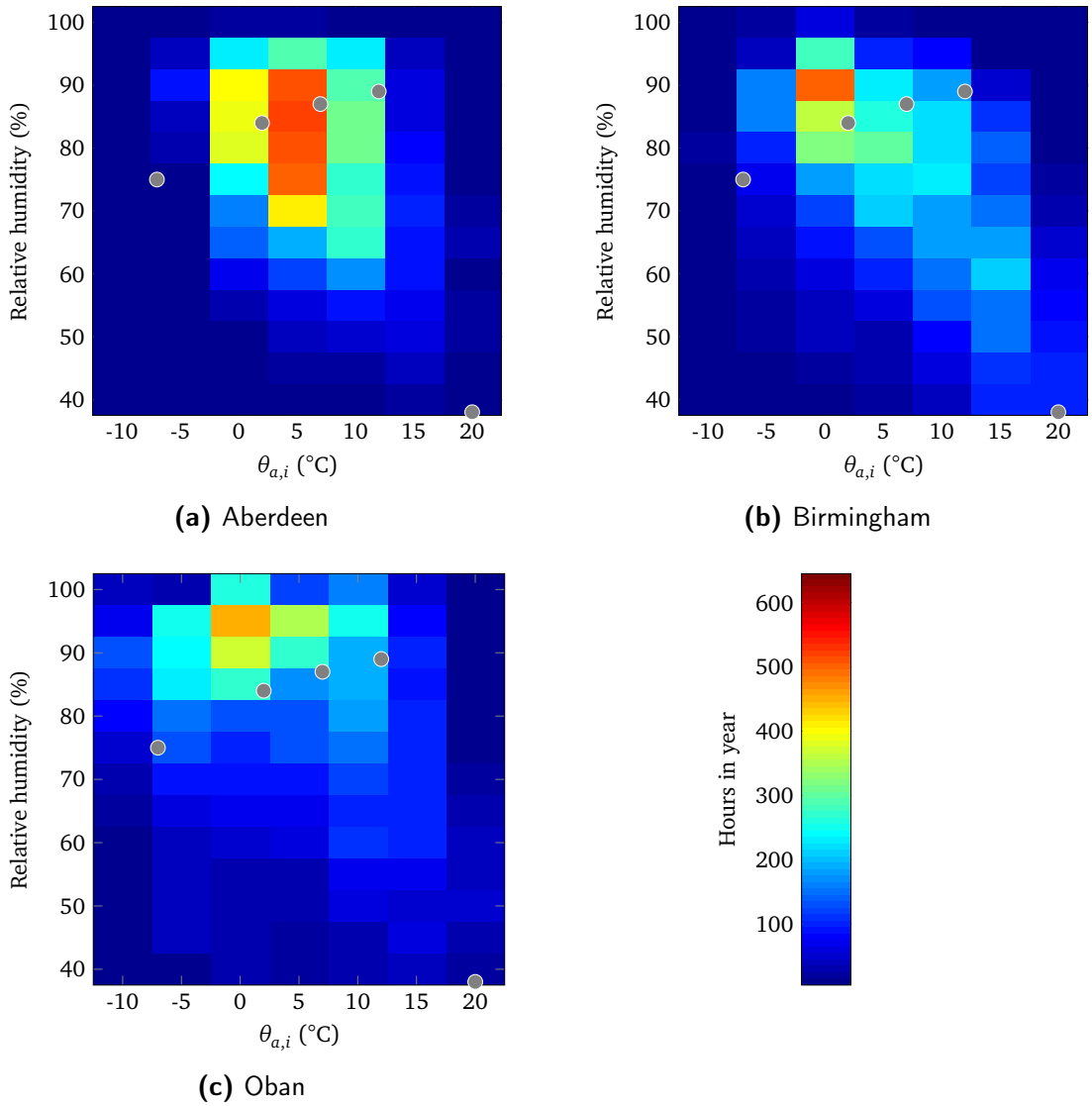

(a) Aberdeen

(b) Birmingham

(c) Oban

Figure 7.1: Histograms of annual climate data

In contrast, the most frequently occurring relative humidity levels in Oban are markedly higher than EN 14511 levels (though the spread is broader than for Aberdeen). When simulating ASHP in this location using the proposed modelling method, the results are likely to over-predict performance. The most frequently occurring relative humidity levels in Birmingham are also higher than EN 14511, though less so than Oban. Some over-prediction also seems likely.

7.2.4 Summary

In conclusion, the limited nature of EN 14511 test data restricts the modelling method to fixed output ASHP, and means that large assumptions must be made in order to represent

transient behaviour. Additionally, defrost cycles cannot be explicitly modelled, meaning the method's dynamic status is questionable. The averaged impact of defrost cycles is accounted for, however the variation in this impact as humidity levels change is not. The latter of these factors requires that care is taken when simulating using climate data in which typical humidity levels are markedly different to those used in EN 14511 tests. The following subsection discusses potential extensions to standard testing which would help address these limitations.

7.3 Suggested areas for strengthening standard testing

It is recognised that enabling dynamic modelling is currently at best a secondary aim of standard heat pump testing such as EN 14511. Primary aims are likely to be to support the market by providing confidence to buyers, and to encourage improvements in the technology. However extensions to the EN 14511 methodology would enable it to also better provide for dynamic modelling. Two key areas where testing could be strengthened relate to defrost behaviour. The expansion of tests to a greater range of humidity level, and the provision of additional data from existing on defrost duration frequency and energy use, would both enable improvements to the representation of performance under frosting conditions. A third is the inclusion of part load tests for both variable and fixed output ASHPs. This could allow information on transient behaviour to be extracted.

An area where potential extensions to testing were considered but are not recommended is that of water flow rate. Although this influences ASHP performance, there is insufficient variation in the flow rates used in EN 14511 testing for its impact to be discerned by regression analysis, and it is therefore omitted from the proposed modelling method. Analysis carried out in section 6.2 suggested that sensitivity of ASHP performance to water flow rate is low, and further the mass flow rates used in tests seem to be within the ranges that ASHP are typically designed for (this may be no coincidence). The omission of water flow rate as a variable is therefore unlikely to be an issue for the majority of simulation scenarios. Extending the EN 14511 test protocol to encompass a greater range of water flow rates is not considered worthwhile. This conclusion may need to be revisited in coming years however, as the EU pushes for the adoption of variable speed circulation pumps.

7.3.1 Defrost cycle reporting and humidity levels used

As described in the previous section, the fact that all EN 14511 tests at a particular air temperature have the same humidity level means that the impact of humidity on ASHP performance cannot be determined. A more useful approach for the modeller would be if at least a subset of the test points were run at multiple humidity levels. This may mean, taking the example of the test points with an air temperature of 2 °C, running tests with 55%, 75% and 95% relative humidity rather than just 84%.

The proposed method does not represent defrost cycles explicitly, but rather models integrated performance - the time-averaged impact of defrost cycles is included in regression models. Were test points extended to include multiple humidity levels, relative humidity could be included as a variable in the regression models for thermal output and power load. Alternatively, as the boundary of the zone in which frosting has an impact is strongly defined, a better approach to modelling may be the three-part approach of Afjei and Wetter [40]. The model would consist of regression models of steady state, peak (unfrosted) performance (these could be based on test points at 55% relative humidity); secondary regression models, subtracted from the first, representing the averaged losses due to defrost cycles at the current conditions; and a component representing transient behaviour.

The approach of representing integrated performance was shown to be insufficient for some ASHP at least, though improvements to defrost control in most modern ASHP may reduce this issue. An explicit representation of defrost cycles would be desirable for studies where the minute-to-minute behaviour of the ASHP is of interest. A simplified first principles approach like that of Vocale et al. [19] would perhaps require fewest changes to the EN 14511 test standard: a small change in reporting, such as the addition of average evaporator temperature and air outlet temperature at each test point would be sufficient. It would be a compromise in terms of accuracy however, and would not distinguish ASHP with highly efficient defrost cycles from those with wasteful ones: the data set analysed in appendix A showed there is a wider range of performance levels.

An empirical approach such as those described by Kelly and Cockroft [33] and Petinot [14] seem likely to offer better accuracy. These require as a minimum information on the time between defrost cycles as well as their energy use and duration - ideally at multiple

humidity levels. Additionally this approach would require not just integrated performance over the whole test to be reported, but also peak performance (that is, average performance once defrost periods are stripped out). This would make test reports considerably more complex, though would not itself require additional tests to be run.

7.3.2 Part load testing

Increasing part load testing of ASHP would enable the modelling of variable output ASHP, as well as aid in the determination of transient parameters. EN 14511 itself omits part load tests by requiring that, if the ASHP being tested is a variable output unit, all controls must be set to their maximum. European standard EN 14825 [37] does includes a process for part load testing, however it forms part of a method for calculating seasonal performance. The part load factors at which a heat pump must be tested are not set for all heat pump units but depend on the relationship between the heat demand of the building model and the particular heat pump's thermal output in given weather conditions. The number of test points are very limited and could not easily be integrated into a dynamic modelling method.

In contrast a (now superceded) development draft of EN 14825 [60] focussed solely on part load testing. This proposed heat pumps were tested again at the same test points as EN 14511 stipulated, but at 50% output. It could be applied to both variable output and fixed output ASHPs, in the latter case by forcing the ASHP to switch on and off at set intervals.

This would have resulted in a reasonably simple set of test data, and a straightforward way of extending the method to variable output ASHP by just including a part load factor variable in regressions.

If high resolution data sets from part load testing of fixed output ASHP could be made available, this would also provide perfect calibration data for their transient parameters. The method for determining their values set out in IEA Annex 42, and later adopted by the Kelly and Cockroft for their ASHP model, would be ideal for this task. This requires high resolution data covering a step change in operation, precisely what occurs at start up and shut down. A virtual test bench is then set up in a suitable modelling environment, such as ESP-r, with the same boundary conditions for the model as in the test data. Optimisation software is then used to run multiple simulations, changing the values of transient parameters each time until a sufficiently close match between test data and simulation are achieved. Such a

process was not applied and tested here due to the lack of suitable data.

Part of EN 14511's role is to help inform National Calculation Methodologies, and these methodologies are beginning to encompass dynamic simulation. One can imagine that ultimately, the purpose of standards such as EN 14511 becomes less about generating tables of performance data, and more about generating the coefficients for an official modelling method. A prerequisite of this approach is the identification of a universal modelling method that can be applied to all examples of a technology.

It appears from this work that the regression modelling aspect of the proposed method largely achieves this universality requirement, though testing on full rather than partial sets of EN 14511 test result would be desirable. There is potential for issues where defrost cycles and part load operation have a strong interaction, as this is not captured by EN 14511 tests, and it is unlikely that the method would provide reliable results for climates with humidity levels different to those used in tests.

7.3.3 Section summary

In summary, the findings of this work suggest that there are two key areas in which extensions to standard testing of ASHP would benefit the production of dynamic models.

The first is the addition to test reports of data on defrost cycle frequency, duration and energy use at existing test points, to enable explicit representations of defrost cycles to be developed. Some benefit would be gained just by publishing peak and integrated performance. It would also be desirable if tests at each air temperature were repeated with different humidity levels, as this is likely to have an impact on defrost cycles and integrated performance.

The second is the addition at a part load test for both fixed and variable output heat pumps, to enable calibration of transient parameters. Full high resolution data from these tests would need to be made accessible to modellers.

7.4 Future uses of dynamic ASHP modelling

The introduction to this thesis described three expected uses for a dynamic ASPH modelling method based on EN 14511 data. The first was in research studies aimed at improving

installation practices, motivated by UK field trial data which showed very mixed performance levels. The second was in research studies into the use of ASHP to aid in grid balancing. The third was in a future dynamic simulation-based National Calculation Methodology.

The second of these uses is seen as the most likely. Long term emissions targets such as the EU's commitment to an 80-95% reduction on 1990 levels by 2050) will require an extensive decarbonisation of the heating sector - which will involve at least a partial switch from gas to electricity generated by renewables. How to economically accommodate an increasing proportion of uncontrolled renewable generation within the electricity network is a key question that will need to be solved for this to succeed. This has driven a large number of studies involving combinations of heat pumps, thermal storage and elements of demand response. Dynamic simulation is an important tool for investigating novel systems and controls quickly and economically.

The idea of using dynamic simulation as part of building standards regulation for *domestic* buildings is from time to time raised. However, any such advance appears a long way off at best. In order for dynamic simulation to offer better results than the calculation methods currently in use, substantially more data on the building is likely to be required. It is therefore seen as unlikely, at least until such time as advances in modelling techniques, data collection technology or information management processes reduces the burden.

The focus of this work has been on the modelling of ASHP at a domestic scale. There is considerable potential for the use of the techniques in *non-domestic* settings, however. With regard to research use, the same motivations apply as with the domestic sector. Demand response, thermal storage and heat recovery from, for example, industrial processes or sewage are all the focus of current development.

There are, of course, a much wider range of heating system types in use in commercial buildings. However as far as an AHSP is concerned, there are really just two possibilities: either they will use water as a heat transfer medium, or there will be a direct heat transfer to air. In the former case, the same modelling principles and issues encountered here will apply.

With regard to regulatory compliance, dynamic simulation is already used in the case of non-domestic buildings. In the UK, it can be used for demonstrating compliance with the Approved Document L2A of the UK Building Regulations for new, non-domestic buildings. It

is required for the production of Energy Performance Certificates for buildings with complex features.

A dynamic ASHP modelling method along the lines of that proposed could therefore be more useful in a commercial setting. Some progress will be required before this is achieved however. The two dynamic simulation tools currently approved for use with regard to regulatory compliance in the UK are Integrated Environmental Solutions Limited Virtual Environment (IES VE) version 7.0.0.0, and Environmental Design Solution Limited TAS (EDSL TAS) version 9.3. Whilst these use dynamic simulation for the building side, plant simulation packages are quasi-steady state, meaning that the method proposed in this work would not be compatible. The high level approach used by these commercial packages is in fact identical to that of the steady state method used in comparative testing of the proposed method (section 6.1). This concluded that for some wet radiator systems at least, the quasi-steady state deployed was not sufficient to prediction of heat pump performance as the dynamics of the heating system as a whole are important.

In the longer term, a move to dynamic plant models as well may occur, either through existing approved software integrating dynamic plant modelling, or through another software package becoming approved. The method employed by some future approved software incorporating dynamic plant modelling can only be guessed at, and therefore it is difficult to comment on the potential applicability of the modelling method developed here. However it is worth noting that the grey box approach used in the proposed method is adaptable: the micro-CHP models developed under IEA Annex 42, with which the proposed modelling method shares many similarities, were successfully implemented in TRNSYS and EnergyPlus as well as ESP-r. There is every reason to believe that a similar process could be carried out for the proposed method.

In addition, the grey box approach of [43] is already included in TRNSYS. This deals with transient behaviour in a different manner (by fitting exponential curves to data). This is closely related to the proposed method: Afjei's exponential curves are equivalent to the solution of the energy balance equation underpinning the proposed method, which is a first order differential. Analytical or numerical solution methods could be applied to the energy balance equation for an ESP-r model to obtain parameters for TRNSYS exponential terms.

7.5 Chapter summary

The aim of this work is the development of a modelling method for ASHP which is suitable for dynamic building energy modelling tools, and which can be informed by data from standard testing. This chapter discusses the success of the proposed modelling method in meeting this aim, its relationship to other modelling methods in the literature, and highlights limitations and areas for further work.

Extensions to standard testing that would enable gaps in the proposed modelling method to be filled are recommended. The main suggestions relate to running additional tests at part loads and adding details on defrost cycles to the data reported. Finally the prospects for wider use of the proposed method are considered.

Chapter 8

Conclusions

The original aim of this work was to develop a method for the production of dynamic models of air-to-water air source heat pumps using just the results of performance testing under the European Standard EN 14511. The motivation was for the model to be of use in research and to inform the development of dynamic methods for National Calculation Methodologies.

A key conclusion is that it is not possible to develop a modelling method which is both dynamic and informed solely by EN 14511 data. The performance reports produced by EN 14511 testing include only average performance over a (typically three hour) test period at various operating conditions, and thus provide no information transient behaviour. No alternative basis for determining transient behaviour was found.

The choice was made to made to prioritise the dynamic strand of the project, and a grey box dynamic modelling method was developed which requires a minimal amount of dynamic data to calibrate.

Even with this relaxing of the input data requirement, it is questionable whether the method is truly dynamic. Standard data does not support the explicit modelling of defrost cycles, and the method is forced to reprsent only the averaged impact of frosting on performance. This means the use of the model is restricted to predicting performance over extended periods.

Some validation testing of the model was possible. Comparative testing against a known dynamic method showed good agreement in some conditions but not others. The discrepancy was traced back to the defrost cycle control employed by the known method. This causes a reduction in performance under frosting conditions at part load which is not captured

in standard test data. There is some evidence that this defrost cycle control method is not representative of the majority of modern ASHP.

Sensitivity analysis was also conducted on two aspects of the model. The first showed that water flow rate has little impact on ASHP performance over the range likely to be encountered, and the proposed method's omission of water flow rate as a variable is unlikely to cause noticeable bias in predictions.

The second aspect tested was the sensitivity of predictions to the values of parameters governing transient behaviour. This was shown to be low. The analysis further suggested that the predictions of a steady state ASHP model may may not be dissimilar to those of the proposed method over extended periods. This would of course mean that the dynamic strand of this work's aim was unnecessary, where only predictions of performance over extended periods are of interest. However it was not possible to draw firm conclusions from the simulations carried out.

Extensions to the standard testing are recommended, which would enable a fully dynamic model to be produced. This would be a required step if fully dynamic plant simulation is to be approved for use in National Calculation Methodologies. Key changes recommended are to add information from current tests on defrost cycle frequency and energy use; and to add at least one part load test, from which high resolution data would be made available. Together these would enable fully dynamic models to be produced.

As the method stands, it is likely to be of some use in research, for example in the development of demand response strategies. However the need for additional calibration data to that provided by standardised testing has eroded the usability advantage it was intended to have over other modelling methods. The grey box approach adopted by the method is likely to be most suitable for use in some future fully-dynamic National Calculation Methodology: however detailed commentary on the compatibility of the method can't be made given as currently approved dynamic software still uses a steady state approach for plant modelling.

Chapter 9

Further work

A number of areas which would benefit from further investigation emerge from this work.

Analysis of the sensitivity of the proposed modelling method to transient parameters suggested it may be possible for a steady state ASHP model within a dynamic plant simulation to produce similar results over extended simulation periods as the proposed method does. It would be valuable to explore this further. A steady state method could be easily calibrated using the data produced by current standard testing. It may be that this project's initial aim of producing a dynamic model was unnecessary when only long term performance is of interest: this would be useful knowledge for the future development of National Calculation Methodologies.

As current dynamic modelling software approved for NCM and compliance use still relies on steady state representations of plant networks, it would also be interesting to compare fully dynamic ESP-r simulation of a given ASHP installation with simulation using their dynamic building/steady state plant. This was explored to some degree in the validation chapter of this work, and the results cast doubt on the ability of steady state plant models to accurately represent ASHP performance with a wet radiator system and no weather or load compensation. If this also applies to other heating system typographies, it may suggest further development of approved software is required - and possibly a move to fully dynamic plant modelling.

Further validation work focussing on the approach taken by the proposed method and others with regard to the "integrated" representation of defrost cycles would also be helpful. Whilst the approach was found not sufficient in the comparative testing undertaken in this

work, it is not known whether the comparator model was truly representative of the majority of ASHP. If it is found that an explicit methods is required, this could also support a move by approved software to dynamic plant modelling.

Should the results of the above suggest that dynamic plant modelling would be of benefit to NCMs, further work would be required to confirm which of the proposed extensions to standard testing recommended in 7 are required: the two key recommendations, for part load testing to determine transient parameters and for the reporting of additional data on defrost cycles to enable explicit defrost models would be the main targets. An increase in part load testing would have the additional benefit of enabling the extension of the method to variable output ASHP.

A key uncertainty in the modelling method is the impact on performance of humidity levels different to those used in EN 14511 tests. Further work to address this uncertainty would also be of benefit. Section 7.3 discussed potential extensions to the test process which would be of benefit. In the meantime, a comprehensive experimental study of the relationship between humidity and integrated performance for individual ASHP units may provide information which could be used to improve the method. The need for such a study has also been remarked upon by other authors.

...

Bibliography

[1] Wärmepumpen-Testzentrum, Buchs, Switzerland, 2013. WPZ Bulletin, Edition 02-2013. URL http://institute.ntb.ch/fileadmin/Institute/IES/pdf/WPZ_Bulletin_02-2013.pdf.

[2] Parliament of the United Kingdom, 2014. The Domestic Renewable Heat Incentive Scheme Regulations 2014. URL www.legislation.gov.uk/uksi/2014/928/contents/made.

[3] Energy Saving Trust, 2010. Getting warmer: a field trial of heat pumps. URL http://www.energysavingtrust.org.uk/content/download/1801485/4898250/version/9/file/Getting_warmer_a_field_trial_of_heat_pumps_report.pdf.

[4] Cooper, S. J. G., Dowsett, J., Hammond, G. P., McManus, M. C., and Rogers, J. G., June 2013. Potential of Demand Side Management to Reduce Carbon Dioxide Emissions Associated with the Operation of Heat Pumps. *Journal of Sustainable Development of Energy, Water and Environment Systems*, 1(2):94–108.

[5] Kelly, N. J., Tuohy, P. G., and Hawkes, A. D., 2014. Performance assessment of tariff-based air source heat pump load shifting in a UK detached dwelling featuring phase change-enhanced buffering. *Applied Thermal Engineering*, 71(2):809–820. Date of Acceptance: 09/12/2013.

[6] Jin, H. and Spitler, J. D., 2002. A Parameter Estimation Based Model of Water-to-water Heat Pumps for Use in Energy Calculation Programs. *ASHRAE Transactions*, 108(1):3–17.

[7] Approved Document L2A, 2013. *Conservation of fuel and power in new buildings other than dwellings*. NBS, Newcastle, UK.

[8] BS EN 14511, 2013. *Air conditioners, liquid chilling packages and heat pumps with electrically driven compressors for space heating and cooling*. British Standards Institution.

[9] European heat Pump Association, 2016. Ehpa Quality Label. URL http://www.ehpa.org/ehpa-quality-label/.

[10] University of Strathclyde. ESP-r. URL http://www.esru.strath.ac.uk/Programs/ESP-r.htm.

[11] Cuevas, C., Lebrun, J., Lemort, V., and Winandy, E., 2010. Characterization of a scroll compressor under extended operating conditions. *Applied Thermal Engineering*, 30(6-7):605–615.

[12] Glen Dimplex Deutschland GmbH, 2014. Technical data LA 12tu. URL LA12TUhttp://www.dimplex.de/pdf/en/produktattribute/produkt_1725609_extern_egd.pdf.

[13] Uhlmann, M. and Bertsch, S. S., 2012. Theoretical and experimental investigation of startup and shutdown behavior of residential heat pumps. *International Journal of Refrigeration*, 35 (8):2138–2149.

[14] Petinot, R., 2011. *Assessment of Seasonal Performance of CO2 Heat Pump by Dynamic Modelling*. MSc Thesis, University of Strathclyde, Glasgow.

[15] Green, R., 2012. The effects of cycling on heat pump performance. URL `https://www.gov.uk/government/uploads/system/uploads/attachment_data/file/65695/7389-effects-cycling-heat-pump-performance.pdf`.

[16] Wellig, B., Imholz, M., Albert, M., and Hilfiker, K., 2008. Defrosting the fin tube evaporators of air/water heat pumps using ambient air. In *9th International Energy Agency Heat Pump Conference, Zurich CH*.

[17] Daikin AC (Americas), Inc, 2011. Engineering Data: Daikin Altherma DACA-EEDEN11-720. URL `http://www.daikinac.com/content/assets/DOC/DACA-EEDEN11-720%20Daikin%20Altherma%20Engineering%20Data.pdf`.

[18] Hubacher, B. and Ehrbar, M., 2000. *Verbesserung des abtauens bei luftbeaufschlagten Verdampfern: analyse gängiger abtauverfahren*. Bundesamt für Energie, Switzerland.

[19] Vocale, P., Morini, G. L., and Spiga, M., 2014. Influence of Outdoor Air Conditions on the Air Source Heat Pumps Performance. *Energy Procedia*, 45:653–662.

[20] Piucco, R., Hermes, C. J., Melo, C., and Barbosa, J., 2008. A Study of Frost Nucleation on Flat Surfaces: Theoretical Model and Experimental Validation. *International Refrigeration and Air Conditioning Conference*.

[21] Guo, X.-M., Chen, Y.-G., Wang, W.-H., and Chen, C.-Z., 2008. Experimental study on frost growth and dynamic performance of air source heat pump system. *Applied Thermal Engineering*, 28(17–18):2267–2278.

[22] Tassou, S. and Marquand, C., 1987. Effects of evaporator frosting and defrosting on the performance of air-to-water heat pumps. *Applied Energy*, 28(1):19–33.

[23] Albert, M., Sahinagic, R., Gasser, L., Wellig, B., and Hilfiker, K., 2008. Prediction of ice and frost formation in the fin tube evaporators for air/water heat pumps. In *9th International Energy Agency Heat Pump Conference, Zurich CH*.

[24] Chen, Y.-g. and Guo, X.-m., 2009. Dynamic defrosting characteristics of air source heat pump and effects of outdoor air parameters on defrost cycle performance. *Applied Thermal Engineering*, 29(13):2701–2707.

[25] Wang, W., Feng, Y. C., Zhu, J. H., Li, L. T., Guo, Q. C., and Lu, W. P., 2013. Performances of air source heat pump system for a kind of mal-defrost phenomenon appearing in moderate climate conditions. *Applied Energy*, 112:1138–1145.

[26] Karlsson, F., 2007. *Capacity control of residential heat pump heating systems*. PhD Thesis, Chalmers University of Technology, Gothenburg, Sweden.

[27] Microgeneration Certification Scheme, 2013. MCS 007 - Product certification scheme requirements: heat pumps issue 4.1. URL `http://www.microgenerationcertification.org/images/MCS_007_Issue_4.1.pdf`.

[28] ANSI/ASHRAE Standard 37, 2005. *Methods of Testing for Rating Electrically Driven Unitary Air-Conditioning and Heat Pump Equipment*. American Society of Heating, Refrigerating and Air-Conditioning Engineers.

[29] AHRI Standard 550/590, 2011. *Performance rating of water-chilling and heat pump water-heating packages using the vapour compression cycle*. Air-Conditioning, Heating, and Refrigeration Institute.

[30] BS EN 14511, 2007. *Air conditioners, liquid chilling packages and heat pumps with electrically driven compressors for space heating and cooling*. British Standards Institution.

[31] Dimplex UK Ltd. Air-eau Technical Planning Manual LA MI Issue 2. URL `http://www.dimplex.co.uk/assets/kb/operating_instructions/0/Air-Eau_LA_MI_Planning_Manual_Issue_2.pdf`.

[32] *MATLAB and Statistics Toolbox Release 2013a*. The MathWorks, Inc., Natick, Massachusetts.

[33] Kelly, N. J. and Cockroft, J., 2011. Analysis of retrofit air source heat pump performance: Results from detailed simulations and comparison to field trial data. *Energy and Buildings*, 43 (1):239–245.

[34] Beausoleil-Morrison, I. and others, 2008. *An Experimental and Simulation-based Investigation of the Performance of Small-scale Fuel Cell and Combustion-based Cogeneration Devices Serving Residential Buildings: Final Report of Annex 42 of the International Energy Agency's Energy Conservation in Buildings and Community Systems Programme*. Natural Resources Canada Ottawa.

[35] Wemhoener, C., Afjei, T., and Dott, R., 2008. IEA HPP Annex 28 – standardised testing and seasonal performance calculation for multifunctional heat pump systems. *Applied Thermal Engineering*, 28(16):2062–2069.

[36] BS EN 15316-4-2, 2008. *Heating systems in buildings. Method for calculation of system energy requirements and system efficiencies. Space heating generation systems, heat pump systems*. British Standards Institution.

[37] BS EN 14825, 2013. *Air conditioners, liquid chilling packages and heat pumps, with electrically driven compressors, for space heating and cooling. Testing and rating at part load conditions and calculation of seasonal performance*. British Standards Institution.

[38] Baster, E., Murphy, G., Counsell, J., Allison, J., and Counsell, S., 2013. Symbolic modelling and predictive assessment of air source heat pumps. *Building Services Engineering Research and Technology*, 34(1):23–39.

[39] Jenkins, D., Tucker, R., Ahadzi, M., and Rawlings, R., 2008. The performance of air-source heat pumps in current and future offices. *Energy and Buildings*, 40(10):1901–1910.

[40] Afjei, T. and Wetter, M., 1997. TRNSYS Type 401: Compressor heat pump including frost and cycle losses. URL `http://www.transsolar.com/__software/download/en/ts_type_401_en.pdf`.

[41] Jin, H. and Spitler, J., 2003. Parameter estimation based model of water-to-water heat pumps with scroll compressors and water/glycol solutions. *Building Services Engineering Research and Technology*, 24(3):203–219.

[42] Bendapudi, S. and Braun, J. E., 2002. A Review of Literature on Dynamic Models of Vapor Compression Equipment. Technical Report 4036-5, ASHRAE. URL `http://www.nist.gov/tc75/docs/1043-RP_Dynamic_Modeling_Literature_Review.pdf`.

[43] Afjei, T. and Dott, R., 2011. Heat pump modelling for annual performance, design and new technologies. In *12th Conference of International Building Performance Simulation Association, Sydney*.

[44] Fisher, D. E., Rees, S. J., Padhmanabhan, S. K., and Murugappan, A., 2006. Implementation and Validation of Ground-Source Heat Pump System Models in an Integrated Building and System Simulation Environment. *HVAC&R Research*, 12(sup1):693–710.

[45] Carbonell, D., Cadafalch, J., Pärisch, P., and Consul, R., 2012. Numerical analysis of heat pump models: comparative study between equation-fit and refrigerant cycle based models. Technical Report 2012.004, International Energy Agency Task 44. URL `http://task44.iea-shc.org/data/sites/1/publications/2012.004.pdf`.

[46] Bertsch, S. S. and Groll, E. A., 2008. Two-stage air-source heat pump for residential heating and cooling applications in northern U.S. climates. *International Journal of Refrigeration*, 31 (7):1282–1292.

[47] Madani, H., Claesson, J., and Lundqvist, P., 2011. Capacity control in ground source heat pump systems part II: Comparative analysis between on/off controlled and variable capacity systems. *International Journal of Refrigeration*, 34(8):1934–1942.

[48] Lepore, R., Remy, M., Dumont, E., and Frère, M., 2012. Dynamic lumped-parameter model of a heat pump designed for performance optimization. *Building Simulation*, 5(3):233–242.

[49] da Silva, D. L., Hermes, C. J., and Melo, C., 2011. First-principles modeling of frost accumulation on fan-supplied tube-fin evaporators. *Applied Thermal Engineering*, 31(14–15):2616–2621.

[50] Getu, H. and Bansal, P., 2011. New frost property correlations for a flat-finned-tube heat exchanger. *International Journal of Thermal Sciences*, 50(4):544–557.

[51] Clarke, J. A., 2001. *Energy Simulation in Building Design*. Routledge.

[52] Hensen, J., 1991. *On the thermal interaction of building structure and heating and ventilating system*. PhD Thesis, Eindhoven University of Technology.

[53] Uhlmann, M. and Bertsch, S. S., 2011. Dynamic modelling of heat pumps. In *10th International Energy Agency Heat Pump Conference, Tokyo, Japan*.

[54] Bloomfield, D., 1985. Appraisal techniques for methods of calculating the thermal performance of buildings. *Building Services Engineering Research and Technology*, 6(1):13–20.

[55] Irving, A., 1988. Validation of dynamic thermal models. *Energy and Buildings*, 10(3):213 – 220.

[56] Scottish Government, 2015. Scottish House Condition Survey: Key Findings 2014. URL `www.gov.scot/Topics/Statistics/SHCS/Downloads`.

[57] Scottish Office, 1990. Technical Standards for compliance with The Building Standards (Scotland) Regulations 1990. URL `www.gov.scot/Resource/0045/00458881.pdf`.

[58] Cantor, J. and Harper, G. D. J., 2011. *Heat pumps for the home*. Crowood Press, Ramsbury, Marlborough, Wiltshire, [England].

[59] USA Department of Energy. EnergyPlus Energy Simulation Software - Weather Data. URL `http://apps1.eere.energy.gov/buildings/energyplus/weatherdata_about.cfm`.

[60] DD CEN/TS 14825, 2003. *Air conditioners, liquid chilling packages and heat pumps with electrically driven compressors for space heating and cooling — Testing and rating at part load conditions*. British Standards Institution.

Appendix A

Equation fit examples

The equation fit method set out in this work has been applied to EN 14511 data for 41 different ASHPs, obtained from a Swiss independent test centre [1]. Graphs of the fit achieved in each case appear in this appendix, and are discussed in section 5.2.

A.1 Categorisation of the fit achieved

The models have been assessed to determine as far as possible the success of the fitting process. They are divided into 3 categories: those with a satisfactory fit, those which may be usable with caution, and those which are unsatisfactory. It was found that the Φ_{ss} regression models were the critical factor: the P regression models were, with one exception, all satisfactory. This is due to the fact that defrost cycles have a far greater impact on thermal output than power, leading to more complex trends within data sets.

It was found that statistical tools were not totally satisfactory in determining the category of a model: whilst useful for discounting models with poor fit, some models with high R^2 value and low residuals never the less displayed trends which were highly unlikely given the underlying physics of the system. This is not an uncommon issue when data sets are small as they are here (generally consisting of 8 or 9 data points). Full EN 14511 data sets contain 18 data points, and for these, statistical tools will be a better guide.

Two tests were therefore necessary: are models a good representation of the data set; and, are models consistent with the underlying physics of the system? The first of these was dealt with by looking at R^2 values and relative error (the difference between each test result and the value predicted by the model, given as a proportion of the test result). Considering Φ_{ss} models first, there was a close match between models with an R^2 value less than 0.95 and those with a relative error greater than 10%: four failed both criteria, and one further model failed the former though not the latter. All 5 are categorised as unsatisfactory. Only two of the P models failed on either criteria: however these ASHP were amongst the group whose Φ_{ss} models had already failed.

The second test was more subjective. Based on the theory set out in chapter 2, one would expect Φ_{ss} to increase with air temperature, and to have either a weak or negative correlation with water temperature. Power load is expected to either increase or have a weak correlation with air temperature, and to increase with water temperature. This behaviour may, of course, be modified by the internal controls implemented by the manufacturer, or by localised effects (defrost cycles). It is therefore acceptable for models to exhibit behaviour different to that suggested by theory if it is supported by sufficient data points: but models which exhibit non-physical behaviour without sufficient support should be treated with suspicion.

No issues were found with power load regression models. However, many of the Φ_{ss} exhibit unsupported non-physical behaviour to some degree. Problems with fit typically manifested themselves in one of two ways:

- An uptick in Φ_{ss} predictions at low air temperatures, without this being supported by data points.
- The expected weak or negative correlation of Φ_{ss} with water temperature is breached for some part of the range of air temperatures, without this being supported by data points. The most common manifestation of this is that in many models, the 45 °C curve, rather than being midway between the 35 °C and 55 °C lines, will overlap one of them (generally at low air temperature) without this being supported by data points.

A.2 Reasons for unsatisfactory fit

In every case, the lack of data points was at least a contributory factor. A full set of EN 14511 test points under the current standard consists of 24 data points: six different air temperatures multiplied by four different water outlet temperatures — 35 °C, 45 °C, 55 °C and most recently 65 °C has been added. It would appear few ASHPs are currently capable of 65 °C, as no sets of data were seen which included these points. However, 18 data points could certainly be expected.

Almost all the sets of test data published by WPZ include only eight or nine data points. Only one of the points with a water output temperature of 45 °C is included, that for air temperature 7 °C. They also include no mare than three of the points with a water output temperature of 55 °C.

Whilst this does not appear to be an issue where the published data points describe clear trends, it can be when combined with other issues.

It is notable that for all of the seven ASHPs whose models are judged to be unsatisfactory, thermal output at test points with an air temperature of 2 °C was well below the trend suggested by other data points. The mean relative error at the test point air 2 °C and water temperature 35 °C is −15%, contrasting with −5% for ASHPs whose models were judged to be satisfactory: almost all have only a small dip at this point. This test point is close to the top of the region where frosting occurs, and indeed is where frost is likely to accumulate most quickly, as warmer air holds more moisture.

The data published by WPZ does not include much information on the physical design of the ASHPs tested. It does, however state “type of construction”, refrigerant used, and whether the ASHP incorporates an inverters and output control capability. There appears to be a correlation between each of these and the categorisation of the models, though admittedly sample size is not huge.

There are two main construction types. In the first, the refrigerant cycle is completely contained within a single unit. Some are designed for installation outdoors, whereas others are installed indoors. The second type are “split units”. In this format the evaporator and condenser are housed in separate units. The evaporator is installed outdoors, and the condenser unit indoors. [1] Five out of the seven the unsatisfactory models were of ‘split’ construction type, compared to three in seven for the 25 satisfactory models. It difficult to say whether this is coincidence or whether there is some intrinsic link. No reasons could be found as to why split units might have less predictable performance: there was no significant

[1] It should be stressed that although this format is familiar from small air conditioning units, these are generally air-to-air, whereas the data sets analysed here are all air-to-water heat pumps.

correlation between construction type and relative error at the test point air 2 °C and water temperature 35 °C which indicate inefficient defrost, for example.

There were three different refrigerant types in use across the set of 42 ASHP tests: R404, R407C, and R410A. Five of the seven unsatisfactory models used R410A, compared to just three of the 25 satisfactory models. There is no clear reason as to why the performance of ASHPs using R410A my be less predictable, though a possibility is that the use of R410A at high pressure ratios is challenging, due to a high discharge temperature. This may mean that ASHP which are not carefully designed may not be able to complete the tests at −15 °C. The mean number of data points included in data sets for ASHP using R410A was lower than the mean for the group as a whole.

Finally, six of the 42 data sets relate to ASHP with output control capability. Of these six, four are amongst the ASHP judged to be unsatisfactory. The EN 14511 test process requires that ASHP are operated at their maximum setting; generally this would means that AHSP with output control exhibit exactly the same trends as fixed output units. In five of the six cases, test results show no definite sign of output control actually being used, non the less three of the models proved unsatisfactory.

The sixth ASHP (number 200, fig. A.40, page 169) does show clear signs of output control, as thermal output does not have an increasing trend with air temperature, and power load has a clear negative trend. It would appear the manufacturer has used internal controls which artificially limit the maximum setting at higher air temperatures, perhaps to reduce part load cycling and improve performance in warmer conditions. If the control had been implemented such that a smooth thermal output curve is produced, this would be unlikely to present an issue: however it can be seen that thermal output data points have an irregular distribution, contributing to the resulting model's unsatisfactory categorisation.

Finally, four of the seven unsatisfactory ASHP models relate to data sets in which the data points themselves have minor breaches of the expected correlations between thermal output and air and water temperatures which are not readily explained by control strategies, and which have been magnified as the regression models try to extrapolate to parts of the temperature ranges without test data. An example is fig. A.37, on page 168. It is likely that with full data sets, a satisfactory fit could have been achieved - so long as trends not readily explained by theory are supported by data points, they are not a reason to discard a model.

In conclusion, ASHPs with poorly controlled or inefficient defrost mechanisms can cause problems for the fitting method when the total number of data points is low (less than ten). Even with the a full set of data, the fit will be less good, as the sharp dip in performance at around 5 °C will be smoothed by the quadratic curve of the model. As Chapter 5 discussed, third or fourth order models were trialled but offered little benefit - more detailed representations of defrost impacts, which would require extension to EN 14511 test data, would be required.

Whilst no causal links could be established, further common features in cases with unsatisfactory fit are split configuration; variable output capability; and the use of R410A as the refrigerant. Additional caution may be required when applying the method to ASHP with these features.

A.3 Models with satisfactory fit

In the following pages, graphs depicting the test data and models for those ASHPs judged to have achieved a satisfactory fit are presented first. Graphs of those categorised as requiring caution are then depicted. Finally, as examples of errors encountered, graphs of ASHP models judged to be unsatisfactory are presented.

Parameters of the models categorised as either satisfactory or usable with caution are given in appendix A.6 on page 171.

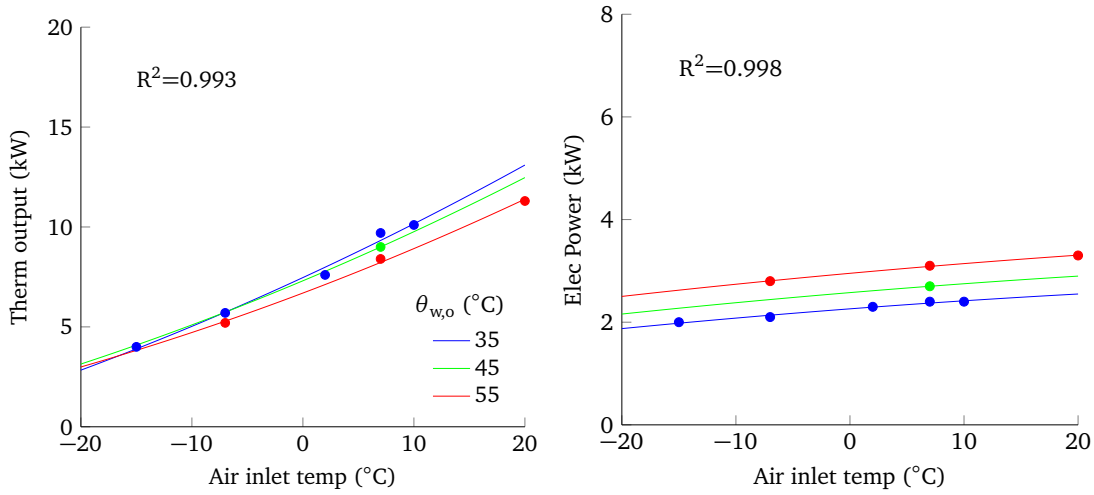

Figure A.1: ASHP 102 thermal output and power load

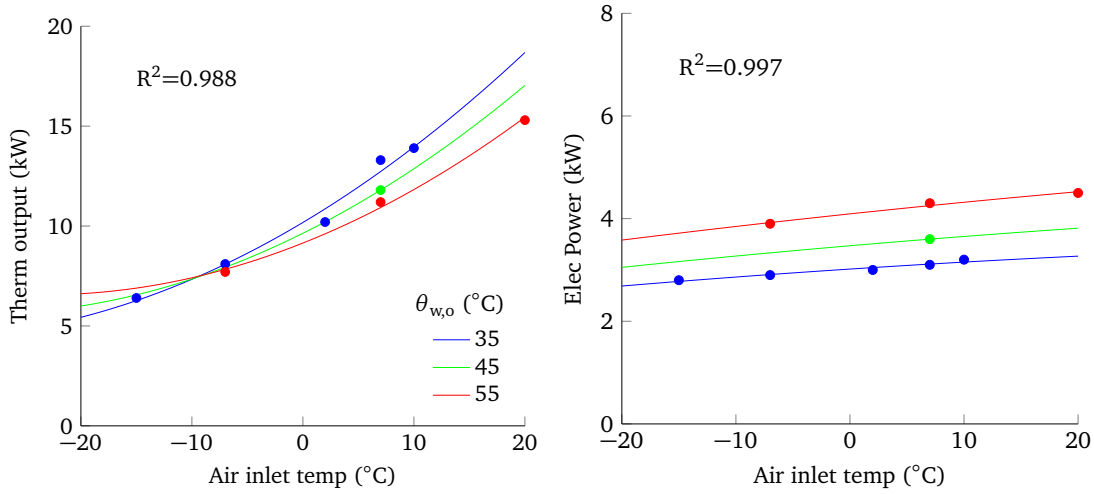

Figure A.2: ASHP 103 thermal output and power load

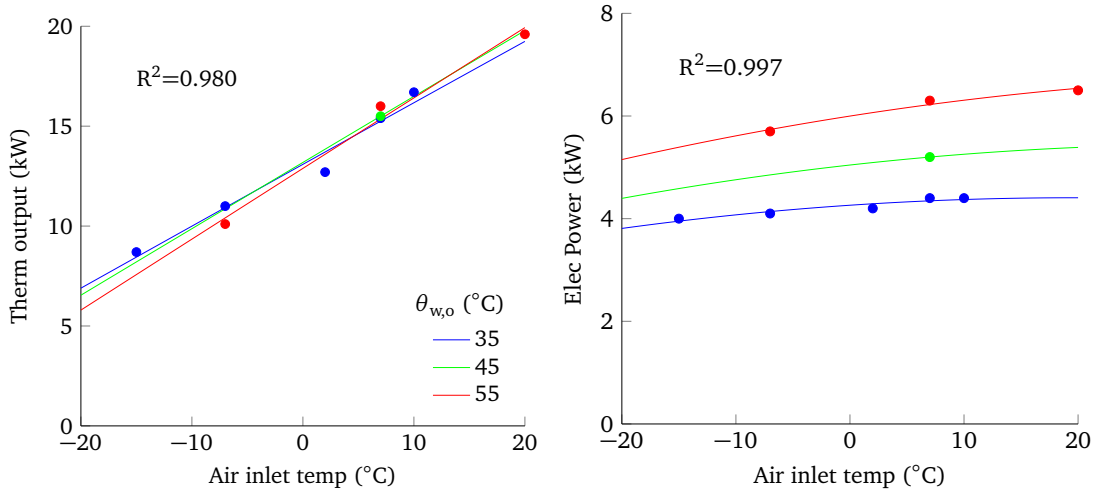

Figure A.3: ASHP 107 thermal output and power load

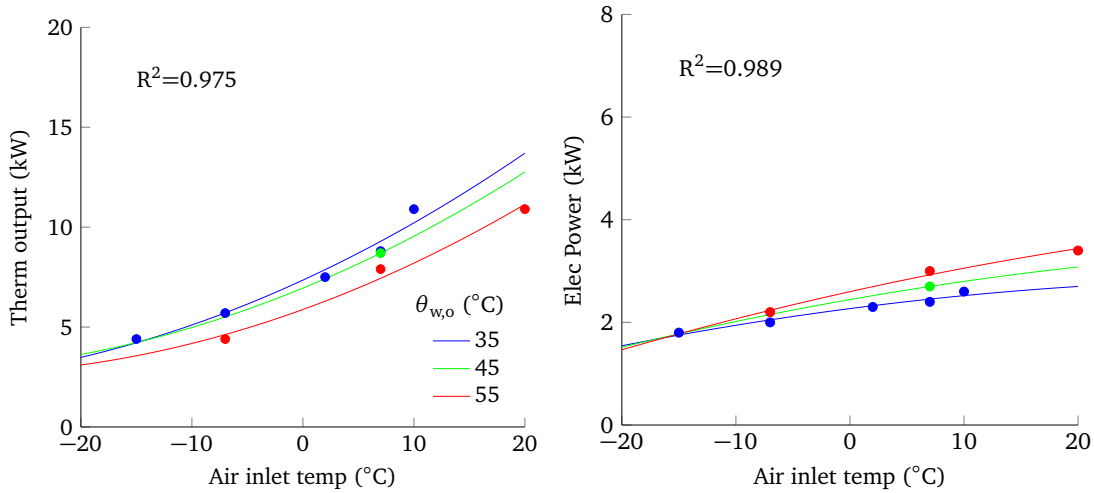

Figure A.4: ASHP 113 thermal output and power load

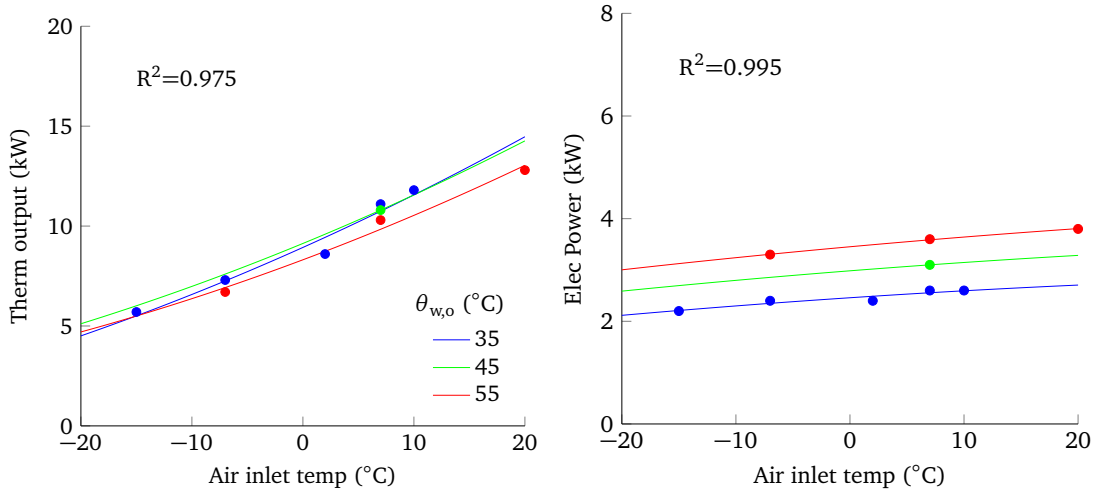

Figure A.5: ASHP 115 thermal output and power load

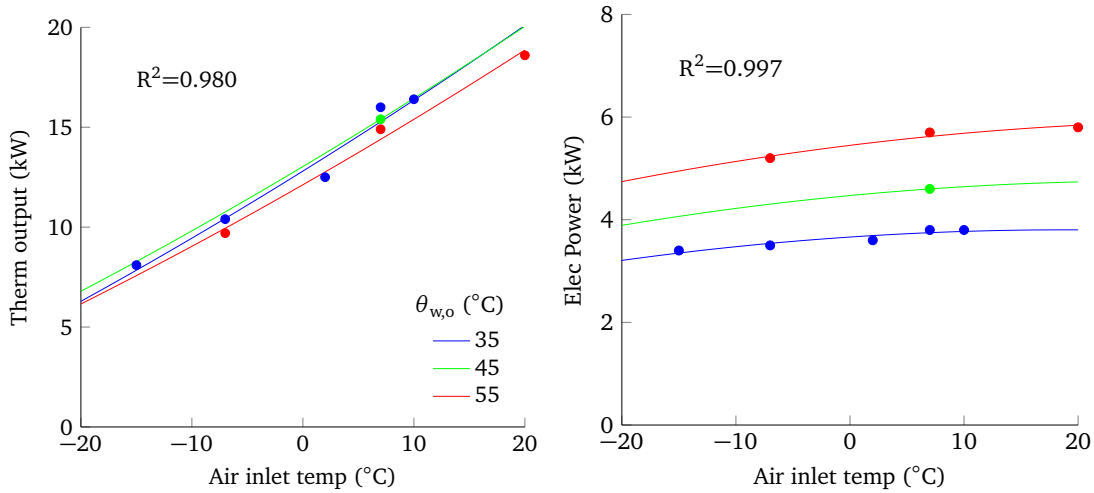

Figure A.6: ASHP 118 thermal output and power load

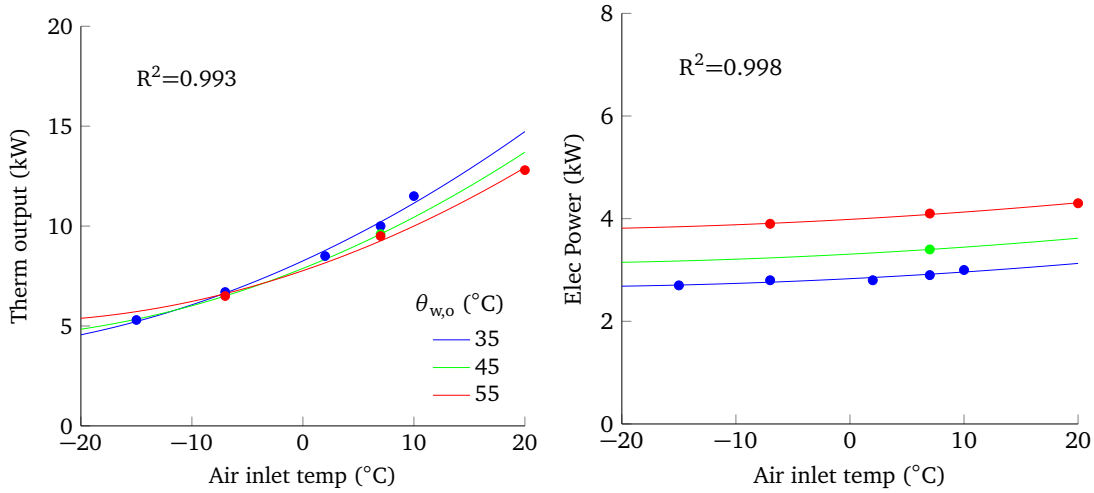

Figure A.7: ASHP 119 thermal output and power load

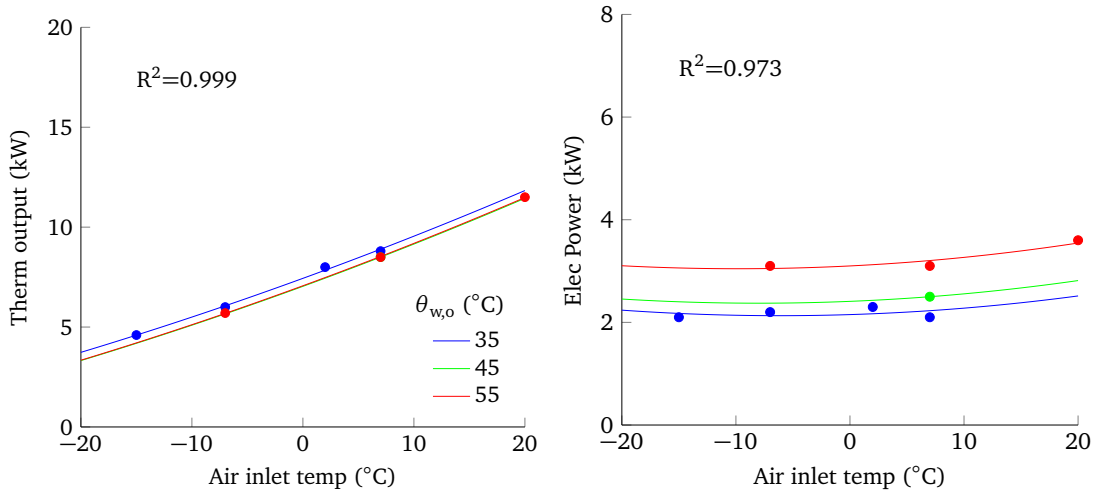

Figure A.8: ASHP 128 thermal output and power load

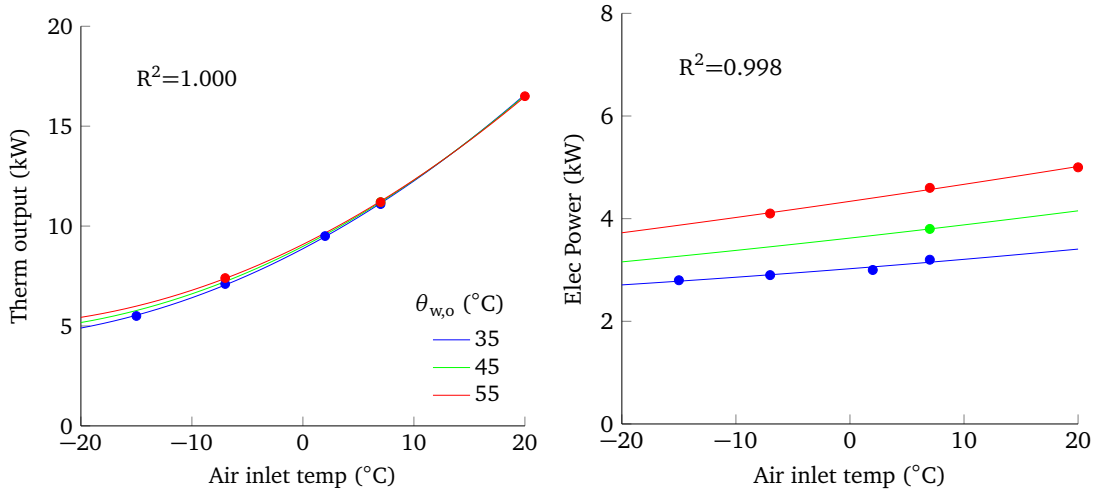

Figure A.9: ASHP 130 thermal output and power load

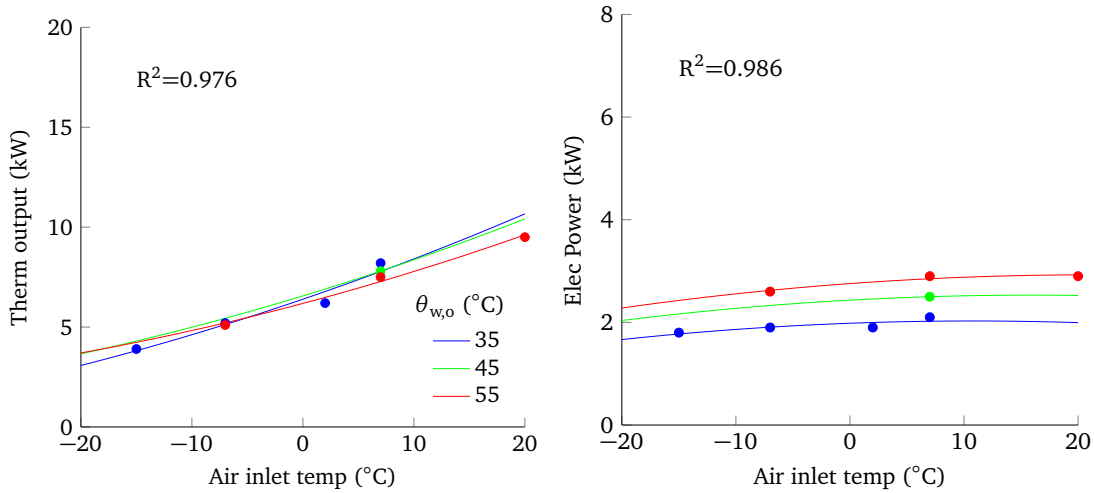

Figure A.10: ASHP 132 thermal output and power load

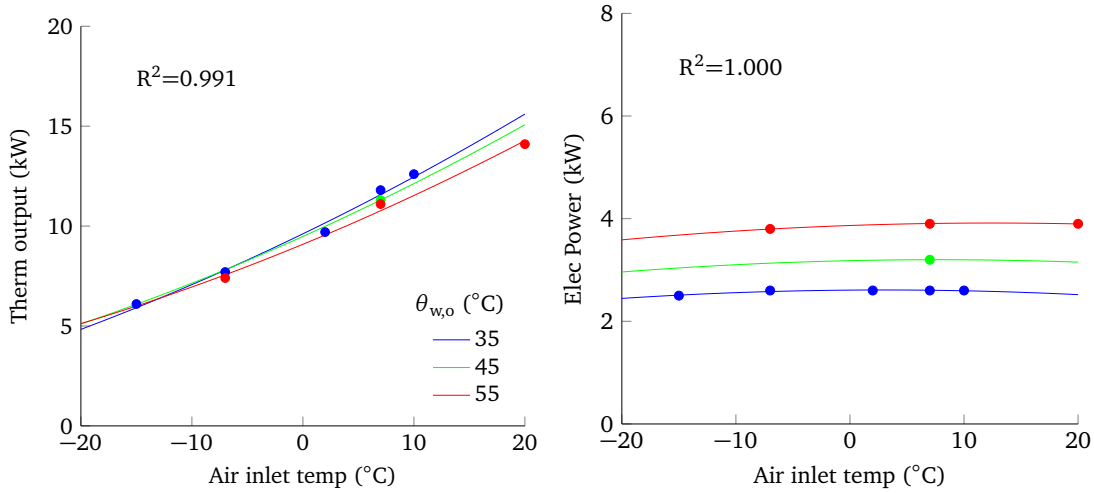

Figure A.11: ASHP 134 thermal output and power load

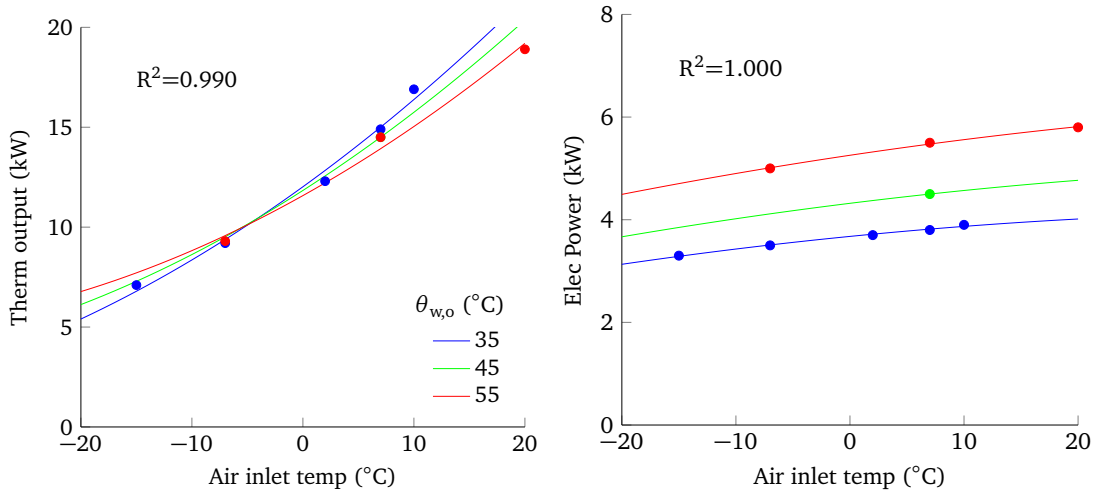

Figure A.12: ASHP 136 thermal output and power load

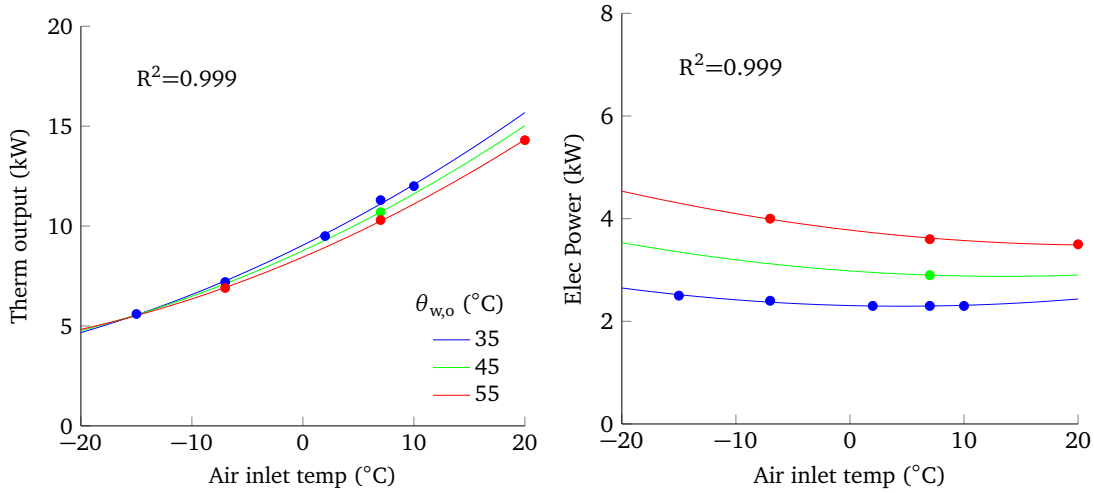

Figure A.13: ASHP 138 thermal output and power load

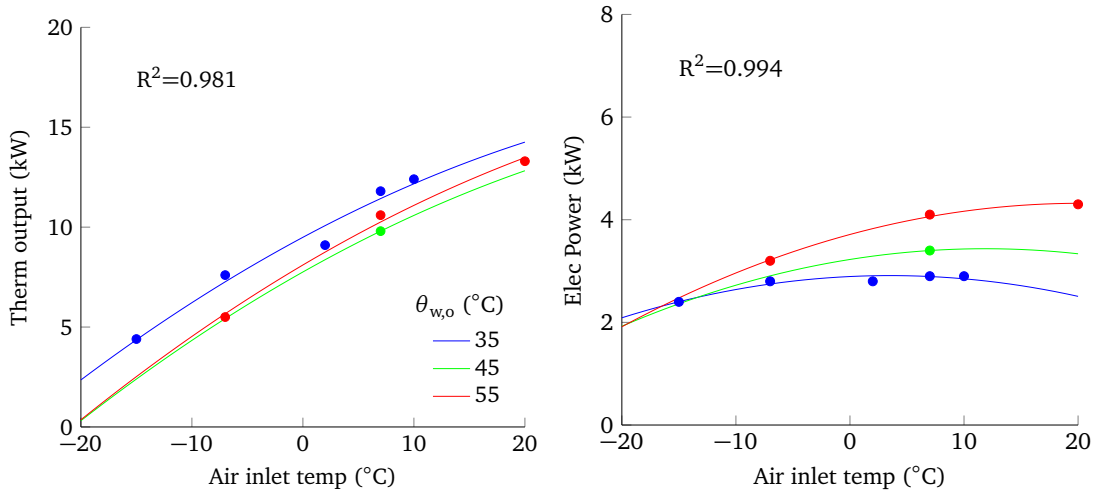

Figure A.14: ASHP 140 thermal output and power load

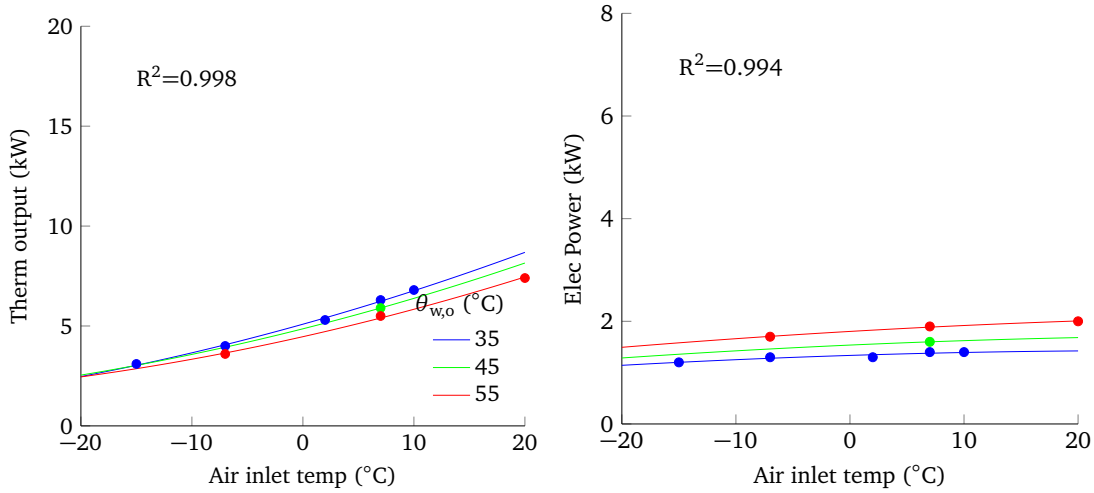

Figure A.15: ASHP 147 thermal output and power load

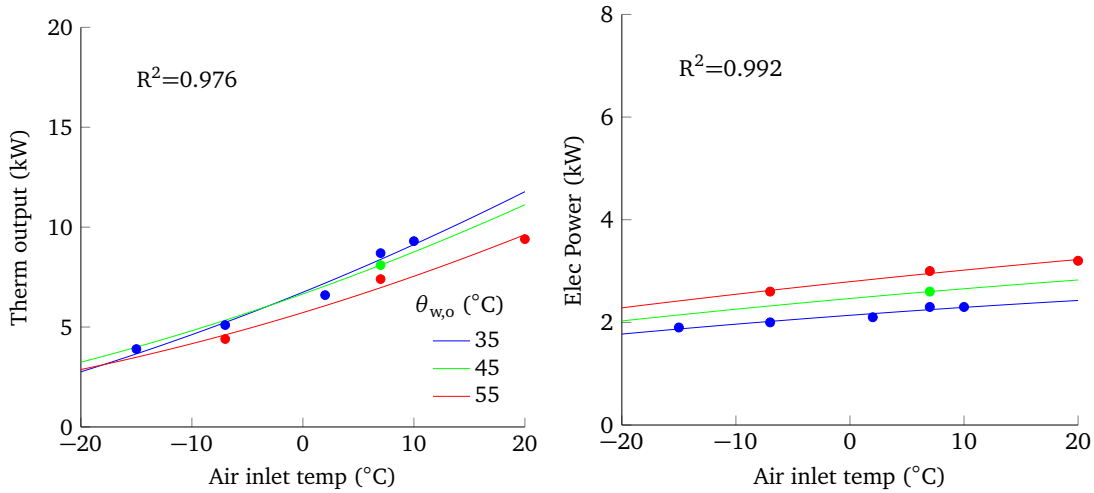

Figure A.16: ASHP 149 thermal output and power load

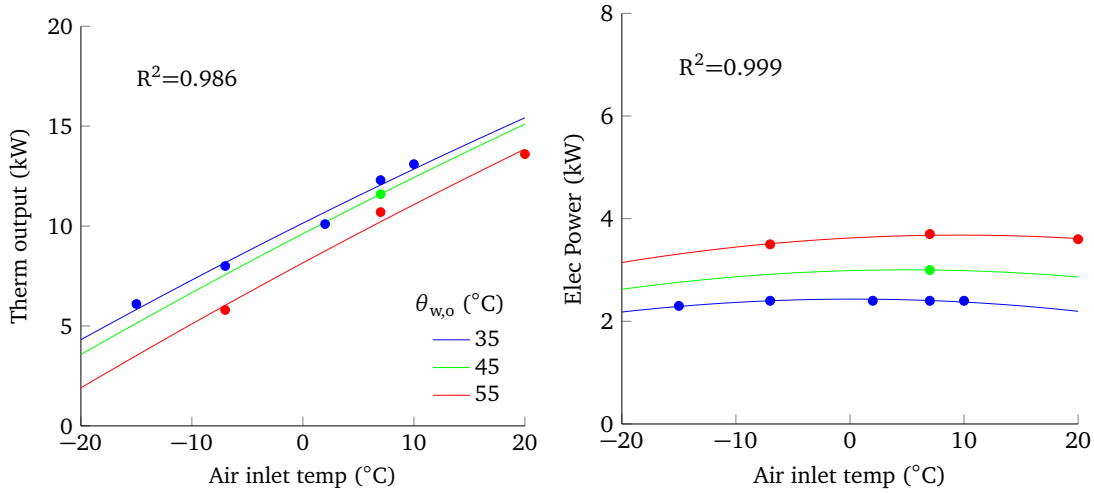

Figure A.17: ASHP 159 thermal output and power load

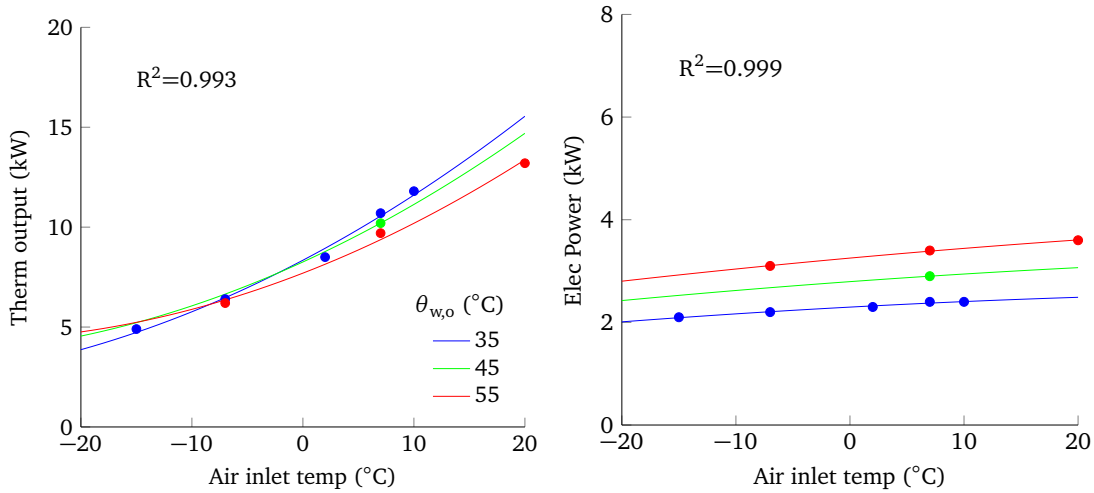

Figure A.18: ASHP 170 thermal output and power load

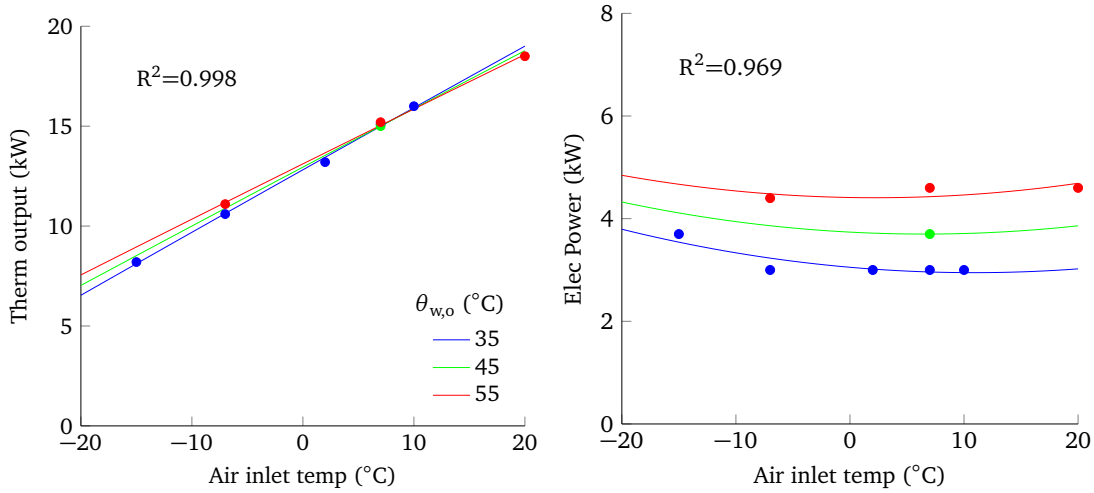

Figure A.19: ASHP 171 thermal output and power load

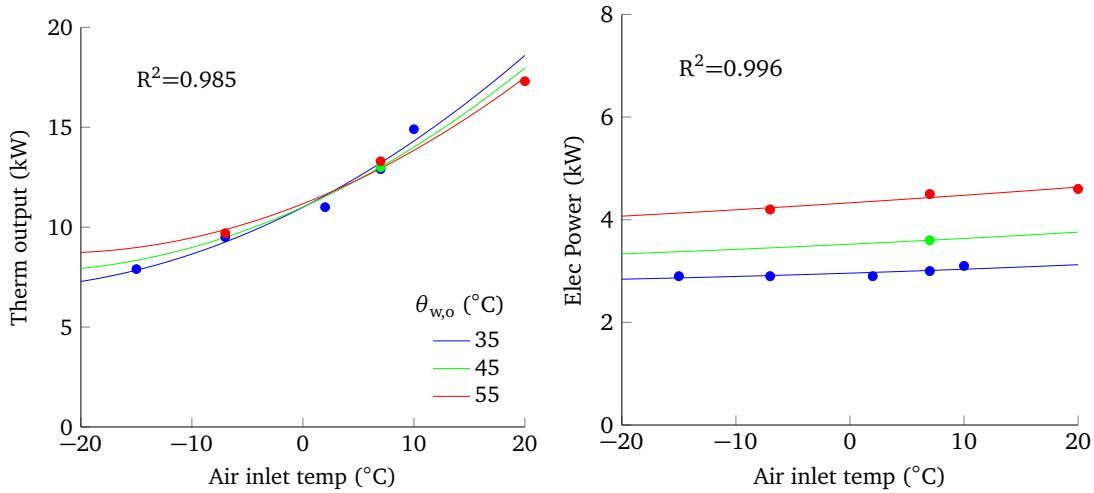

Figure A.20: ASHP 189 thermal output and power load

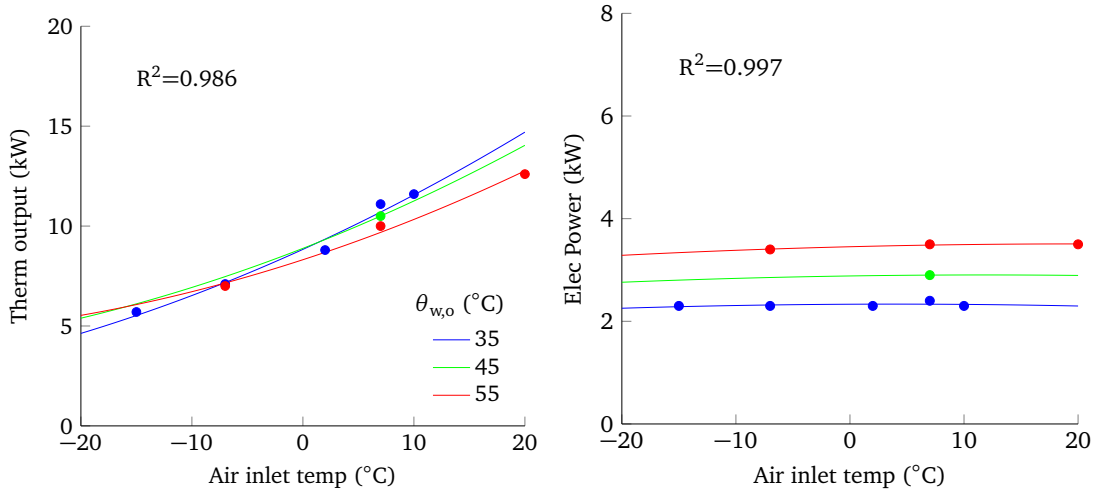

Figure A.21: ASHP 190 thermal output and power load

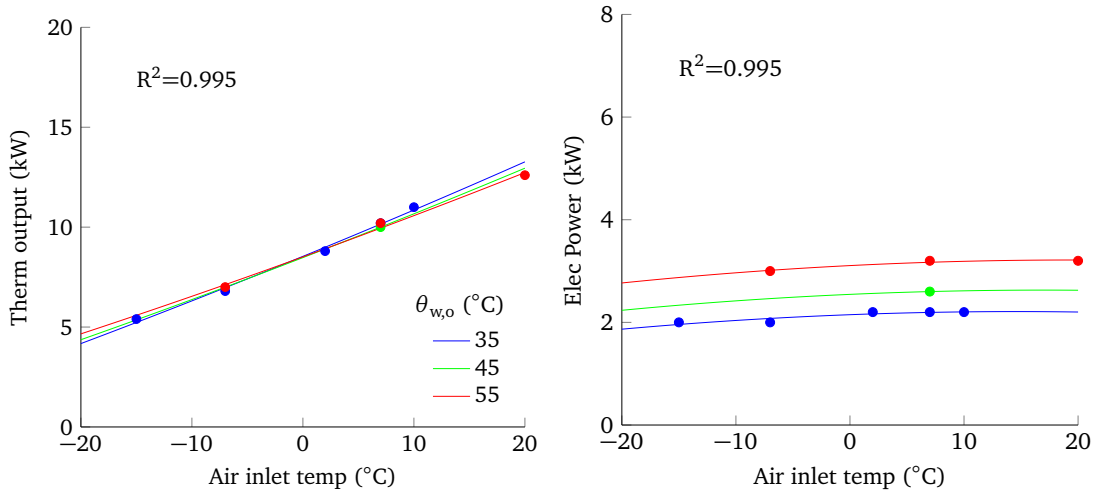

Figure A.22: ASHP 191 thermal output and power load

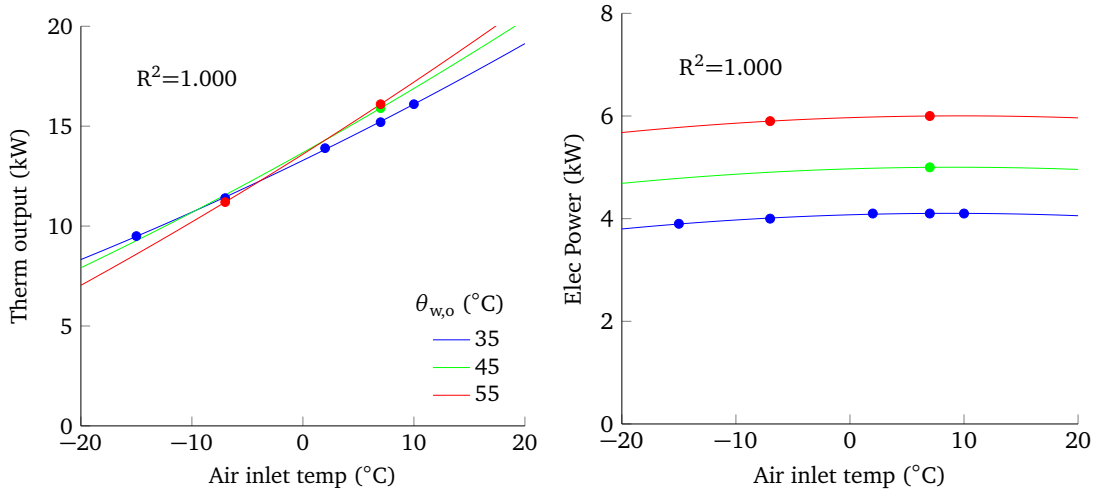

Figure A.23: ASHP 195 thermal output and power load

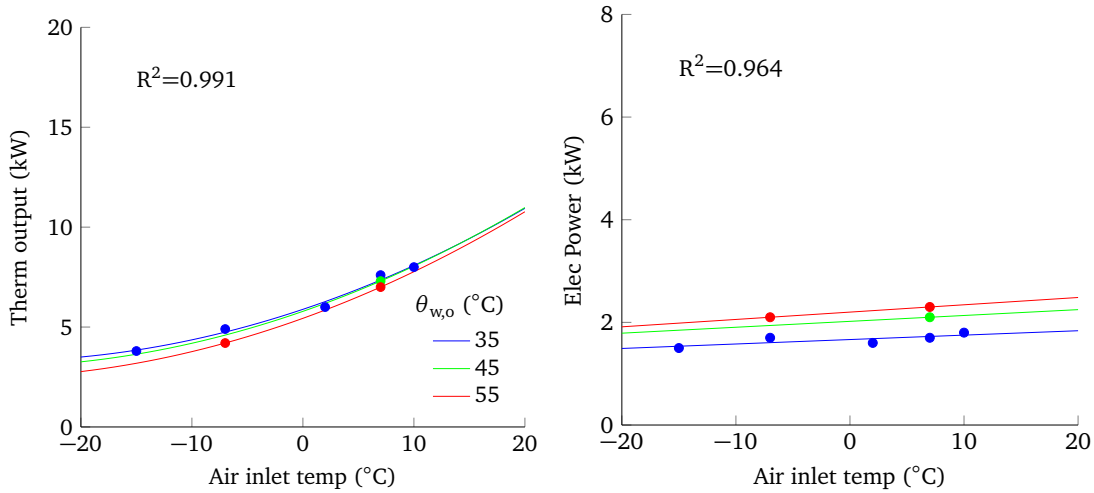

Figure A.24: ASHP 198 thermal output and power load

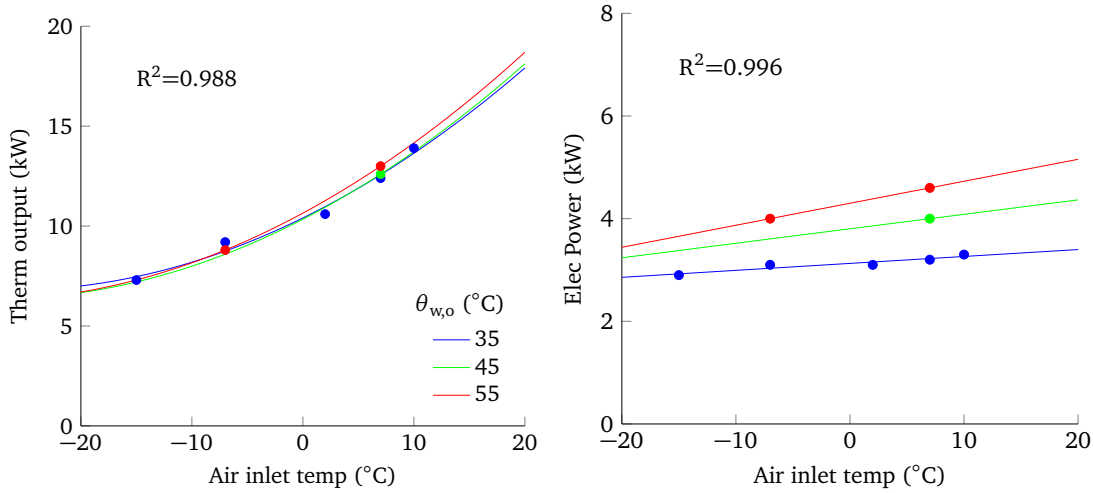

Figure A.25: ASHP 199 thermal output and power load

A.4 Models requiring caution

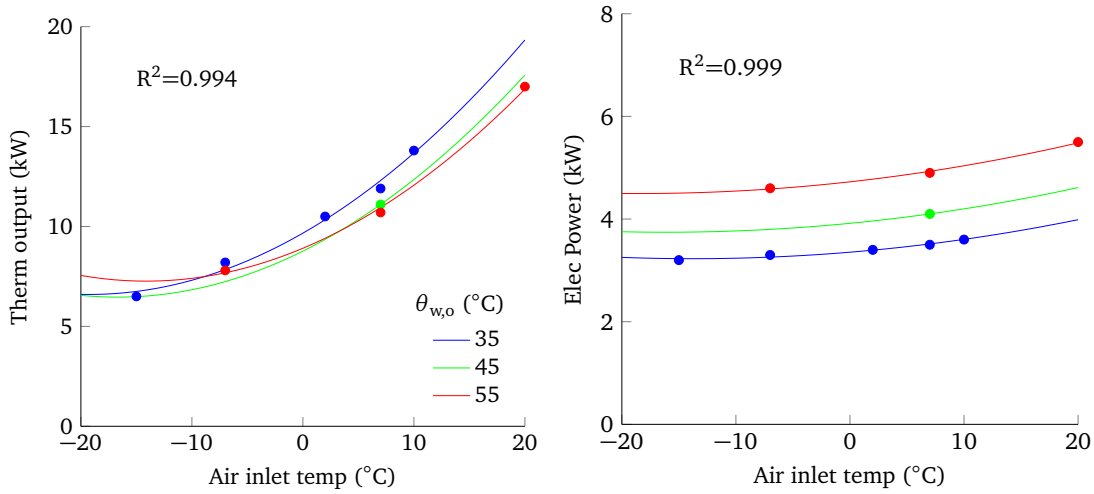

Figure A.26: ASHP 120 thermal output and power load

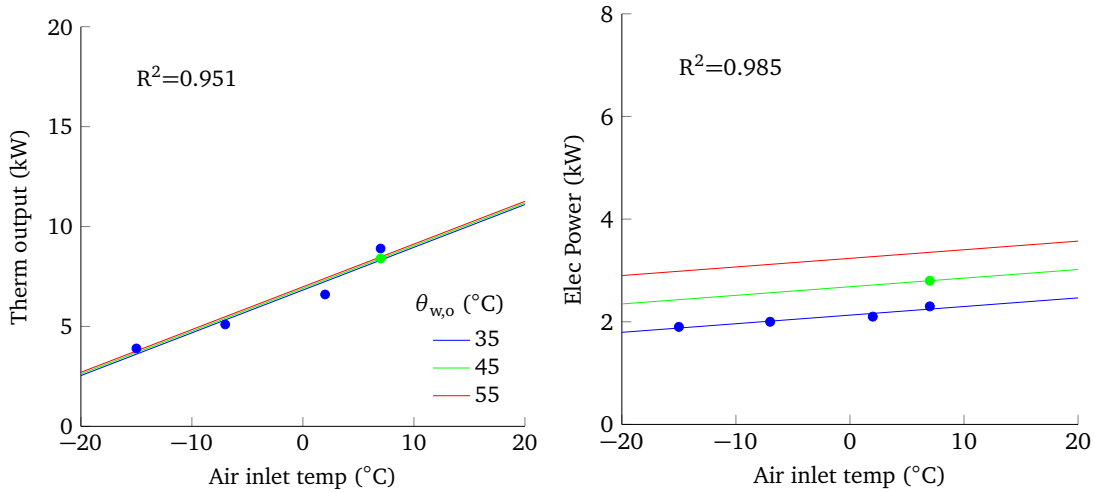

Figure A.27: ASHP 127 thermal output and power load

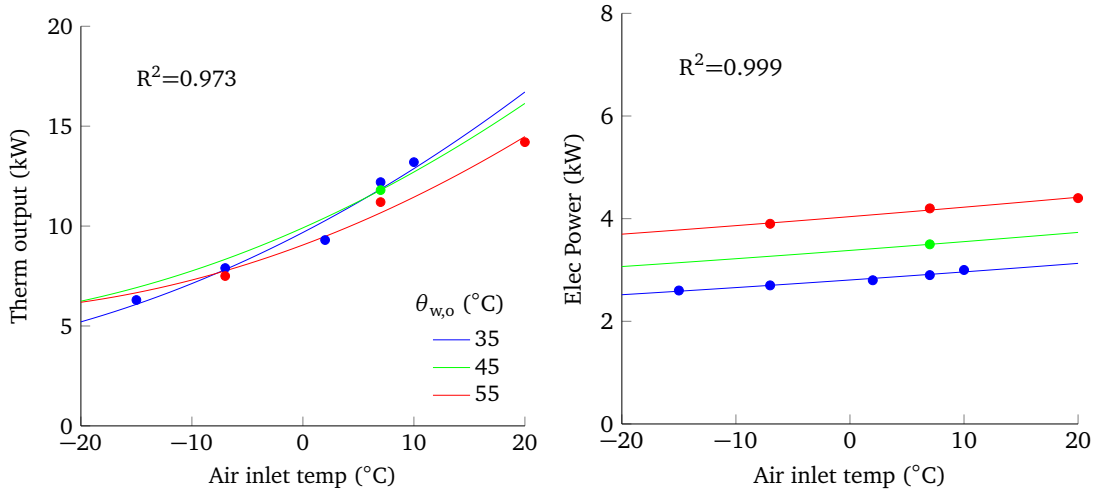

Figure A.28: ASHP 131 thermal output and power load

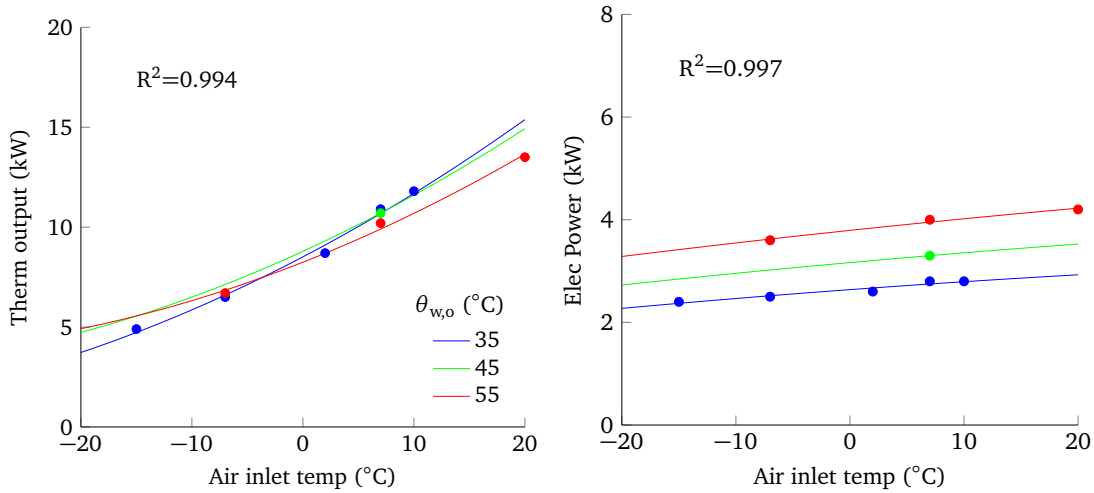

Figure A.29: ASHP 135 thermal output and power load

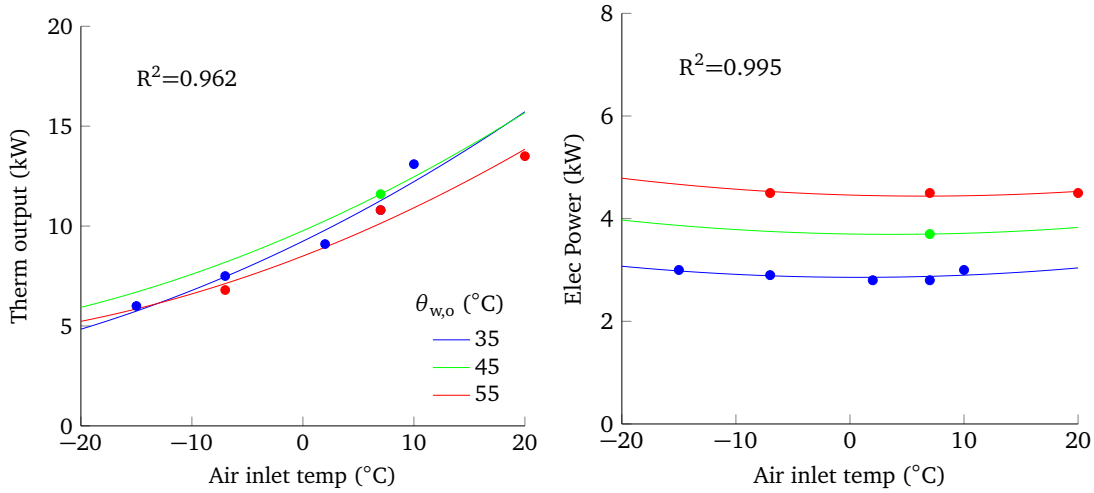

Figure A.30: ASHP 146 thermal output and power load

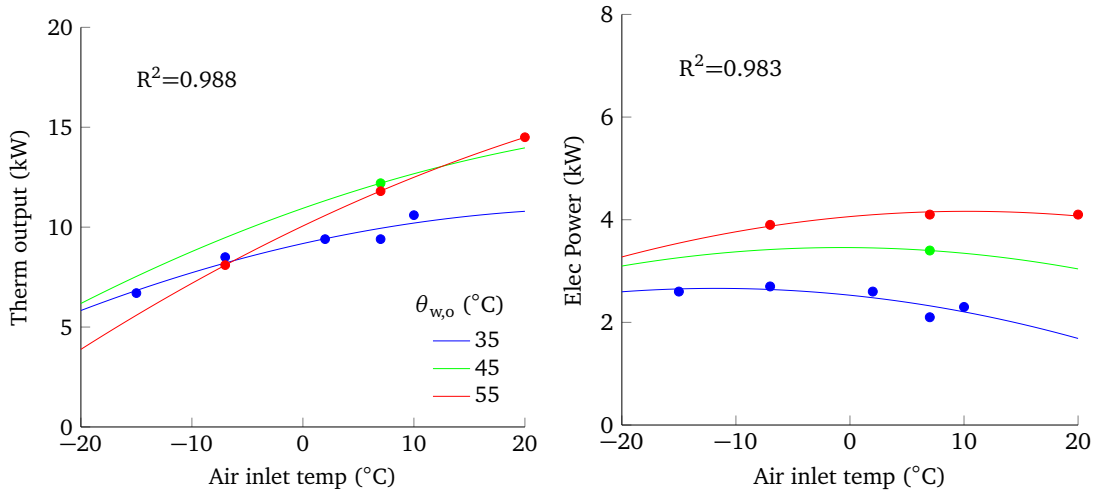

Figure A.31: ASHP 150 thermal output and power load

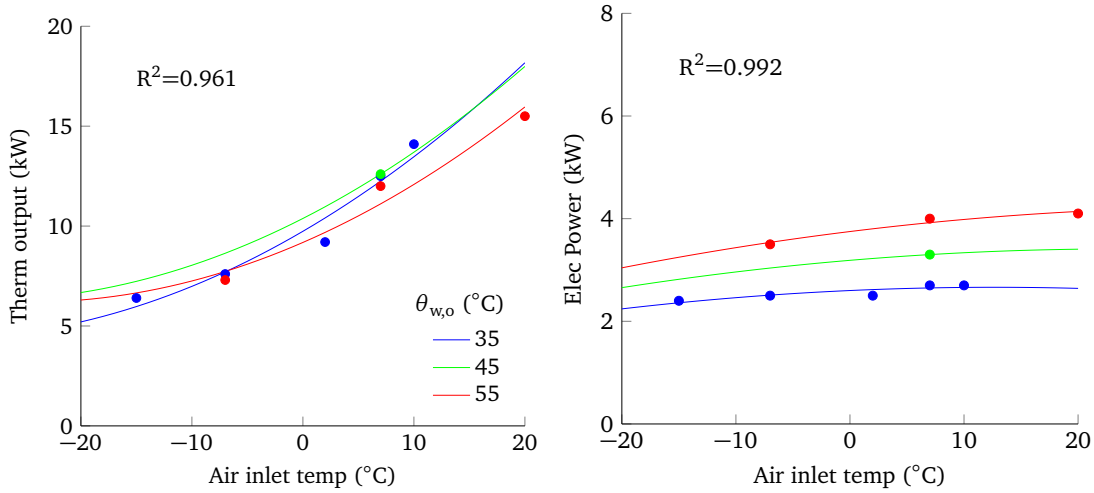

Figure A.32: ASHP 164 thermal output and power load

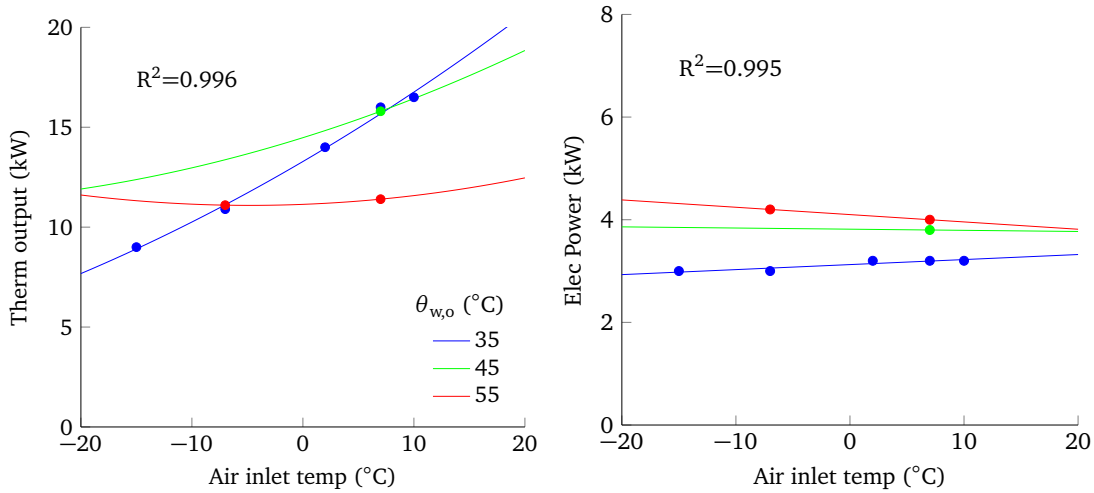

Figure A.33: ASHP 201 thermal output and power load

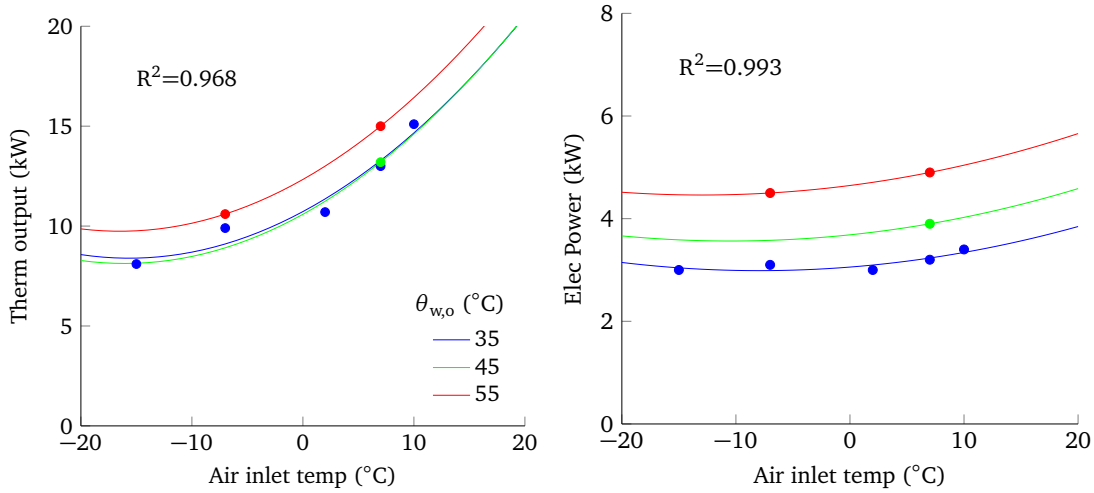

Figure A.34: ASHP 211 thermal output and power load

A.5 Models with unsatisfactory fit

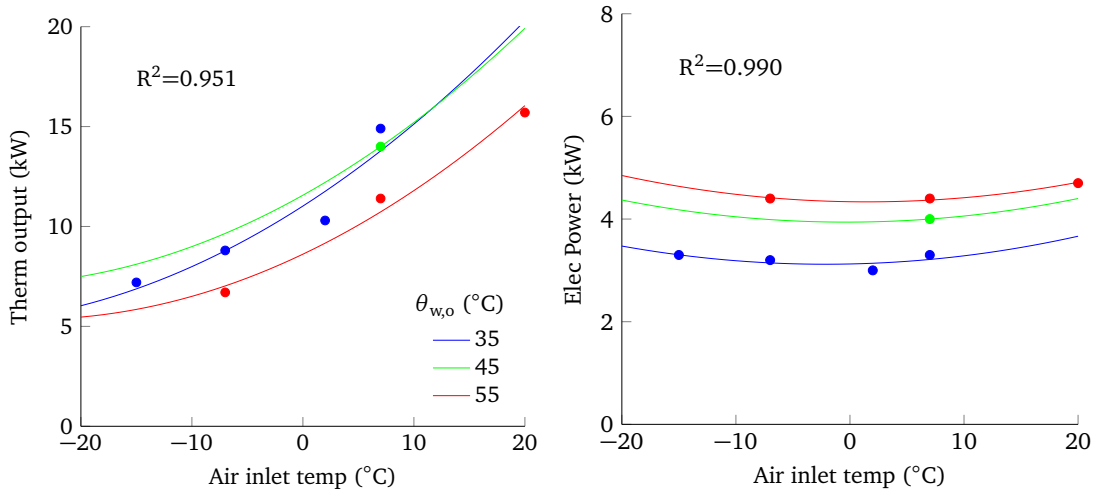

Figure A.35: ASHP 124 thermal output and power load

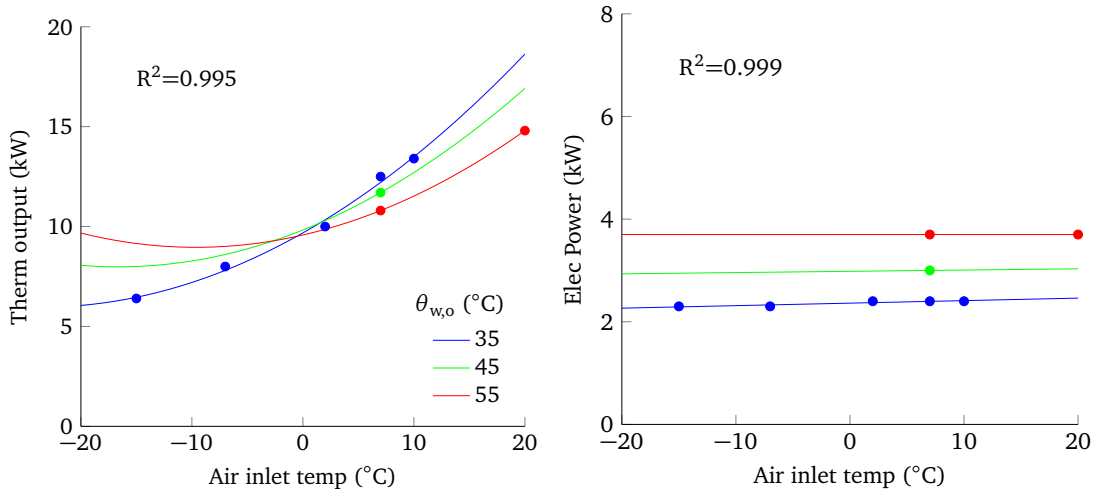

Figure A.36: ASHP 141 thermal output and power load

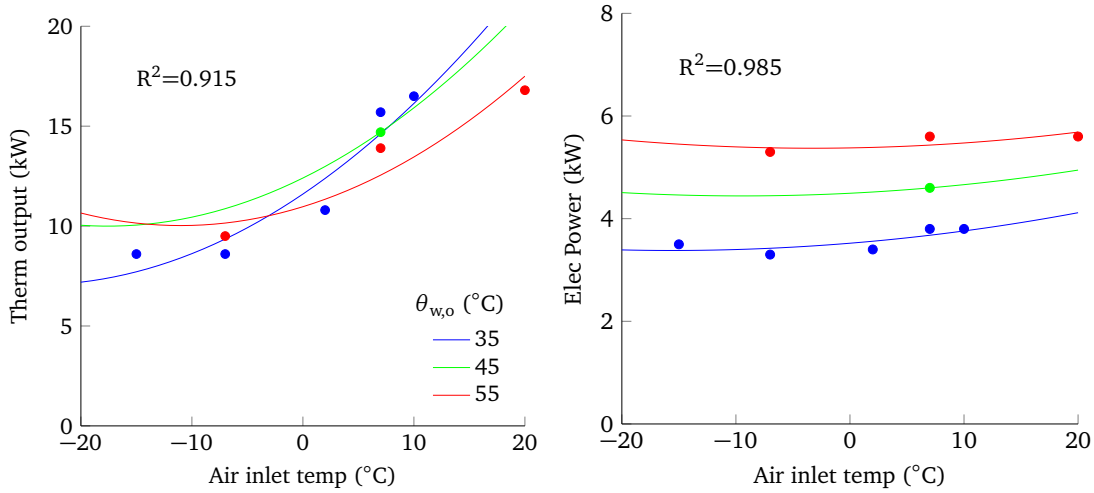

Figure A.37: ASHP 160 thermal output and power load

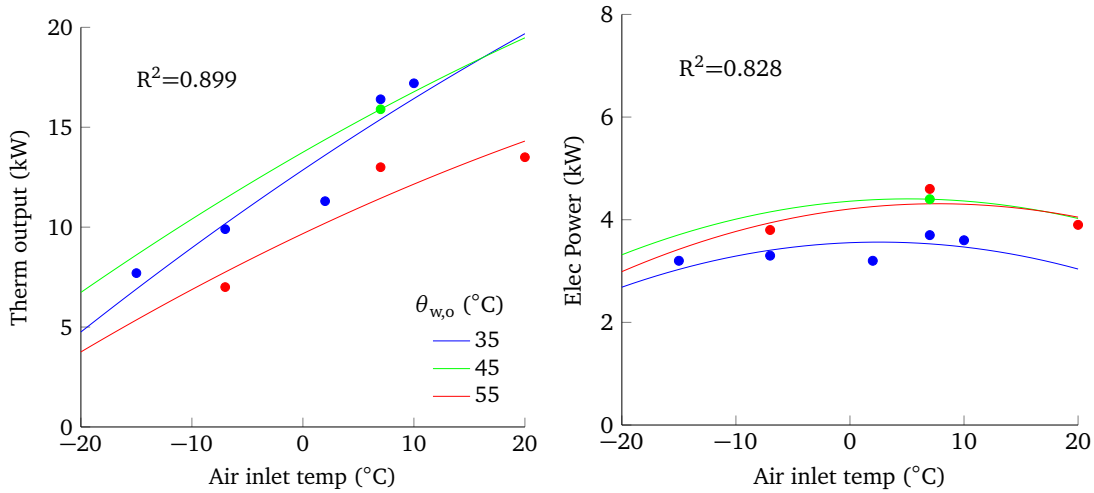

Figure A.38: ASHP 183 thermal output and power load

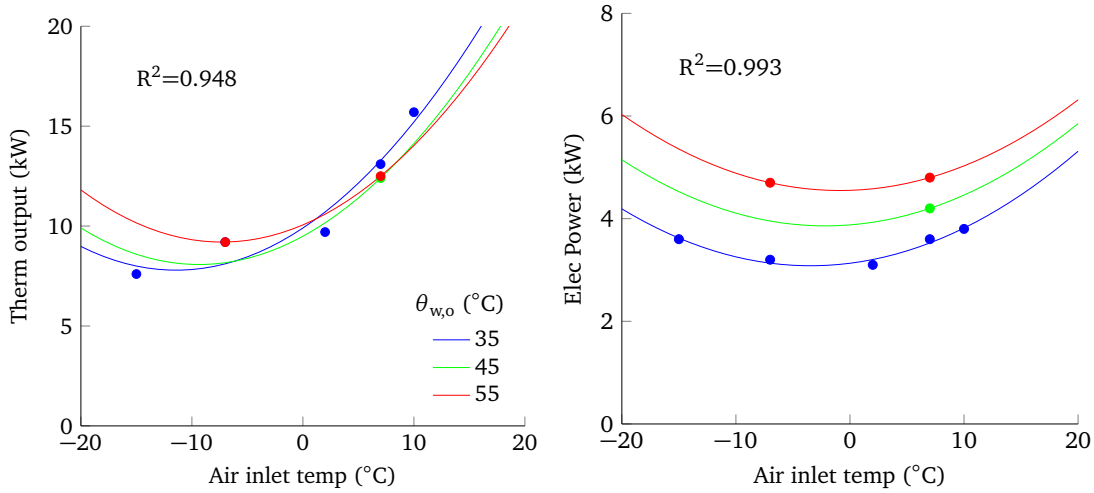

Figure A.39: ASHP 197 thermal output and power load

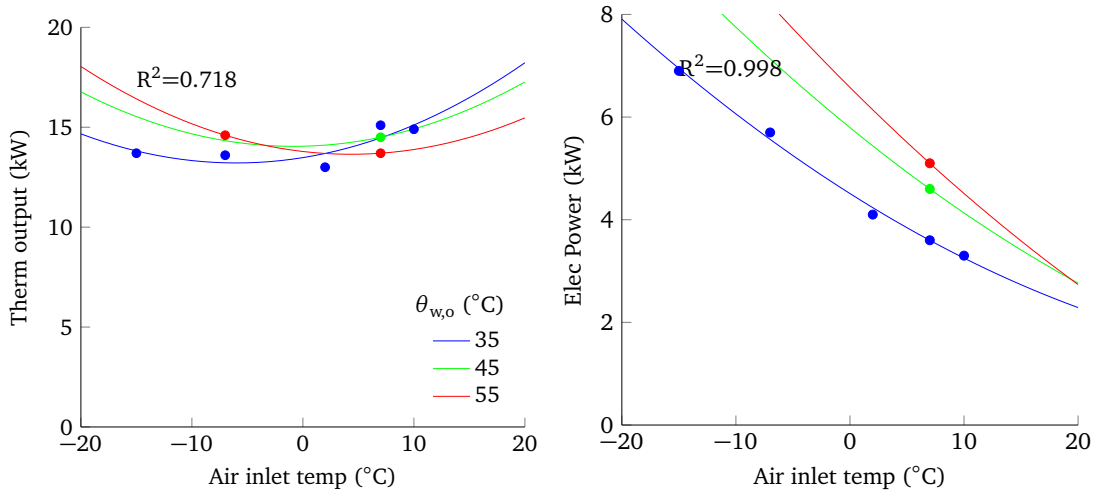

Figure A.40: ASHP 200 thermal output and power load

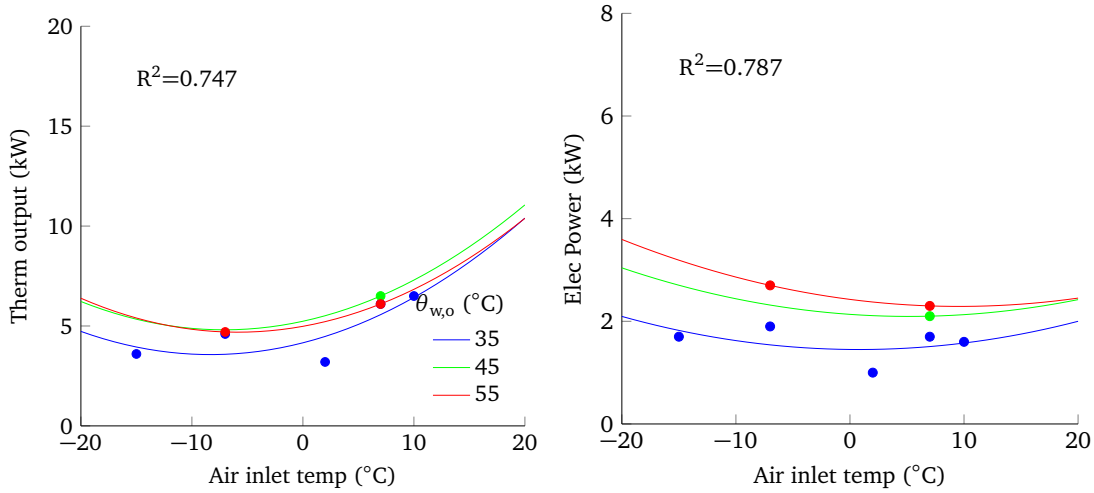

Figure A.41: ASHP 204 thermal output and power load

A.6 Calibration parameter tables

$$\Phi_{ss} = a_0 + a_1\theta_{w,o} + a_2\theta_{a,i} + a_3\theta_{w,o}\theta_{a,i} + a_4\theta_{w,o}^2 + a_5\theta_{a,i}^2 \tag{A.1}$$

$$P_{ss} = b_0 + b_1\theta_{w,o} + b_2\theta_{a,i} + b_3\theta_{w,o}\theta_{a,i} + b_4\theta_{w,o}^2 + b_5\theta_{a,i}^2 \tag{A.2}$$

ASHP no.	102	103	107	113	115	118	119	128
a_0	4.4754	12.466	9.6558	3.4273	0.22071	3.037	11.647	12.226
a_1	3.38E-01	5.25E-01	2.31E-01	3.51E-01	3.20E-01	3.93E-01	3.69E-01	2.00E-01
a_2	1.65E-01	-7.42E-02	1.67E-01	2.30E-01	4.27E-01	4.78E-01	-1.43E-01	-2.12E-01
a_3	-2.33E-03	-5.52E-03	2.23E-03	-2.73E-03	-2.04E-03	-1.37E-03	-3.29E-03	5.66E-05
a_4	1.25E-03	4.70E-03	-5.50E-05	3.11E-03	1.39E-03	9.69E-04	3.47E-03	8.63E-04
a_5	-2.26E-03	2.53E-04	-1.97E-03	-3.37E-03	-5.09E-03	-5.70E-03	1.32E-03	2.15E-03
R^2 value	0.993	0.988	0.980	0.975	0.975	0.980	0.993	0.999
b_0	1.6257	2.7427	2.8634	1.4881	0.1789	2.167	2.7284	4.6511
b_1	1.12E-02	-1.21E-03	-1.97E-02	-6.83E-03	5.38E-03	-7.13E-03	8.85E-03	-3.19E-04
b_2	7.65E-03	-2.14E-02	1.01E-02	2.60E-02	7.50E-02	1.31E-02	-3.20E-02	-1.47E-01
b_3	1.62E-04	4.51E-04	9.89E-04	1.02E-03	2.68E-04	6.29E-04	6.43E-05	2.07E-04
b_4	-1.20E-04	-9.88E-05	-3.83E-04	-3.66E-04	-1.20E-04	-3.94E-04	1.89E-04	5.63E-04
b_5	3.00E-04	8.35E-04	8.53E-04	-1.05E-04	-2.81E-04	8.47E-04	9.97E-04	2.16E-03
R^2 value	0.998	0.997	0.997	0.989	0.995	0.997	0.998	0.973

Figure A.42: ASHP calibration parameters (Satisfactory fit, part 1)

ASHP no.	130	132	134	136	138	140	147	149	159
a_0	8.3493	1.5358	8.0044	12.094	9.6773	31.996	4.601	0.38879	4.6846
a_1	3.20E-01	2.63E-01	3.40E-01	5.60E-01	3.41E-01	2.44E-01	2.09E-01	3.25E-01	2.41E-01
a_2	1.73E-02	2.34E-01	9.18E-02	1.06E-02	-1.07E-02	-1.01E+00	4.27E-02	3.30E-01	3.19E-01
a_3	-8.02E-04	-2.10E-03	-2.02E-03	-4.54E-03	-1.89E-03	1.52E-03	-1.52E-03	-2.83E-03	1.05E-03
a_4	4.68E-03	1.19E-03	1.51E-03	3.52E-03	2.82E-03	-2.97E-03	1.22E-03	1.31E-03	-7.02E-04
a_5	-7.31E-05	-2.72E-03	-1.31E-03	-3.63E-04	-2.12E-04	1.04E-02	-8.22E-04	-4.23E-03	-4.64E-03
R^2 value	1.000	0.976	0.991	0.990	0.999	0.981	0.998	0.976	0.986
b_0	1.8708	-0.60106	1.4733	3.7114	0.89097	2.9446	1.1378	0.99484	1.1205
b_1	-8.55E-03	-5.64E-03	-8.51E-03	2.94E-03	3.11E-02	-7.65E-02	-3.19E-03	3.83E-03	-1.95E-02
b_2	1.22E-02	9.62E-02	1.30E-02	-5.20E-02	1.94E-02	-2.85E-02	-5.63E-03	3.26E-02	2.34E-02
b_3	7.43E-04	3.96E-04	2.96E-04	5.46E-04	-1.04E-03	2.48E-03	2.92E-04	3.58E-04	5.66E-04
b_4	8.32E-05	-3.83E-04	-3.12E-04	-2.55E-04	5.88E-04	-1.49E-03	-1.32E-04	-9.55E-05	-6.11E-04
b_5	5.94E-04	-6.40E-04	5.55E-04	1.46E-03	6.01E-04	7.72E-04	3.22E-04	1.03E-06	4.01E-04
R^2 value	0.998	0.986	1.000	1.000	0.999	0.994	0.994	0.992	0.999

Figure A.43: ASHP calibration parameters (Satisfactory fit, part 2)

ASHP no.	170	171	189	190	191	195	198	199
a_0	4.9316	12.595	12.143	3.7889	9.5304	8.2579	4.2952	13.504
a_1	4.26E-01	3.75E-01	3.95E-01	3.76E-01	2.72E-01	1.30E-01	1.62E-01	2.25E-01
a_2	1.80E-01	9.22E-04	-5.92E-02	2.52E-01	-4.56E-02	2.25E-01	8.87E-02	-1.53E-01
a_3	-3.84E-03	-1.80E-03	-3.20E-03	-3.55E-03	-1.28E-03	3.99E-03	6.96E-04	1.36E-03
a_4	3.41E-03	-1.10E-04	4.86E-03	2.08E-03	4.58E-04	1.10E-03	3.34E-03	5.13E-03
a_5	-2.36E-03	1.55E-04	7.54E-04	-3.09E-03	4.93E-04	-2.33E-03	-1.24E-03	1.83E-03
R^2 value	0.993	0.999	0.985	0.986	0.995	1.000	0.991	0.988
b_0	0.26748	0.57005	2.899	0.54891	2.06	1.7489	-0.94727	-0.6264
b_1	-2.29E-03	-4.63E-02	-5.36E-03	-6.72E-03	3.40E-03	5.24E-03	-1.24E-03	-3.78E-02
b_2	6.45E-02	7.28E-02	-4.08E-02	4.77E-02	-2.63E-02	4.85E-02	1.05E-01	1.38E-01
b_3	4.07E-04	7.70E-04	3.55E-04	2.23E-04	1.42E-04	3.45E-05	2.82E-04	1.47E-03
b_4	-1.21E-04	8.87E-04	5.79E-05	-1.41E-04	-2.88E-04	-3.68E-04	-2.79E-06	-2.48E-06
b_5	-1.86E-04	-5.39E-05	1.21E-03	9.19E-05	8.23E-04	5.12E-04	-8.71E-04	-8.85E-04
R^2 value	0.999	0.969	0.996	0.997	0.995	1.000	0.964	0.996

Figure A.44: ASHP calibration parameters (Satisfactory fit, part 3)

ASHP no.	120	127	131	135	146	150	164	201	211
a_0	21.043	6.5337	0.29408	1.0977	-6.7093	-17.848	-7.0243	-26.568	26.001
a_1	4.68E-01	2.14E-01	4.28E-01	4.19E-01	3.71E-01	-1.23E-01	4.69E-01	8.57E-01	2.70E-01
a_2	-5.08E-01	8.19E-03	4.59E-01	3.55E-01	7.69E-01	1.24E+00	8.01E-01	1.93E+00	-7.65E-01
a_3	-4.26E-03	0.00E+00	-4.01E-03	-3.65E-03	-2.84E-03	7.06E-03	-4.13E-03	-1.52E-02	8.04E-04
a_4	8.25E-03	0.00E+00	3.20E-03	2.60E-03	2.59E-03	-2.17E-03	4.87E-03	2.24E-03	9.53E-03
a_5	5.22E-03	0.00E+00	-5.44E-03	-4.10E-03	-8.96E-03	-1.32E-02	-9.21E-03	-2.27E-02	9.40E-03
R^2 value	0.994	0.951	0.973	0.994	0.962	0.988	0.961	0.996	0.968
b_0	3.3194	0.19359	1.4334	1.5823	-0.7654	-3.2717	0.32125	-2.4833	3.4798
b_1	7.34E-03	1.68E-02	1.05E-02	3.83E-03	8.97E-03	-9.74E-02	-2.06E-02	5.19E-02	-1.88E-03
b_2	-4.20E-02	5.53E-02	2.49E-02	1.26E-02	1.18E-01	2.22E-01	7.00E-02	2.31E-01	-7.04E-02
b_3	3.15E-04	0.00E+00	1.35E-04	3.58E-04	-2.80E-04	2.13E-03	8.74E-04	-1.20E-03	5.54E-04
b_4	6.65E-04	0.00E+00	4.51E-05	-9.55E-05	4.99E-04	-9.69E-04	-3.95E-04	6.10E-07	1.10E-03
b_5	1.23E-03	0.00E+00	4.09E-04	5.01E-04	-4.24E-04	-1.62E-03	-1.39E-04	-2.03E-03	1.66E-03
R^2 value	0.999	0.985	0.999	0.997	0.995	0.983	0.992	0.995	0.993

Figure A.45: ASHP calibration parameters (Fit usable with caution)

Appendix B

Implementation of the model in ESP-r

Section 5.4 outlined the changes made to the ESP-r source code to implement the proposed modelling method. The changes are all within the portion of code relating to the existing ASHP component known as the "coefficient generator". This code appears below. The larger changes are highlighted in the code by comments, and enclosed by the initials "EB". The relevant line numbers are:

- 121-130: declares new variables (coefficients of regression models).
- 166-196: initialises new variables, and substitutes water inlet temperature variable for water outlet temperature.
- 268-280: code to ensure UA value is set to zero whilst ASHP is operating.
- 350-383: implements controls for back up heating model.
- 386-404: implements new power load regression model
- 408-430, 440-449: replaces existing model's COP regression model with new Φ_{ss} regression model.
- 461-469, 495-500: adjusts collation of power loads in line with new modelling approach.

```
1  C ******************** CMP45C ********************
2  C CMP45C generates for plant component IPCOMP with plant db code 450 ie.
3  C 1 node (ISV=20) WCH air-source heat pump feeding a hydronic heating system.
4  C the matrix equation coefficients COUT (in order: self-coupling, cross-
5  C coupling, and present-time coefficients) for energy balance (ISTATS=1),
6  C 1st phase mass balance (ISTATS=2), or 2nd phase mass (ISTATS=3)
7
```

```
C      ADATA: 1 Mass of component (solids+liquid) (kg)
C             2 Mass weighted average specific heat node (J/kgK)
C             3 UA modulus for component (W/K)

C      BDATA: 1 COP model [1 - fixed COP 2 - modified Carnot COP; 3- f(dT) 4 - polynomial]
C             2 Model coef a0
C             3 Model coef a1
C             4 Model coef a2
C             5 Model coef a3
C             6 Device power draw (kW) model [1 - fixed 2- polynomial]
C             7 Model coef b0
C             8 Model coef b1
C             9 Model coef b2
C            10 Model coef b3
C            11 Compressor pf (-)
C            12 Pump rating (W)
C            13 Pump pf (-)
C            14 Flowrate at rated pump power (l/s)
C            15 Fan power (W)
C            16 Fan pf (-)
C            17 Controller power (W)
C            18 Controller pf (-)
C            19 Tout max (degC)
C            20 Tin max (degC)
C            21 Defrost cycle trigger ambient temp (degC)
C            22 Defrost cycle time calc (1-user def 2-f(RH))
C            23 Defrost cycle  calc coefficient b1/fixed defrost cycle  time  (-)
C            24 Defrost cycle  calc coefficient b2 (-)
C            25 Defrost cycle  lockout time (mins)
C            26 Min defrost time (mins)
C            26 Max defrost time (mins)
C            27 Temp compensation on/off (-)
C            28 Nominal water return temperature (Deg C)
C            29 Nominal water return deadband (Deg C)
C            30 Ambient temperature for temp compensation start [Deg C]
C            31 Ambient temperature for temp compensation end [Deg C]
C            32 Temp compensation gradient [deg C return/deg C ambient] (degCr/degCa)


C      CDATA: 1 Call for heat [0 or 1] (-)

C Node 1 represents the condenser heat exchanger and couples to the hydronic heating circuit.
C The device has an internal pump and so an explicit pump model is not needed in system
C models containing this component. This particular device model is suitable for ON/OFF type
C control and will require modification if PID-type control is to be applied. The model
C internally controls the water inlet temperature.

      SUBROUTINE CMP45C(IPCOMP,COUT,ISTATS)
       use h3kmodule
      implicit none
#include "plant.h"
#include "building.h"

      COMMON/OUTIN/IUOUT,IUIN
      COMMON/TC/ITC,ICNT
      COMMON/TRACE/ITCF,ITRACE(MTRACE),IZNTRC(MCOM),ITU

      COMMON/ITERINDEX/ITERNU !plant iteration number

      COMMON/SIMTIM/IHRP,IHRF,IDYP,IDYF,IDWP,IDWF,NSINC,ITS
      COMMON/Pctime/TIMSEC
      COMMON/PCTC/TC(MPCOM)

      COMMON/PCEQU/IMPEXP,RATIMP

      COMMON/C9/NPCOMP,NCI(MPCOM),CDATA(MPCOM,MMISCD)

      COMMON/C12PS/NPCDAT(MPCOM,9),IPOFS1(MCOEFG),IPOFS2(MCOEFG,MPVAR)
      COMMON/PCVAL/CSVF(MPNODE,MPVAR),CSVP(MPNODE,MPVAR)
      COMMON/PCVAR/PCTF(MPCON),PCRF(MPCON),PUAF(MPNODE),PCQF(MPNODE),
     &             PCNTMF(MPCOM),
     &             PCTP(MPCON),PCRP(MPCON),PUAP(MPNODE),PCQP(MPNODE),
     &             PCNTMP(MPCOM)
      COMMON/PCOND/CONVAR(MPCON,MCONVR),ICONTP(MPCON),
     &             ICONDX(MPCOM,MNODEC,MPCONC)
      COMMON/PCRES/QDATA(MPCOM),PCAOUT(MPCOM,MPCRES),napdat(mpcom)
      common/pcnam/pcname(mpcom)

      COMMON/CLIMIP/QFPP,QFFP,TPP,TFP,QDPP,QDFP,VPP,VFP,DPP,DFP,HPP,HFP

      COMMON/ASHPvar1/CompMass,AveSpHt,UAMod,CarEffMod,BUchktim,
     &BUsetpt,BUgrad,BUcap,BUtimer,BUtimerp,Compa2,Compa3,      ! EBU
     &CompressPf,PumpRating,PumpPf,RatedFlow,
     &FanRating,FanPf,CtlRating,CtlPf,ToutMax,TinMax,DefrostT,
     &DefrostTime,Defrostb0,Defrostb1,DefrostLockout,DefrostMinTime,
     &DefrostMaxTime,NomRetT,NomRetTDeadB,TempCompS,TempCompE,
     &TempCompc0,DefrostDur,DefrostLockDur,ReturnTp,BUONOFF

      COMMON/ASHPvar2/BUtype,CompModel,DefrostCalc,AmbientTempComp,  ! EBU
     &DeviceONOFFp,DeviceONOFF

      COMMON/ASHPvar3/CallforHeat,InDeadB,DefrostLock,InDefrost

      REAL SMALL
      PARAMETER (SMALL=1.0E-20)
```

```
103
104         LOGICAL  CallforHeat , InDeadB , DefrostLock , InDefrost
105
106         INTEGER  BUtype , CompModel , DefrostCalc , AmbientTempComp ,
107        &DeviceONOFFp , DeviceONOFF                                    ! EBU
108
109         REAL  CompMass , AveSpHt , UAMod, CarEffMod ,                  ! EBU
110        &Compa2 , Compa3 , CompressPf ,                                 ! EBU
111        &PumpRating , PumpPf , RatedFlow , FanRating , FanPf , CtlRating , CtlPf ,
112        &ToutMax , TinMax , DefrostTime , DefrostT , Defrostb0 , Defrostb1 ,
113        &DefrostLockout , DefrostMinTime , DefrostMaxTime , NomRetT , NomRetTDeadB ,
114        &TempCompS , TempCompE , TempCompc0 , DefrostDur , DefrostLockDur , BUchktim ,
115        &BUsetpt , BUgrad , BUcap , BUtimer , BUtimerp , ReturnTp , BUONOFF    ! EBU
116
117         REAL  DefrostStat , CompPower , CompressPower , COP , CtlPower , DeviceFlow ,
118        &FanPower , HeatOutput , PumpPower , ReturnSP , ReturnSPH , ReturnSPL , RHamb,
119        &TotApparentPower , TotReacPower , TotRealPower
120
121 C ========================================== EB: Start ==========
122 C New variables declared. These hold the parameters of the
123 C regression models; ASHP node temperature; and UAonoff. The last
124 C is a switch required because thermal output regression model
125 C already includes heat loss to environment
126       REAL  Qa0EB , Qa1EB , Qa2EB , Qa3EB , Qa4EB , Qa5EB , Qa6EB , Qa7EB
127       REAL  Pb0EB , Pb1EB , Pb2EB , Pb3EB , Pb4EB , Pb5EB , Pb6EB , Pb7EB
128       REAL  OutputT
129       INTEGER  UAonoff
130 C ========================================== EB: end ============
131
132       INTEGER  InbInk
133       REAL  SHTFLD
134
135       INTEGER  IUOUT , IUIN , ITC , ICNT , ITCF , ITRACE , IZNTRC , ITU , ITERNU ,
136      &IHRP , IHRF , IDYP , IDYF , IDWP , IDWF , NSINC , ITS , IMPEXP
137       INTEGER  NPCDAT , IPOFS1 , IPOFS2 , ICON1 , INOD1 , napdat ,
138      &IPCOMP , ISTATS , I , ICONDX , ICONTP , IX1 , NCI , NITMS , NPCOMP
139
140       REAL  TIMSEC , TC , RATIMP , CSVF , CSVP , PCTF , PCRF , PUAF , PCQF , PCNTMF ,
141      &PCTP , PCRP , PUAP , PCQP , PCNTMP , CONVAR , QFPP , QFFP , TPP , TFP , QDPP , QDFP , VPP
142       REAL  VFP , DPP , DFP , HPP , HFP , Tamb , ReturnT , Td , Ta , TL , TH , ALPHA , CM , C1 ,
143      &TmpDev
144
145       REAL  COUT(MPCOE) , QDATA , PCAOUT , CDATA
146
147       LOGICAL  CLOSE , CLOSEA
148
149       CHARACTER  OUTS*248 , PCNAME*15
150
151       INTEGER  IPCOMP_LEN !lenght of ipcomp
152
153 C Trace output
154       IF(ITC.GT.0.AND.NSINC.GE.ITC.AND.NSINC.LE.ITCF.AND.
155      &    ITRACE(37).NE.0) WRITE(ITU,*) '␣Entering␣subroutine␣CMP45C'
156
157 C **NB** Variable Assignment and initilalisation in CMP40S
158
159 C Initialize pointers to inter-connection(s) ICON, and node(s) INOD
160       ICON1=ICONDX(IPCOMP,1,1)
161       INOD1=NPCDAT(IPCOMP,9)
162
163       call eclose(PCNTMF(IPCOMP),-99.00,0.001,closea)
164       IF(closea) UAMod=0.
165
166 C ================================== EB: Start ==================
167 C coefficients for the heat output and power load equation
168 C fit models
169       Qa0EB=9.3254E+00
170       Qa1EB=-2.7807E-02
171       Qa2EB=3.3410E-01
172       Qa3EB=-1.8018E-03
173       Qa4EB=-7.7566E-04
174       Qa5EB=1.2888E-03
175       Qa6EB=0
176       Qa7EB=0
177
178       Pb0EB=2.3426E+00
179       Pb1EB=-2.3194E-02
180       Pb2EB=-5.3952E-03
181       Pb3EB=7.0933E-04
182       Pb4EB=4.3611E-04
183       Pb5EB=-1.5218E-04
184       Pb6EB=0
185       Pb7EB=0
186
187 C Read most recent node temperature (this is effectively the output temperature
188 C for the future timerow. Finalised future timerow temperatures are of course not
189 C known at this stage, but the solver makes use of iteration - and it appears
190 C CONVAR gets overwritten each iteration. So the value read below is the penultimate
191 C iteration of the output temperature. From examining results, this is practically the
192 C same as final output temperature, with small differences only occuring when heat
193 C generation changes rapidly at the start and end of heating periods.)
194 C       OutputT=CSVP(INOD1,1)
195       OutputT=CONVAR(1,1)
196 C ================================== EB: end ====================
197
```

```
198
199
200 C Read ambient temperature
201       Tamb=TFP    ! TFP is FUTURE time row ambient temperature
202
203 C Set initial operation mode based on CDATA.
204       IF(CDATA(IPCOMP,1).GT.0.0) THEN
205         CallForHeat=.true.
206
207 C Pump circulates while there is a call for heat.
208         PumpPower=PumpRating
209         DeviceFlow=RatedFlow
210       ELSE
211         CallforHeat=.false.
212         DeviceFlow=0.
213         PumpPower=0.
214       ENDIF
215
216
217 C Calculate the return water temperature set point if temperature compensation is active.
218       ReturnSP=NomRetT !default return temperature
219       ReturnSPL=ReturnSP-0.5*(NomRetTDeadB)
220       ReturnSPH=ReturnSP+0.5*(NomRetTDeadB)
221       IF(ReturnSP.GT.TinMax) ReturnSP=TinMax
222
223       IF(AmbientTempComp.GT.0)THEN
224
225         IF(Tamb.GE.TempCompS.AND.Tamb.LT.TempCompE)THEN
226           ReturnSP=((Tamb-TempCompS)*TempCompc0)+NomRetT
227           ReturnSPL=ReturnSP-0.5*(NomRetTDeadB)
228           ReturnSPH=ReturnSP+0.5*(NomRetTDeadB)
229
230 C Case where Tamb > Temp compensation saturation point
231         ELSEIF(Tamb.GE.TempCompE)THEN
232           ReturnSP=((TempCompE-TempCompS)*TempCompc0)+NomRetT
233           ReturnSPL=ReturnSP-0.5*(NomRetTDeadB)
234           ReturnSPH=ReturnSP+0.5*(NomRetTDeadB)
235         ENDIF
236         IF(ReturnSP.GT.TinMax)THEN
237           ReturnSP=TinMax
238           ReturnSPH=ReturnSP
239         ENDIF
240       ENDIF
241
242 C Determine whether machine should be on or off based on return water temperature.
243       ReturnT=CONVAR(ICON1,1)
244       DeviceONOFFp=DeviceONOFF
245       IF(CallforHeat)THEN
246
247 C Check to see if the device is in the dead band.
248         IF(ReturnT.GE.ReturnSPL.AND.ReturnT.LE.ReturnSPH)THEN
249           InDeadB=.true.
250         ELSE
251           InDeadB=.false.
252         ENDIF
253
254 C Evaluate the device status.
255         IF(ReturnT.GT.ReturnSPH)THEN
256           DeviceONOFF=0
257         ELSEIF(ReturnT.LT.ReturnSPL)THEN
258           DeviceONOFF=1
259         ELSEIF(DeviceONOFFp.EQ.1.AND.InDeadB)THEN
260           DeviceONOFF=1
261         ELSEIF(DeviceONOFFp.EQ.0.AND.InDeadB)THEN
262           DeviceONOFF=0
263         ENDIF
264       ELSE
265         DeviceONOFF=0
266       ENDIF
267
268 C ========================================== EB start ============================
269 C Heat loss to enviroment is already included in HeatOutput regression models.
270 C UAonoff is effectively a switch preventing double counting of heat losses:
271 C UAonoff = 0 when ASHP is on, and 1 when it is off. In all later
272 C calculations,"UAMod" is replaced with "UAMod*UAonoff". This is coded inside a
273 C switch (COPModel is an un-used user-selectable integer variable) so that comparisons
274 C can be easily made without recompiling.
275       IF(CompModel.GT.0)THEN
276         UAonoff=1-DeviceONOFF
277       ELSE
278         UAonoff=1
279       ENDIF
280 C ========================================== EB end  ============================
281
282 C Establish the device COP
283       IF(DeviceONOFF.GT.0)THEN
284
285 C Determine the defrost status of the device (do only once per timestep so check
286 C iteration number.
287         IF(DefrostCalc.GT.0)THEN
288
289           IF(.NOT.InDefrost)THEN
290 C Update the defrost time.
291             IF(DefrostCalc.eq.1)THEN
292               DefrostTime=Defrostb0
```

```
293               ELSE
294                 RHamb=HFP
295   C Calculate defrost time to the nearest minute.
296                 DefrostTime=float(nint(Defrostb0+Defrostb1*RHamb))
297               ENDIF
298
299   C Impose limits on defrost time
300               IF(DefrostTime.GT.DefrostMaxTime)
301         &DefrostTime=DefrostMaxTime
302               IF(DefrostTime.LT.DefrostMinTime)
303         &DefrostTime=DefrostMinTime
304
305   C Issue warning about timestep length if it is longer than the Defrost time.
306               IF(DefrostTime.LT.TIMSEC/60.)THEN
307                 WRITE(OUTS,'(a,f7.4,a,f7.4,a)')
308         &'ASHP Warning: time step ',TIMSEC/60.,' > defrost cycle time',
309         &DefrostTime,' reduce the time step to avoid problems.'
310                 CALL EDISP(IUOUT,OUTS)
311               ENDIF
312             ENDIF
313
314   C Set defrost state.
315             IF(Tamb.LE.DefrostT)THEN
316               IF(.NOT.InDefrost)THEN
317                 IF(.NOT.DefrostLock)THEN
318                   InDefrost=.TRUE.
319                   DefrostDur=0.0
320                 ENDIF
321               ENDIF
322             ELSE
323               InDefrost=.FALSE.
324               DefrostLock=.FALSE.
325             ENDIF
326
327   C Increment timers
328               IF(InDefrost.and.ITERNU.eq.1)
329         &DefrostDur=DefrostDur+0.5*timsec/60.
330
331               IF(DefrostLock.and.ITERNU.eq.1)
332         &DefrostLockDur=DefrostLockDur+0.5*timsec/60.
333
334   C Update state for next ts
335             IF(DefrostDur.GT.DefrostTime)THEN
336               InDefrost=.false.
337               DefrostDur=0.0
338               DefrostLock=.true.
339               DefrostLockDur=0.0
340             ENDIF
341
342             IF(DefrostLockDur.GT.DefrostLockout)THEN
343               DefrostLock=.false.
344               DefrostLockDur=0.0
345             ENDIF
346
347           ENDIF !end of defrost code.
348   C ---------------------------
349
350   C ========================================== EB: Start ==================
351   C ---- backup heating
352
353   C BUtype=1 -> no backup heating
354
355   C BUtype=2 -> if after BUchktim minutes, Treturn has not reached BUsetpt, control turns
356   C on backup.
357
358   C BUtype=3 -> if after BUchktim minutes, rate of increase of Treturn is less than BUgrad,
359   C control turns on backup.
360
361           if(BUtype.eq.2)then
362             if((BUtimer.ge.BUchktim).and.(BUtimerp.lt.BUchktim))then
363               if(ReturnT.lt.(ReturnSP-BUsetpt))then
364                 BUONOFF=1 !switch on BU
365               endif
366             endif
367           elseif(BUtype.gt.2)then
368             if((BUtimer.ge.BUchktim).and.(BUtimerp.lt.BUchktim))then
369               if(ReturnT.lt.(ReturnTp+BUgrad*0.5*timsec/60))then
370                 BUONOFF=1 !switch on BU
371               endif
372             endif
373           endif
374
375   C       if((DeviceONOFF.eq.0).and.(DeviceONOFFp.eq.1))BUONOFF=0
376           if(ITERNU.eq.1)then
377             BUtimerp=BUtimer
378             BUtimer=BUtimer+0.5*timsec/60.
379             ReturnTp=ReturnT
380           endif
381
382
383   C ========================================== EB: end ====================
384
385
386   C ========================================== EB: Start ==================
387   C EB Previous options for power load regression model type
```

```
c removed: new power load regression model hard-wired.
C Further, variable Td used in regression models is now
C defined as output rather than return water temperature.

C Calculate the TOTAL device power draw (W)
c         IF(CompModel.eq.1)THEN
c           CompPower=1000.*(Compa0) !fixed power consumption
c         ELSEIF(CompModel.eq.2)THEN
            Td=OutputT
            Ta=Tamb
c           CompPower=1000.*(Compa0+(Compa1*Ta)+(Compa2*Td))
c         ENDIF
c         if(CompPower.LT.0.0)CompPower=0.0
          CompPower=1000*(Pb0EB+Pb1EB*Td+Pb2EB*Ta+Pb3EB*Td*Ta+Pb4EB*Td*Td
     &              +Pb5EB*Ta*Ta+Pb6EB*(Td**3)+Pb7EB*(Ta**3))
          CtlPower=0.
C ================================================ EB: end ====================

          FanPower=FanRating

C ================================================ EB: Start ==================
C EB: Previous options for COP equation fit model type removed
C COP no longer forms part of calculation so set to zero.
C
C Calculate the COP based on the user-specified method.
c         IF(COPModel.EQ.1)THEN
c           COP=COPa0 !fixed COP
c         ELSEIF(COPModel.EQ.2)THEN
c           TL=Tamb+273.15
c           TH=ReturnT+273.15
c           COP=CarEffMod*((1-(TL/TH))**(-1)) !modified carnot COP
c         ELSEIF(COPModel.EQ.3)THEN !quadratic based on Td-Ta
c           TL=Tamb
c           TH=ReturnT
c           COP=COPa0+(COPa1*(TH-TL))+(COPa2*(TH-TL)**2.)
c         ELSEIF(COPModel.EQ.4)THEN
c           COP=COPa0+COPa1*Tamb+COPa2*Tamb**2.+COPa3*Tamb**3.
c         ELSE
c           WRITE(OUTS,'(a)')'Error␣in␣ASHP,␣COP␣model␣#'
c           CALL EDISP(IUOUT,OUTS)
c         ENDIF
          COP=0.0
C ================================================ EB: End ====================

C Set limits on calculated values of COP
          IF(COP.LT.0.0) COP=0.0
          IF(COP.GT.12.0) COP=12.0

          IF(InDefrost)THEN
            HeatOutput=0.0
          ELSE

C ================================================ EB: Start ==================
C EB: Heat output is defined directly, rather than being
C the product of COP and power load as before.
C           HeatOutput=COP*CompPower
            Ta=Tamb
            Td=OutputT
            HeatOutput=1000*(Qa0EB+Qa1EB*Td+Qa2EB*Ta+Qa3EB*Ta*Td
     &          +Qa4EB*Td*Td+Qa5EB*Ta*Ta+Qa6EB*(Td**3)+Qa7EB*(Ta**3))
     &          +BUONOFF*BUcap
C ================================================ EB: End ====================

            IF(HeatOutput.LT.0) THEN
              write(*,*) "Error:␣heat␣output␣<␣0!␣",HeatOutput, COP,
     &CompPower
              STOP
            ENDIF
          ENDIF
        ELSE

C Device is 'off' set parameters accordingly (assume controller is still operating).

C ================================================ EB: Start ==========
C Control power variable from previous model now represents standby/off mode power
          CompPower=0.
          CtlPower=CtlRating
C           CompPower=CtlPower
          BUONOFF=0           ! EBU turn off backup heating
          BUtimer=0.
          BUtimerp=0.
C ================================================ EB: End ============
          HeatOutput=0.
          FanPower=0.
          COP=0.
          InDefrost=.false.
          DefrostLock=.false.


        ENDIF

C Generate coefficients for energy balance equation
        IF(ISTATS.EQ.1) THEN

C Establish the nodal thermal capacities.
```

```
483           CM=CompMass*AveSpHt
484
485   C node 1 water
486           C1=DeviceFlow*SHTFLD(3,CONVAR(ICON1,1))
487
488   C Establish heat loss modulus
489           CALL ECLOSE(PCNTMF(IPCOMP),99.,0.0001,CLOSE)
490           IF(CLOSE) UAMod=0.0
491
492   C Calculate the electrical demand of the device assumung the controller is ON.
493   C          CtlPower=CtlRating      ! EB - control power dealt with earlier
494
495   C ========================================= EB: Start ==================
496   C Circulation pump power added to calculation of total power draw.
497
498   C          TotRealPower=CompPower+CtlPower
499             TotRealPower=CompPower+CtlPower+PumpPower+BUONOFF*BUcap
500   C +======================================== EB : End ===================
501
502   c Calculate the compressor power draw.
503             CompressPower=CompPower-(PumpPower+FanPower+CtlPower)
504             IF(CompressPower.LT.0.0)CompressPower=0.0
505   C         TotRealPower=CompPower+PumpPower+CtlPower+FanPower
506
507             TotReacPower=(((CompressPower/CompressPf)**2)
508          &-(CompressPower**2))**0.5
509          &+(((PumpPower/PumpPf)**2)-(PumpPower**2))**0.5
510          &+(((CtlPower/CtlPf)**2)-(CtlPower**2))**0.5
511          &+(((FanPower/FanPf)**2)-(FanPower**2))**0.5
512
513             TotApparentPower=((TotRealPower**2)+(TotReacPower*2))**0.5
514
515   C Calculate current component time-constant TC
516             TC(IPCOMP)=CM/AMAX1(SMALL,(C1+UAMod))
517
518   C Set up implicit/explicit weighting factor ALPHA (1 = fully implicit)
519             IF(IMPEXP.EQ.1) THEN
520                ALPHA=1.
521             ELSE IF(IMPEXP.EQ.2) THEN
522                ALPHA=RATIMP
523             ELSE IF(IMPEXP.EQ.3) THEN
524               IF(TIMSEC.GT.0.63*TC(IPCOMP)) THEN
525                  ALPHA=1.
526               ELSE
527                  ALPHA=RATIMP
528               END IF
529             ELSE IF(IMPEXP.EQ.4) THEN
530                 CM=0.
531                 ALPHA=1.
532             END IF
533
534
535   C ========================================= EB: Start ==================
536   C EB The following lines are as they were in the previous version, other
537   C than all mentions of UAMod are replaced with UAMod*UAonoff
538   C
539   C Establish matrix equation self- and cross-coupling coefficients.
540             COUT(1)=ALPHA*(-C1-(UAMod*UAonoff))-CM/TIMSEC    ! EB UAonoff added
541   C Matrix cross coupling coefficients.
542             COUT(2)=ALPHA*C1
543   C Establish the present and known coefficient i.e. RHS
544             COUT(3)=((1.-ALPHA)*(PCRP(ICON1)+PUAP(INOD1))-CM/TIMSEC)
545          &            *CSVP(INOD1,1)
546          &            +(1.-ALPHA)*(-PCRP(ICON1))*PCTP(ICON1)
547          &            -ALPHA*UAMod*UAonoff*PCNTMF(IPCOMP)          ! EB  UAonoff
548          &            -ALPHA*HeatOutput
549          &            -(1.-ALPHA)*PCQP(INOD1)
550          &            -(1.-ALPHA)*PUAP(INOD1)*PCNTMP(IPCOMP)
551
552   C Store "environment" variables future values
553              PCTF(ICON1)=CONVAR(ICON1,1)
554              PCRF(ICON1)=C1
555              PCQF(INOD1)=HeatOutput
556              PUAF(INOD1)=UAMod*UAonoff           ! EB  UAonoff added
557   C ========================================= EB: End ====================
558
559   C ========================================= EB: Start ==================
560   C EB Some additional outputs are changed to aid model development.
561              NAPDAT(IPCOMP)=9
562              PCAOUT(IPCOMP,1)=HeatOutput
563   C          PCAOUT(IPCOMP,2)=COP
564              PCAOUT(IPCOMP,2)=UAMod*UAonoff      !EB  UAonoff added
565              PCAOUT(IPCOMP,3)=Tamb
566              PCAOUT(IPCOMP,4)=DeviceONOFF
567              PCAOUT(IPCOMP,5)=ReturnSP
568              PCAOUT(IPCOMP,6)=TotRealPower
569   C            PCAOUT(IPCOMP,7)=TotReacPower
570   C            PCAOUT(IPCOMP,8)=TotApparentPower
571              PCAOUT(IPCOMP,7)=OutputT
572              PCAOUT(IPCOMP,8)=BUONOFF*BUcap
573   C            if(Indefrost)then
574   C              PCAOUT(IPCOMP,9)=1.0
575   C            elseif(DefrostLock)then
576   C              PCAOUT(IPCOMP,9)=-1.0
577   C            else
```

```
578 C              PCAOUT(IPCOMP,9)=0.0
579 C            endif
580              PCAOUT(IPCOMP,9)=PCTP(ICON1)
581 C ========================================== EB: End ================
582
583 C-------------------------------------------------------------------------------
584 C Make select results available in XML and CVS output.
585 C-------------------------------------------------------------------------------
586            IPCOMP_LEN = lnblnk(pcname(IPCOMP))
587
588             call AddToReport(rvPltHOut%Identifier,
589      &            HeatOutput,
590      &            pcname(IPCOMP)(1:IPCOMP_LEN))
591
592             call AddToReport(rvPltCOP%Identifier,
593      &            COP,
594      &            pcname(IPCOMP)(1:IPCOMP_LEN))
595
596             call AddToReport(rvPltTambient%Identifier,
597      &            Tamb,
598      &            pcname(IPCOMP)(1:IPCOMP_LEN))
599
600             tmpdev=float(DeviceONOFF)
601             call AddToReport(rvPltDeviceONOFF%Identifier,
602      &            tmpdev,
603      &            pcname(IPCOMP)(1:IPCOMP_LEN))
604
605             call AddToReport(rvPltReturnTSP%Identifier,
606      &            ReturnSP,
607      &            pcname(IPCOMP)(1:IPCOMP_LEN))
608
609            call AddToReport(rvPltRealPow%Identifier,
610      &            TotRealPower,
611      &            pcname(IPCOMP)(1:IPCOMP_LEN))
612
613             call AddToReport(rvPltReacPow%Identifier,
614      &            TotReacPower,
615      &            pcname(IPCOMP)(1:IPCOMP_LEN))
616
617            call AddToReport(rvPltApparPow%Identifier,
618      &            TotApparentPower,
619      &            pcname(IPCOMP)(1:IPCOMP_LEN))
620
621            DefrostStat=PCAOUT(IPCOMP,9)
622            call AddToReport(rvPltDefrostStat%Identifier,
623      &            DefrostStat,
624      &            pcname(IPCOMP)(1:IPCOMP_LEN))
625
626
627 C 1st phase mass (ie. "water") balance coefficients
628       ELSE IF(ISTATS.EQ.2) THEN
629          COUT(1)=1.
630          COUT(2)=0.
631          COUT(3)=DeviceFlow
632
633 C 2nd phase mass (ie. "vapour") balance coefficients
634       ELSE IF(ISTATS.EQ.3) THEN
635          COUT(1)=1.
636          COUT(2)=0.
637          COUT(3)=0.
638       END IF
639
640
641 C Trace.
642       IF(ITC.GT.0.AND.NSINC.GE.ITC.AND.NSINC.LE.ITCF.AND.
643      &   ITRACE(37).NE.0) THEN
644          WRITE(ITU,*) ' Component       ',IPCOMP,':'
645          WRITE(ITU,*) ' 1 node (ISV=20) Air Source Heat Pump'
646          WRITE(ITU,*) ' Matrix node(s) ',INOD1
647          WRITE(ITU,*) ' Connection(s)   ',ICON1
648          IF(ISTATS.EQ.1) THEN
649             WRITE(ITU,*) ' CM      = ',CM,' (J/K)'
650             WRITE(ITU,*) ' C1      = ',C1,' (W/Ks)'
651             WRITE(ITU,*) ' Flow    = ',DeviceFlow,' (l/s)'
652             WRITE(ITU,*) ' TC      = ',TC(IPCOMP),' (s)'
653             WRITE(ITU,*) ' ALPHA   = ',ALPHA,' (-)'
654             WRITE(ITU,*) ' UAMod   = ',UAMod*UAonoff,' (W/K)'          ! EB  UAonoff added
655             WRITE(ITU,*) ' Tamb    = ',Tamb,' (C)'
656             WRITE(ITU,*) ' ReturnT = ',ReturnT,' (C)'
657             WRITE(ITU,*) ' ReturnSP        = ',ReturnSP,' (C)'
658             WRITE(ITU,*) ' ReturnSPH       = ',ReturnSPH,' (C)'
659             WRITE(ITU,*) ' ReturnSPL       = ',ReturnSPL,' (C)'
660             WRITE(ITU,*) ' InDeadB         = ',InDeadB,' (-)'
661             WRITE(ITU,*) ' CallforHeat     = ',CallforHeat,' (-)'
662             WRITE(ITU,*) ' DeviceONOFF     = ',DeviceONOFF,' (-)'
663             WRITE(ITU,*) ' DeviceONOFFp    = ',DeviceONOFFp,' (-)'
664             WRITE(ITU,*) ' COP             = ',COP,' (-)'
665             WRITE(ITU,*) ' AmbientTempComp = ',AmbientTempComp,' (C)'
666             WRITE(ITU,*) ' TempCompS       = ',TempCompS,' (C)'
667             WRITE(ITU,*) ' TempCompE       = ',TempCompE,' (C)'
668             WRITE(ITU,*) ' DefrostCalc     = ',DefrostCalc,' (-)'
669             WRITE(ITU,*) ' AmbientRH       = ',RHamb,' (%)'
670             WRITE(ITU,*) ' DefrostTime     = ',DefrostTime,' (mins)'
671             WRITE(ITU,*) ' DefrostDur      = ',DefrostDur,' (-)'
```

```
672                 WRITE(ITU,*) ' InDefrost       = ',Indefrost,' (-)'
673                 WRITE(ITU,*) ' DefrostLock     = ',DefrostLock,' (-)'
674                 WRITE(ITU,*) ' DefrostLockout  = ',DefrostLockout,' (mins)'
675                 WRITE(ITU,*) ' DefrostLockDur  = ',DefrostLockDur,' (mins)'
676                 WRITE(ITU,*) ' HeatOutput      = ',HeatOutput,' (W)'
677                 WRITE(ITU,*) ' CompPower       = ',CompPower,' (W)'
678                 WRITE(ITU,*) ' FanPower        = ',FanPower,' (W)'
679                 WRITE(ITU,*) ' PumpPower       = ',PumpPower,' (W)'
680                 WRITE(ITU,*) ' CtlPower        = ',CtlPower,' (W)'
681               END IF
682               WRITE(ITU,*) ' Matrix coefficients for ISTATS = ',ISTATS
683               NITMS=6
684               WRITE(ITU,*) (COUT(I),I=1,NITMS)
685               IF(ITU.EQ.IUOUT) THEN
686                  IX1=(IPCOMP/4)*4
687                  IF(IX1.EQ.IPCOMP.OR.IPCOMP.EQ.NPCOMP) call epagew
688               END IF
689             END IF
690
691             IF(ITC.GT.0.AND.NSINC.GE.ITC.AND.NSINC.LE.ITCF.AND.
692            &   ITRACE(37).NE.0) WRITE(ITU,*) ' Leaving subroutine CMP45C'
693
694             RETURN
695             END
```